# CHARACTERIZATION OF DEGRADATIVE PROTEIN QUALITY CONTROL MECHANISMS USING MODEL SUBSTRATES DERIVED FROM TEMPERATURE SENSITIVE ALLELES

by

Sophie Comyn

M.Sc., The University of Alberta, 2011

B.Sc., The University of British Columbia, 2007

A THESIS SUBMITTED IN PARTIAL FULFILLMENT
OF THE REQUIREMENTS FOR THE DEGREE OF

**Doctor of Philosophy**

in

THE FACULTY OF GRADUATE AND POSTDOCTORAL STUDIES

(Genome Science and Technology)

The University of British Columbia

(Vancouver)

December 2016

# Abstract

The purpose of protein homeostasis (proteostasis) is to maintain proteome integrity, thereby promoting viability at both the cellular and organism levels. Exposure to a range of acute stresses often produces misfolded proteins, which present a challenge to maintaining proteostatic balance. The accumulation of misfolded proteins can lead to the formation of potentially toxic protein aggregates, which are characteristic of a number of neurodegenerative diseases such as Alzheimer's and Parkinson's. Therefore, a number of protein quality control pathways exist to promote protein folding by molecular chaperones or target terminally misfolded proteins for degradation via the ubiquitin proteasome system or autophagy. Within the cytosol the mechanisms responsible for targeting substrates for proteasomal degradation remain to be fully elucidated.

In this thesis, we established and employed thermosensitive model substrates to screen for factors that promote proteasomal degradation of proteins misfolded as the result of missense mutations in *Saccharomyces cerevisiae*. Using a genome-wide flow cytometry based screen we identified the prefoldin chaperone subunit Gim3 as well as the E3 ubiquitin ligase Ubr1. An absence of Gim3 leads to the accumulation of model substrates in cytosolic inclusions and their delayed degradation. We propose that Gim3 promotes degradation by maintaining substrate solubility.

In the course of screening for factors involved in degradative protein quality control, we identified secondary mutations in the general stress response gene *WHI2* among a number of E3 ligase deletion strains. We demonstrate that an absence of *WHI2* is responsible for the observed impairment in the proteolytic degradation of Guk1-7. We propose a link between mutations in *WHI2* to a deficiency in

the Msn2/4 transcriptional response, thereby altering the cell's capacity to degrade misfolded cytosolic proteins.

Collectively, the data in this thesis generated with the Guk1-7 model substrate underscores how changes in the elaborate protein quality control network can perturb proteostasis. Given that proteostasis is altered in a number of diseases ranging from cancer to ageing, identifying the factors that mediate protein quality control and understanding the interplay between members of the proteostatic network are important not only for understanding the basic biological processes but also for potential therapeutic applications.

# Preface

Chapter 1 is partially based on a first author publication. *Comyn SA, Chan GT, Mayor T. (2014). False start: cotranslational protein ubiquitination and cytosolic protein quality control. J Proteomics 100:92-101. doi: 10.1016/j.jprot.2013.08.005*. This is a peer reviewed review article. I co-wrote most of the manuscript with Thibault Mayor, whereas Gerard Chan helped with some sections. I prepared the figure.

Chapter 2 is based on a first author publication. *Comyn SA, Young BP, Loewen CJ, Mayor T. (2016). Prefoldin promotes proteasomal degradation of cytosolic proteins with missense mutations by maintaining substrate solubility. PLoS Genetics 12(7):e1006184. doi: 10.1371/journal.pgen.1006184*. I performed all of the experiments and Barry Young prepared the barcoded yeast deletion collection used for the screen and all subsequent validation experiments. I and Thibault Mayor co-wrote the manuscript with input from Drs. Barry Young and Christopher Loewen. The plasmid BPM866 (pFA6a-mCherry-KanMX6) and the yeast strain YTM1919 (Hsp42-mCherry), which were used in this study, were made by Mang Zhu using a codon optimized mCherry template prepared by Dr. Patrick Chan.

Chapter 3 is based on a first author publication being prepared for submission. *Comyn SA, Flibotte S, Spear ED, Michaelis S, Mayor T. Recurrent background mutations in WHI2 alter proteostasis and impair degradation of cytosolic misfolded proteins in Saccharomyces cerevisiae*. All the experiments were designed by myself and Thibault Mayor. I performed most of the experiments and co-wrote the manuscript with Thibault Mayor. Illumina library preparation and whole genome sequencing was conducted by Ana Kuzmin at the NextGen Sequencing facility at the UBC Biodiversity Research Centre. Dr. Stéphane Flibotte performed the se-

quencing analysis which led to the identification of the *WHI2* mutation. Eric Spear and Susan Michaelis performed experiments that are not presented in this thesis but form part of this publication.

# Table of Contents

# List of Tables

# List of Figures

# Glossary

| | |
|---|---|
| ΔΔG | Free energy change |
| ABCE1 | ATP binding cassette subfamily E member 1 |
| ADP | Adenosine diphosphate |
| ANOVA | Analysis of variance |
| ARS | Autonomously replicating sequence |
| Asi1 | Amino acid sensor independent |
| Atg8 | Autophagy related |
| ATP | Adenosine triphosphate |
| Bmh2 | Brain modulosignalin homologue |
| bp | Base pair |
| Bra7 | Fluorocytosine resistance |
| Btn2 | Batten disease |
| CCT | Chaperonin containing TCP-1 |
| Cdc48 | Cell division cycle |
| CEN | Yeast centromere |
| CETSA | Cellular thermal shift assay |
| CHX | Cycloheximide |
| CHIP | C-terminus of Hsc70-interacting protein |
| CFTR | Cystic fibrosis transmembrane conductance regulator |
| CPY | Carboxypeptidase |
| CytoQ | Cytosolic quality control compartment |
| Das1 | Dst1-delta6-azaurail sensitivity |
| DBD | DNA binding domain |
| Deg1 | Depressed growth rate |
| DIC | Differential interference contrast |
| DNA | Deoxynucleic acid |

| | |
|---|---|
| Doa10 | Suppressor of mRNA stability mutant |
| DsRed | Discosoma sp. red fluorescent protein |
| E1 | Ubiquitin activating enzyme |
| E2 | Ubiquitin conjugating enzyme |
| E3 | Ubiquitin ligase enzyme |
| EDTA | Ethylenediamine tetraacetic acid |
| EGFP | Enhanced GFP |
| ER | Endoplasmic reticulum |
| ERAD | ER associated degradation |
| ERISQ | Excess ribosomal protein quality control |
| EV | Empty vector |
| FACS | Fluorescence activated cell sorting |
| Fap1 | FKBP12-associated protein |
| FDA | Food and drug administration |
| Fes1 | Factor exchange for Ssa1p |
| FITC | Fluorescein isothiocyanate |
| g | Gravity |
| GDP | Guanosine diphosphate |
| GFP | Green fluorescent protein |
| Gim | Gene involved in microtubule biogenesis |
| Glo4 | Glyoxalase |
| GMP | Guanosine diphosphate |
| GPD | Triose-phosphate dehydrogenase |
| GPS | Global protein stability analysis |
| Guk1 | Guanylate kinase |
| Gus1 | Glutamyl-tRNA synthetase |
| Hbs1 | Hsp70 subfamily B suppressor |
| HCl | Hydrogen chloride |
| HECT | Homologous to the E6AP carboxyl terminus domain |
| HEPES | 4-(2-hydroxyethyl)-1-piperazineethanesulfonic acid |
| HGMD | Human gene mutation database |
| HOP | Hsp90 organizing protein |
| Hrd1 | HMG-coA reductase degradation |

| | |
|---|---|
| Hrt3 | High level expression reduces Ty3 transposition |
| HSD | Honest significant difference |
| Hsp | Heat shock protein |
| Hul5 | HECT ubiquitin ligase |
| INQ | Intranuclear quality control compartment |
| IPOD | Immobile protein deposit |
| IRES | Internal ribosome entry site |
| JUNQ | Juxtanuclear quality control compartment |
| kDa | Kilo dalton |
| Ltn1 | RING domain mutant killed by Rtf1 deletion |
| $\mu$g | Microgram |
| $\mu$L | Microlitre |
| $\mu$m | Micrometer |
| mL | Millilitre |
| mM | Millimolar |
| M | Molar |
| Mr | Molecular weight |
| min | Minute |
| MAT | Mating type |
| MPP11 | DnaJ Hsp family member C2 |
| Msn | Multicopy suppressor of SNF1 mutation |
| Mup3 | Methionine uptake |
| n | Number |
| NAC | Nascent chain associated complex |
| NaCl | Sodium chloride |
| NEDD4 | Neural precursor cell expressed, developmentally downregulated 4 |
| NEF | Nucleotide exchange factor |
| NEMF | Nuclear export mediator factor |
| NES | Nuclear export sequence |
| NLS | Nuclear localization sequence |
| NMP | Nucleoside monophosphate kinase |
| NP-40 | Nonidet P-40 |
| Npl4 | Nuclear protein localization |

| | |
|---|---|
| OD | Optical density |
| ORF | Open reading frame |
| P | P-value |
| p62 | Nucleoporin 62 |
| PAH | Phenylalanine hydroxylase |
| PBS | Phosphate buffered saline |
| PCR | Polymerase chain reaction |
| PDB | Protein data bank |
| Pep4 | Carboxy peptidase Y-deficient |
| Pgk1 | 3-phosphoglycerate kinase |
| PKA | Protein kinase A |
| PMSF | Phenylmethane sulfonyl fluoride |
| PolyQ | Polyglutamine |
| Prb1 | Proteinase B |
| Pro3 | Proline requiring |
| Prc1 | Proteinase C |
| RAC | Ribosome associated complex |
| RBR | RING-between-RING |
| Rim15 | Regulator of IME2 |
| RING | Really interesting new gene |
| RNA | Ribonucleic acid |
| Rpt6 | Regulatory particle triple-A protein |
| RQC | Ribosome quality control complex |
| Rqc1 | Ribosome quality control 1 |
| Rsp5 | Reverses Spt-phenotype |
| S | Soluble |
| San1 | Sir antagonist |
| SD | Standard deviation |
| SDG | Saccharomyces genome database |
| SDS | Sodium dodecyl sulfate |
| SDS-PAGE | Sodium dodecyl sulfate polyacrylamide gel electrophoresis |
| Sec61 | Secretory |
| SILAC | Stable isotope labelling with amino acids in cell culture |

| | |
|---|---|
| Sir4 | Silent information regulator |
| Sis1 | Slt4 suppressor |
| SNV | Single nucleotide variant |
| Ssa | Stress sensitive subfamily A |
| Ssb | Stress sensitive subfamily B |
| Sse1 | Stress seventy subfamily E |
| Sti1 | Stress inducible |
| STRE | Stress response elements |
| t | Time |
| T | Total cell lysate |
| TAD | Transcriptional activating domain |
| Tae2 | Translation-associated element 2 |
| TAP | Tandem affinity purification |
| Tcp | Tailless complex polypeptide |
| Tom1 | Trigger of mitosis |
| TOR | Target of rapamycin |
| TPR | Tetratricopeptide repeat domain |
| TRiC | TCP-1 ring complex |
| Tx-100 | Triton X-100 |
| Ub | Ubiquitin |
| Ubc | Ubiquitin conjugating |
| Ube2W | Ubiquitin conjugating enzyme E2 W |
| Ubp | Ubiquitin specific protease |
| Ubr1 | Ubiquitin protein ligase E3 component N-recognin 1 |
| Ufd | Ubiquitin fusion degradation |
| Ugp1 | UDP-glucose pyrophosphorylase |
| UPS | Ubiquitin proteasome system |
| UTR | Untranslated region |
| VHL | von Hippel Landau |
| Whi2 | Whiskey |
| X | Times |
| Ydj1 | Yeast dnaJ |
| YPD | Yeast extract peptone dextrose |

# Acknowledgements

I would like to thank everyone who has contributed to the work contained in this thesis and who has helped me throughout the course of my degree. I would like to express my appreciation to my supervisor, Thibault Mayor, and to my supervisory committee members Christopher Loewen, Vivien Measday, and Michel Roberge for their advice, encouragement, guidance, and mentorship. Thank you to members of the Mayor lab for valuable feedback and camaraderie. To Elizabeth, Allym, Aruna, and Carla, thank you for making me welcome in your lab and for your kindness and generosity. Thank you to Megan Kofoed for all of her assistance with the numerous yeast collections. Thank you to members of the Hansen lab, both past and present, for their friendship and making the office a fun place to be over the past six years. I am especially grateful to Cheryl and Tan for their friendship and insightful discussions. Finally, I would like to express my gratitude to my parents for their support and patience, without which none of this would have been possible.

# Chapter 1

# Introduction

## 1.1 Protein Misfolding and Protein Homeostasis

Protein homeostasis, or proteostasis, preserves proteome integrity and thereby promotes viability at both the cellular and organism levels. To do so, proteostasis is maintained by a network of interconnected pathways that influence the fate of proteins by directing their translation, folding, localization, and degradation [1]. Misfolded proteins are one of many factors that challenge a cell's ability to maintain proteostatic balance.

Protein misfolding can result from a number of processes such as mutation; errors during transcription, RNA processing and translation; trapping of a folding intermediate; failure to incorporate into multimeric complexes; or post-translational damage [2, 3]. The risk to the cell of misfolded or partially folded proteins may be attributed, at least in part, to the exposure of hydrophobic amino acid residues that in the native state would be sequestered to the core of the protein, or at protein-protein interaction interfaces, but once exposed can engage in unspecific interactions with other polypeptides. These exposed hydrophobic regions of misfolded proteins also have an inherent propensity to aggregate, forming associations not native to the cell [4]. For example, artificial beta-sheet proteins expressed in human HEK293T cells were found to coaggregate with proteins that have many functional interaction partners suggesting that the aggregates competitively bind to functional protein-protein interaction interfaces [5]. Moreover, the relative cytotoxicity of the

aggregates correlated with the number of interaction partners ascribed to the coaggregating proteins. More recently, Kim *et al.* identified and analysed aberrant protein interactions involving soluble oligomers and insoluble inclusions of the mutant huntingtin protein [6]. Expressing a fragment of huntingtin, containing the Huntington's disease causing polyglutamine (PolyQ) repeat expansion, they found that insoluble inclusions predominantly interacted with members of the protein quality control machinery representing $\sim$85 proteins. Soluble oligomers interacted with upwards of 800 different proteins representing diverse cellular functions such as transcription, translation, and RNA-binding. Within the cytosol, macromolecular crowding creates an environment that increases the tendency of folding intermediates and misfolded proteins to aggregate, as aggregation is highly concentration dependent [7]. The native conformation of a protein, however, must balance structural stability with conformational flexibility that is associated with protein function [8]. As such, a tightly regulated network of molecular chaperones contend with a constant flux of protein intermediates, misfolded proteins, and aggregate formation [9].

Proteostasis depends on balancing the folding capacity of chaperone networks with the quantity of proteins in non-native conformations (Figure 1.1). When the level of misfolded proteins rises, the folding capacity of the cell can be temporarily augmented to meet the increased demand through the activation of signaling pathways modulated by the transcription factors heat shock factor 1 (Hsf1) and Msn2/4. Stressors that precipitate protein misfolding disrupt equilibrium and if the cellular response is overwhelmed and insufficient to meet the increase in need, then it can lead to the accumulation and aggregation of misfolded proteins [10]. Although the exact mechanism that results in the formation of cellular aggregates has yet to be fully elucidated, their presence is associated with a number of neurodegenerative conditions such as Huntington's, Parkinson's, and Alzheimer's diseases, as well as ageing [11, 12]. Maintaining proteome integrity, therefore, requires an integrated protein quality control network that monitors the proteome, mediates protein refolding by molecular chaperones, and removes terminally misfolded proteins via the ubiquitin proteasome system or autophagy [1].

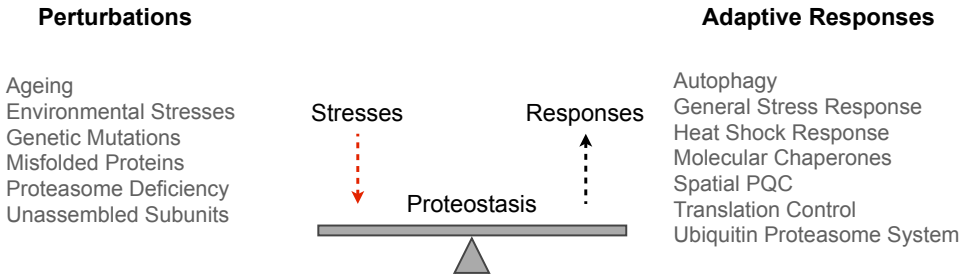


**Figure 1.1:** Proteostasis. Proteostasis depends upon balancing the perturbations that disrupt protein folding with the network of pathways that direct the levels, conformational state, and distribution of the proteome.

## 1.2 Protein Folding and Cytosolic Molecular Chaperones

Molecular chaperones promote protein homeostasis by preventing protein aggregation, assisting protein folding, and targeting terminally misfolded clients for degradation. Broadly, chaperones can be defined as any protein that recognizes and interacts with proteins found in a non-native state for the purpose of stabilizing and promoting folding into an active conformation without forming part of the final structure [10]. There are a number of distinct conserved chaperone families, one of which is the heat shock protein (Hsp) family whose members are classified by their molecular weights (*e.g.* Hsp40, Hsp70, Hsp90, and the small Hsps). Within the context of protein quality control in the eukaryotic cytosol, the main chaperone machineries involved are the: ribosome associated chaperones, Hsp70/40, Hsp90, TRiC/CCT chaperonin, and prefoldin.

### 1.2.1 Nascent Protein Folding

A number of chaperones bind to, or associate with, the ribosome to both promote protein folding and prevent misfolding or aggregation of the nascent polypeptide as it emerges from the ribosome. As translation occurs at a slower rate than protein folding, nascent polypeptide chains emerge from the ribosome in a partially folded aggregation prone state. Also, because the size of the ribosome exit tunnel is such that folding beyond the formation of alpha helical structures is prohibited, only limited folding can proceed until a domain (generally 50 to 300 amino acids in length)

exits the ribosome [13]. Therefore, molecular chaperones interact co-translationaly with nascent polypeptide chains to prevent aggregation and premature non-native folding from occurring before the polypeptide has been fully translated. Moreover, while the ribosome exit sites are positioned in the polysome in such a way as to minimize aggregation of the nascent polypeptides, ribosome associated chaperones are needed to further prevent aggregation of the numerous identical proteins being translated from the polysome [14, 15]. The ribosome associated complex (RAC) and nascent chain associated complex (NAC) are the first chaperone complexes to interact with the nascent polypeptide as it exits the ribosome. In mammals, RAC is formed by the association of Hsp70L1 and the J-domain containing protein MPP11. In yeast, RAC consists of the Hsp70 Ssz1 and the ribosome binding Hsp40 zuotin. Zuotin in turn acts in concert with the Hsp70s Ssb1 and Ssb2 that are also associated to the ribosome [16–18]. Deleting the genes encoding the dimeric NAC complex subunits and Ssb proteins in *Saccharomyces cerevisiae* resulted in decreased viability under conditions of protein folding stress [19]. Moreover, the abundance of ribosomal particles was altered in these mutants suggesting that ribosome biogenesis is linked to the protein folding capacity of the ribosome associated chaperones. Partially folded proteins are transferred by Hsp70 chaperones from the ribosome associated complex to further downstream folding pathways such as Hsp70, prefoldin, and chaperonin.

### 1.2.2 Hsp70, Hsp40, and Hsp90

The Hsp70 family of molecular chaperones promotes protein folding through reiterative cycles of ATP-dependent client capture and release (Figure 1.2). Hsp70s do not function independently, but as part of an Hsp70 core machinery consisting of an Hsp70, an Hsp40 (J domain protein), and a nucleotide exchange factor (NEF) that coordinate their activities to increase the efficiency of Hsp70 client folding [20, 21]. Hsp70 consists of an N-terminal ATPase domain and a C-terminal substrate binding domain that binds to short 5-7 amino acid stretches of hydrophobic residues on client proteins. Dimerization is necessary for Hsp70 chaperone activity and efficient Hsp40 interaction [22]. Initial client binding occurs while Hsp70 is in the ATP-bound state and the Hsp70-client interaction is stabilized through ATP hy-

drolysis. The intrinsic ATPase activity of Hsp70 is relatively low however, and is enhanced by association with an Hsp40. As the number of Hsp40 proteins in the cell greatly outnumbers that of the Hsp70s, it is thought that the repertoire of Hsp40 proteins help target Hsp70 to its clients, or bind them directly to enhance the specificity of the system [23]. How each Hsp40 protein recognizes its cohort of substrates remains to be fully understood. Once Hsp70 is bound to a client protein, Hsp40, via its conserved J domain, stimulates ATP hydrolysis and the subsequent activity of a NEF promotes ADP dissociation and client release. Upon release from Hsp70 the bound hydrophobic region is free to refold, however, it may re-associate with Hsp70 if folding is not complete. There are four non-ribosomal binding Hsp70s (Ssa1-4) in the cytosol of *S. cerevisiae* and their ATP hydrolysis is enhanced by Ydj1 and Sis1 Hsp40 co-chaperones [24]. In addition to Fes1, a confirmed NEF in the yeast cytosol, the Hsp110 Sse1 has also been reported to act as a NEF for the Hsp70s Ssa1 and Ssb1 [24]. The Hsp70 family can act both co- and post-translationaly and are hubs to direct substrates to further downstream chaperone networks such as Hsp90 and chaperonin [25].

Hsp90 acts downstream of Hsp70 and Hsp40 to assist in the folding of nascent transcription factors, protein kinases, and steroid hormone receptors [26]. Substrate transfer from the Hsp70/Hsp40 system to Hsp90 is mediated by the Hsp90 organizing protein (HOP, or Sti1 in yeast) [27]. The tetratricopeptide repeat domain (TPR) of HOP interacts with the MEEVD sequence on the C-terminal of Hsp90 bridging the two chaperone machineries and facilitating substrate transfer. Once bound to a substrate, Hsp90 ATPase activity is stimulated through an interaction with Aha1. Chemical inhibition of Hsp90 function leads to the proteasomal degradation of many Hsp90 substrates potentially as the result of increased interaction with Hsp70 and Hsp70 associated factors [28].

### 1.2.3 TRiC/CCT Chaperonin and Prefoldin

Chaperonin, also known as the TCP-1 ring complex (TRiC) or; the chaperonin containing TCP-1 (CCT), functions in folding newly translated proteins and preventing protein aggregation in the cytosol [29, 30]. Essential in all three domains of life, it has been estimated that upwards of 10% of the eukaryotic proteome transits

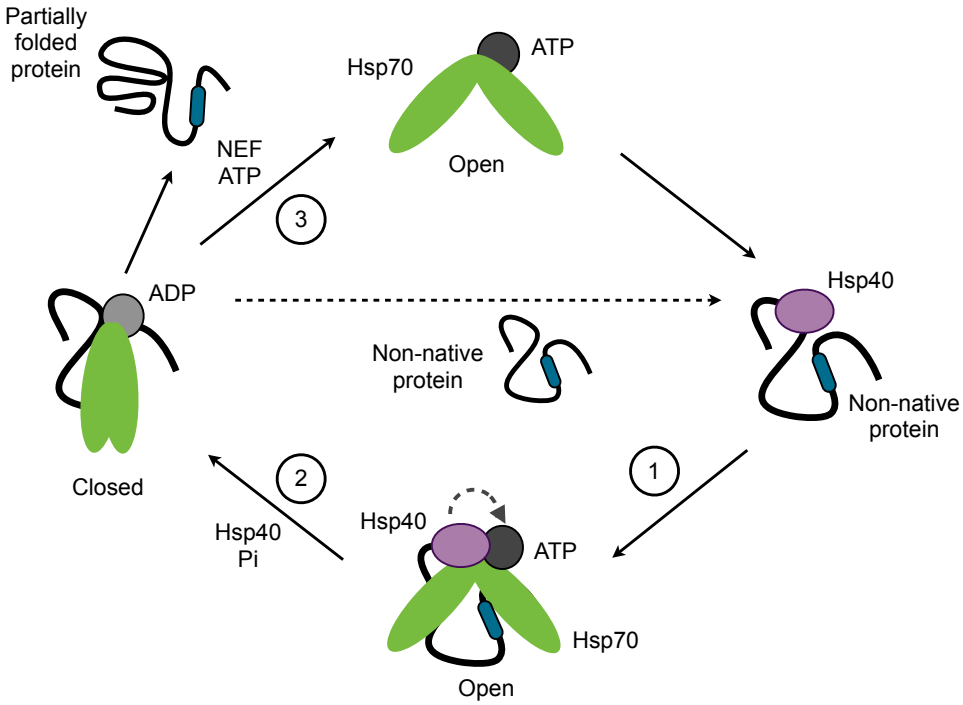


**Figure 1.2:** Hsp70 reaction cycle. 1) Hsp40 binds to misfolded substrates and delivers them to an ATP bound Hsp70. 2) Substrates bind to Hsp70 via hydrophobic patches (blue) and ATP hydrolysis to ADP, accelerated by Hsp40, switches Hsp70 to the closed substrate binding conformation. 3) Hsp40 dissociates from Hsp70 and a nucleotide exchange factor (NEF) exchanges ATP for ADP causing Hsp70 to open and release the misfolded substrate enabling it to fold. Substrates can re-engage with Hsp40 to continue Hsp70 cycling or fold into their native conformation.

through CCT, including cytoskeleton proteins and cell cycle regulators [31]. Chaperonin is a large cylindrical 1 MDa protein complex formed through the stacking of two identical rings, each comprising eight subunits (CCT1-8) [30]. The apical domains of the ring subunits act as a lid to enclose the partially unfolded substrate in the central cavity mitigating the effects of macromolecular crowding on protein folding. In eukaryotes, the chaperonin lid does not close entirely thereby accommodating extended polypeptide chains and single domains of multidomain substrates [32]. CCT engages substrates while in the ATP-bound state with ATP

hydrolysis inducing conformational changes that lead to the closure of the chaperonin lid and substrate encapsulation. Each ring is divided into two hemispheres based on ATP binding affinity that leads to a cycle of asymmetric conformational changes [33]. CCT subunits 3, 6, 7, and 8 constitute one of the hemispheres and have low affinity for ATP under physiological conditions and were found to be dispensable for chaperonin activity [33]. While all eight subunits have a conserved ATP binding domain, their sequences are only $\sim$40% identical. The apical domains of each subunit, therefore, are thought to recognize different substrate motifs, which is underscored by each subunit having its own specific patterns of polar and hydrophobic residues [34]. The pattern of amino acid residues in the each apical domain is thought to allow chaperonin to bind and fold a range of structurally diverse proteins. Although initially identified through its requirement for folding the cytoskeletal proteins actin and tubulin, the eukaryotic chaperonin has been shown to act in the folding of a number of other substrates [35]. The human chaperonin interactome is enriched for proteins predicted to be aggregation prone, which contain multiple domains and have complex topologies [36]. The importance of CCT in human health is underscored by a mutation in CCT5 being identified as the cause of autosomal recessive mutilating sensory neuropathology with spastic paraplegia [37]. CCT is also required for the replication of human pathogens such as HIV and hepatitis C as well as folding a number of cancer associated proteins, such as p53 and the von Hippel Lindau tumor suppressor [38–40].

Prefoldin is a hetero-oligomeric protein complex composed of six subunits ranging in size from 14–23 kDa [41]. Conserved in archaea and eukaryotes, but absent in prokaryotes, the prefoldin hexamer forms a "jellyfish-like" structure with N- and C-terminal coiled-coil regions of each subunit forming "tentacles" that emanate from a central region [42]. Misfolded substrates are transferred from prefoldin to the TRiC/CCT chaperonin in an ATP-independent manner through direct binding of the two chaperone complexes [41]. In addition to its role in aiding nascent proteins, such as actin and tubulin, to attain their functional conformations, the prefoldin chaperone complex has been shown to prevent huntingtin and alpha-synuclein aggregate formation [43, 44].

## 1.3 Molecular Chaperones and Protein Degradation

While molecular chaperones promote protein homeostasis by preventing protein aggregation and promoting protein folding, they can also mediate the targeting of terminally misfolded clients for degradation; either indirectly, by maintaining misfolded proteins in a non-aggregated degradation competent state, or directly through facilitating the recognition and/or transfer of substrates to degradative quality control pathways [45–49]. In an elegant study using the von Hippel Lindau (VHL) tumor suppressor protein as a misfolded model substrate, Frydman and colleagues showed that a different set of chaperone proteins and co-factors mediate folding and degradation, respectively [50]. Hsp90 and the co-chaperone Sti1 were required for degradation but not the folding of VHL, while the converse was true for the chaperonin TRiC/CCT. The Ssa1/2 cytosolic Hsp70s, and the nucleotide exchange factor Sse1 were also required for degradation of VHL, as well as other cytosolic misfolded proteins [50, 51]. Although the yeast Hsp70 cofactor Ydj1 was not required for VHL degradation, it has been shown to mediate the degradation of ER proteins with exposed misfolded cytosolic domains and the degradation of cytosolic proteins after heat shock [52, 53]. Most recently Fes1, another yeast Hsp70 NEF, was shown to promote proteasomal degradation of additional misfolded proteins [54]. In higher eukaryotes, the Bag6 Hsp70 cofactor that can bind to the proteasome via its ubiquitin-like domain is required for the efficient degradation of defective nascent polypeptides [55]. Although the degradation of distinct substrates has been demonstrated to require different chaperones and co-chaperones, in most cases it remains unclear how two competing systems (*i.e.* folding and degradation machineries) triage misfolded proteins in the cell.

## 1.4 Ubiquitin Proteasome System (UPS)

In eukaryotes, the ubiquitin proteasome system plays a critical role in protein quality control by selectively targeting intracellular proteins for degradation through the covalent attachment of polyubiquitin chains. Ubiquitin is a highly conserved 8.5 kDa protein that is primarily conjugated onto lysine residues of target substrates through the activity of an enzymatic cascade involving ubiquitin activating (E1), ubiquitin conjugating (E2), and ubiquitin ligase (E3) enzymes [56]. Substrate

specificity and recruitment is mediated by an E3 ubiquitin ligase, either alone or in combination with an E2 conjugating enzyme. The inherent complexity of the ubiquitin system is reflected in the sheer number of putative E3 ligases (90 and 600) encoded in the genome of yeast and human, respectively [57]. Moreover, the importance of E3 ligases in substrate targeting is emphasized by the fact that the number of putative E3 ligases greatly outnumbers that of E2 conjugating enzymes by approximately 15:1 [58]. E3 ubiquitin ligases belong to one of three families characterized by their namesake domains (Figure 1.3). The really interesting new gene (RING) family are the most abundant E3 ligases with $\sim$600 members in humans and can be found as monomers, dimers, or as part of multisubunit complexes [59]. The RING domain can be located anywhere on the protein and consists of a conserved consensus sequence of cysteine and/or histidine residues, which coordinate with two zinc atoms to stabilize the domain structure [58]. RING E3 ligases act as scaffolds to orient the substrate with an E2-ubiquitin conjugate for efficient ubiquitin transfer. Approximately thirty proteins belong to the homologous to the E6AP carboxyl terminus domain (HECT) family with all known HECT domains located at the C-terminus of the protein. HECT E3 ligases play a direct role in substrate ubiquitination through a stepwise process. First, the HECT E3 ligase, via an N-lobe E2 binding domain, receives an E2-ubiquitin conjugate to then form an E3-ubiquitin conjugate. Ubiquitin is then conjugated to a substrate from the E3 active site via a C-lobe catalytic cysteine [58]. The final family, the RING-between-RING or RBR E3 ligases, are the least abundant containing only 13 members in humans. RBR ligases contain an N-terminal RING domain (RING1), like the RING ligases, followed by in between RING and RING2 domains, which are unique to RBR proteins and do not contain the cysteine RING consensus sequence. In addition, like HECT ligases, RBR ligases form a thioester bond with ubiquitin. Mutations in Parkin, one of the most studied members of this family, are associated with early onset Parkinson's disease [60].

Ubiquitin has seven lysine residues, all of which can be conjugated to ubiquitin molecules to form polyubiquitin chains. The K48 chain linkage is considered to be the predominant signal recognized by the cell for proteasomal degradation. The 26S proteasome is a large 2.5 MDa protein complex responsible for the selective recognition and degradation of ubiquitin conjugated proteins. It is composed of the

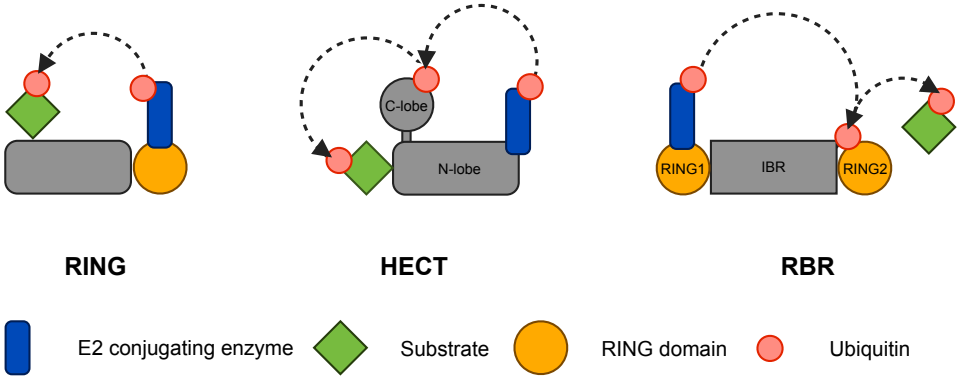


**Figure 1.3:** Schematic of the three E3 ubiquitin ligase families and E3 catalysed ubiquitin transfer.

central barrel-like 20S core particle, which contains the proteolytic peptidases, and two 19S regulatory particles. The regulatory particle is responsible for substrate recognition, ubiquitin chain removal, and protein unfolding and translocation into the catalytic core particle [61, 62]. In addition, the system is under constant flux as ubiquitination can be reversed by deubiquitinating enzymes.

There are multiple pathways that can target misfolded proteins for proteasomal degradation. Different types of protein damage are more prevalent in different cellular compartments owing to the nature of the subcellular environment necessitating compartment-specific quality control pathways, with systems having been described for the ER, nucleus, and cytoplasm [63].

### 1.4.1 ER Associated Degradation (ERAD)

Approximately one third of all eukaryotic proteins are membrane or secreted proteins that must pass through the ER [64]. Protein folding is monitored by ER quality control machinery and non-native or unassembled subunits are targeted for degradation by the ER associated degradation (ERAD) pathway. If misfolded proteins are left to accumulate in the ER, a stress response is triggered in an attempt to rebalance the protein quality control system and to clear misfolded proteins. ERAD was initially discovered through studies of the cystic fibrosis transmembrane conductance regulator (CFTR). While some components of the ERAD path-

way, such as the E3 ligases, are better defined in yeast, the identification of human homologs to several of the yeast genes involved would suggest that ERAD may play a role in ER proteostasis in higher eukaryotes as well. ER proteins targeted for degradation must be retranslocated from the ER in an ATP-dependent manner where they are degraded by the ubiquitin proteasome system [64]. The multispan ER membrane RING E3 ligases Doa10 and Hrd1 ubiquitinate substrates on the cytosolic side of the ER following substrate retranslocation by a complex containing the AAA-ATPase Cdc48, Ufd1, and Npl4 (p97, UFD1, and NPL4 in mammals) (Figure 1.4) [65]. The mechanism determining whether a substrate is targeted by Doa10 or Hrd1 is thought to be based upon the location of the degradation signal. ER lumen and membrane substrates are generally recognized by Hrd1 and cytosolic substrates by Doa10 [66, 67].

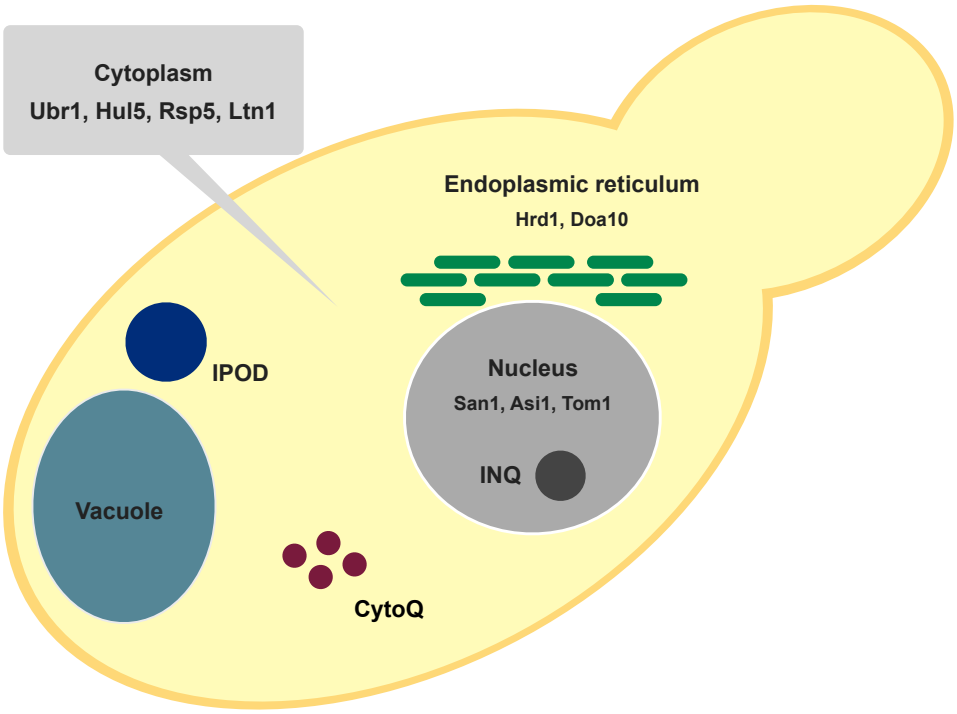


**Figure 1.4:** Schematic representation of the spatial distribution of protein quality control compartments in yeast.

### 1.4.2 Nuclear Protein Quality Control

Despite the fact that the majority of proteasomes are located within the nucleus under non-stress conditions, our understanding of nuclear protein quality control is relatively limited compared to that of the ER and cytoplasm [68]. In yeast, the primary model organism used for nuclear protein quality control studies, the RING E3 ligase San1, in conjunction with the E2 ubiquitin conjugating enzyme Ubc1, is responsible for the ubiquitination of misfolded nuclear proteins, thereby targeting them for degradation by the ubiquitin proteasome system in the nucleus (Figure 1.4) [69–71]. San1 recognizes exposed hydrophobic residues on misfolded proteins that are normally buried in the native conformation [69]. These hydrophobic stretches interact with substrate recognition sites on San1 that are interspersed between N- and C-terminal intrinsically disordered domains [72]. It is thought that these disordered regions, which lack secondary structure, provide flexibility such that San1 can bind to a large number of substrates with different conformations. The AAA-ATPase Cdc48/p97 has also been shown to be required for the degradation of some highly insoluble San1 substrates [73]. While the role of molecular chaperones in nuclear protein quality control remains unclear, the chaperones Sis1 and Sse1 are required for the nuclear targeting of misfolded cytoplasmic proteins [74–76]. Moreover, inhibition of Hsp42 leads to the accumulation of cytoplasmic proteins in the nucleus [77]. This would suggest a mechanism whereby some proteins are normally retained in the cytosol and when this fails it leads to the accumulation and aggregation of proteins within the nucleus. Why misfolded cytoplasmic proteins are imported into the nucleus remains unknown, however, a number of possible explanations have been proposed. The first, is that proteins under 40 kDa in size passively diffuse through nuclear pores into the nucleus. The second, is that nuclear import is an active response in cases where cytoplasmic protein quality control becomes overwhelmed. The third, is that it could be advantageous to separate nuclear degradation from cytosolic protein folding. More work will be required to determine whether one, or all, of these explanations is correct [78, 79]. It remains unclear as to which E3 ligase is required for nuclear protein quality control in mammals.

In addition to San1, two other nuclear E3 ligases have recently been character-

ized. Asi1 is a RING E3 ligase located in the inner nuclear membrane. The Asi complex, consisting of the proteins Asi1-3, acts in parallel with Hrd1 and Doa10 of the ERAD pathway to degrade soluble and integral membrane proteins [80]. It is not yet known if Asi1 has a more general role in nuclear protein quality control, or how its substrates are recognized. Recently, the HECT E3 ligase Tom1 was identified in a screen, along with the E2 conjugating enzymes Ubc4 and Ubc5, to be responsible for targeting overexpressed and unassembled ribosomal proteins for degradation [81]. Tom1 specifically targets residues that would normally be hidden in mature ribosome assemblies. Cells lacking *TOM1* contained aggregated ribosomal proteins. This new pathway named excess ribosomal protein quality control (ERISQ) is conserved as the human Tom1 homolog Huwe1 demonstrated a similar function in human cells.

## 1.5 Cytosolic E3 Ubiquitin Ligases Involved in Protein Quality Control

Several ubiquitin ligases in higher and lower eukaryotes are proposed to target misfolded cytosolic proteins for degradation, a number of which are described in detail below. Many of these E3 ligases act in conjunction with molecular chaperone partners to target their misfolded clients for degradation. Their substrates are diverse ranging from nascent polypeptides that fail to attain their native conformation, stalled translation products, N-terminally destabilized polypeptides, and proteins which have become misfolded. How do E3 ligases recognize their substrates? Does each pathway target a specific subset of misfolded proteins? Do several ubiquitin ligases target the same proteins, potentially recognizing different domains or conformations? The search for the answers to these questions drives current work in the cytoplasmic protein quality control field.

### 1.5.1 CHIP

C-terminus of Hsc70-interacting protein (CHIP) E3 ligase was shown over ten years ago to be part of a major pathway targeting cytosolic misfolded proteins for degradation. A chaperone dependent ligase, CHIP interacts with both Hsp70 and Hsp90 via its TPR domain, as well as with misfolded proteins that are then

ubiquitinated and targeted for degradation [49, 82–84]. Several co-factors were found to influence CHIP activity. For instance, the Bag2 Hsp70 co-chaperone was found to interact and inhibit CHIP activity, favoring folding over degradation of the substrate [85, 86]. In contrast, the related Bag1 Hsp70 co-chaperone that contains a proteasomal interacting ubiquitin-like domain promotes CHIP activity and may facilitate substrate delivery to the proteasome [87, 88]. In addition, CHIP auto-ubiquitination on lysine 2, mediated by the E2 conjugating enzyme Ube2W, enhances the E3 ligase activity of CHIP [89]. Preventing this self-ubiquitination results in a reduction of CHIP's ability to ubiquitinate a variety of substrates. The deubiquitinating enzyme Ataxin 3 has been shown to regulate the ability of CHIP to ubiquitinate itself, as well as regulate the polyubiquitin chain lengths of CHIP substrates [90]. CHIP in turn, has been observed to ubiquitinate the polyglutamine expanded form of Ataxin 3, targeting it for degradation [91]. It is still unclear what criterion determines the targeting of such proteins for degradation. Other ubiquitin ligases, like Parkin (for which mutations are linked to Parkinson's disease) and Dorfin have been implicated in the targeting of cytosolic misfolded proteins, although more recent work indicates that Parkin may instead target defective mitochondria for macroautophagy [92–96]. Intriguingly, these ubiquitin ligases are mostly absent in lower eukaryotes like *S. cerevisiae*.

### 1.5.2 Ubr1

Ubr1 was first identified and characterized as being the E3 ligase of the N-end rule, a pathway whereby the half-life of a protein correlates with the identity of the N-terminal amino acid residue that is recognized by the ubiquitin ligase [97]. Ubr1 recognizes N-end rule substrates through two domains: the UBR box (binds Type I (Arg, Lys, or His) basic N-terminal amino acids) and the ClpS domain (binds Type II (Phe, Leu, Trp, Tyr, Ile) bulky hydrophobic residues) [98]. A number of reports however, now lend support to Ubr1 playing a role in protein degradation independent of the N-end rule [99–101]. Subsequently, it was shown that both San1 and Ubr1 are key E3 ligases in the cytosolic quality control machinery (Figure 1.4) [74]. The cytosolic Ubr1, alone or together with the nuclear ubiquitin ligase San1, was found to target a large variety of cytosolic misfolded proteins

including artificial model substrates, thermosensitive mutant alleles and unfolded kinases [74, 101–104]. In some cases, Ubr1 ubiquitinates cytosolic substrates with the assistance of Sse1 and Ssa1 chaperones, while the nuclear localized San1 ubiquitinates substrates that are delivered to it from the cytosol with the help of the Sis1 Hsp40 [48, 75]. Ubr1 is highly conserved with one mammalian homologue known to play a role in protein quality control [105]. Mutations in human Ubr1 are responsible for the autosomal recessive Johanson-Blizzard syndrome characterized by developmental abnormalities and pancreatic insufficiency [106].

### 1.5.3 Hul5 and Rsp5

Exposure to heat shock stress induces a conserved cytoprotective heat shock response that, in addition to transcriptional induction and repression, results in increased protein ubiquitination and degradation of primarily cytosolic proteins [107–109]. The HECT E3 ligases Hul5 and Rsp5 are both required for the increased ubiquitination of cytosolic proteins observed following heat shock (Figure 1.4) [52, 109]. Hul5 is a proteasome associated protein, with chain elongation activity in opposition to the proteasome bound deubiquitinating enzyme Ubp6 [110, 111]. While Hul5 is mainly nuclear in unstressed cells, it relocalizes to the cytoplasm upon heat shock and its cytosolic localization is required for the targeting of cytosolic misfolded proteins for proteasomal degradation [109]. As an E4 ligase, Hul5 promotes the elongation of polyubiquitin chains initiated by other E3 ligases, thereby increasing substrate processivity at the proteasome [110]. Rsp5 is essential for yeast viability and has a role in a number of cellular processes such as endocytosis, RNA export, and lipid biosynthesis [112–114]. Following heat shock, Rsp5 interacts with the Hsp40 chaperone Ydj1 to promote substrate ubiquitination [52]. Rsp5's role in ubiquitinating proteins following heat shock is conserved as the homolog NEDD4 is also required for heat shock induced ubiquitination in higher eukaryotes [52].

### 1.5.4 Ltn1

Nascent polypeptides on stalled ribosomes have been shown to be ubiquitinated and targeted for proteasomal degradation by the E3 ligase Ltn1 (Figure 1.4) [115].

Ltn1 targets non-stop proteins (derived from non-stop mRNA lacking a termination codon) and proteins containing polylysine stretches for ubiquitination and subsequent degradation in yeast, but was shown not to play a role in general cytosolic quality control when tested against the VHL quality control substrate [115]. Stalled 80S ribosomes are dissociated by the ribosome recycling factors Hbs1-Pelota-ABCE1 into 40S small subunits and 60S nascent chain tRNA complexes that facilitate the recognition of the nascent polypeptide by Ltn1 [116]. Exposed tRNA is recognized by Rqc2 (NEMF in mammals) prohibiting 40S reassociation and promoting Ltn1 recruitment [117]. Ltn1 associates with the 60S ribosome and functions as part of a ribosome quality control complex (RQC) comprising Cdc48, the translation-associated element 2 (Tae2), and the protein ribosome quality control 1 (Rqc1) [118, 119]. Ltn1 binds to ribosomal proteins in a way such that its RING domain is oriented towards the exit tunnel [120]. Following ubiquitination by Ltn1, and as a prerequisite for proteasomal degradation, the tRNA-linked polypeptide is dissociated from the 60S ribosome through the activity of the Cdc48-Ufd1-Npl4 complex [121]. Recently, Ltn1 has also been shown to mediate the degradation of translationally stalled ER proteins [122]. This function requires cytosolic exposure of the nascent polypeptide at the ribosome-Sec61 translocation channel junction [117]. Targeting proteins during cotranslational translocation prevents complete translocation into the ER, thereby eliminating the need to retranslocate the protein back into the cytosol and bypassing the ERAD network. Ltn1's structure, determined by single-particle electron microscopy, is similar to the cullin subunit of the cullin-RING ubiquitin ligases, but has significant conformational variability that could be integral for its function [123]. The importance of Ltn1 is underscored by the results of an N-ethyl-N-nitrosourea mutagenesis screen that identified homozygous *lister* mouse mutants that are viable, but display progressive early onset neurodegeneration [124].

## 1.6 Autophagy

Autophagy, the process whereby cytoplasmic components are degraded by the lysosome, is important for recycling amino acids during nutrient starvation and for the clearance of aggregated proteins and damaged organelles, such as mitochondria

and ribosomes. Three types of autophagy have been described, each categorized by the mechanisms required to deliver substrates to the lysosome [125]. Cellular components destined for degradation via macroautophagy are encapsulated through the formation of double membraned autophagosomes that fuse with the lysosome (or vacuole in fungi) delivering their contents to be degraded by enzymes. In microautophagy, the lysosomal membrane is remodeled to capture cellular components bringing them directly into the lysosome in a fashion reminiscent of phagocytosis. Finally, chaperone-mediated autophagy requires the selective import of unfolded proteins into the lysosome through a combination of chaperone mediated substrate targeting and a set of dedicated receptors and translocation machinery. While autophagy was originally viewed as a non-selective process, whereby the lysosome indiscriminately engulfed portions of the cytosol, many studies now demonstrate that macroautophagy can selectively target protein aggregates and organelles for lysosomal degradation. Moreover, the ubiquitin proteasome system and autophagy are interconnected, as a compensatory increase in autophagy is observed when proteasome activity is impaired or inhibited [126]. Under starvation conditions, ribosomes and proteasomes undergo selective lysosomal degradation in a process called ribophagy and proteaphagy, respectively [127–129]. The E3 ubiquitin ligase Ltn1 protects 60S ribosomal subunits from starvation-induced selective ribophagy in a process antagonised by the deubiquitinating enzyme Ubp3 [130]. Similarly, selective mitochondrial degradation, or mitophagy, is important for maintaining mitochondrial integrity and for limiting the production of potentially harmful reactive oxygen species [131]. Parkin, an E3 ligase of the outer mitochondrial membrane, has been associated with mitophagy suggesting that some outer mitochondrial membrane proteins require ubiquitination in order to promote selective macroautophagy [132]. In cases where damaged proteins presumably can no longer be processed by the proteasome, protein aggregates accumulate adjacent to the vacuole, presumably to be cleared by autophagy [125]. Such aggregates colocalize with Atg8, the homolog to the mammalian autophagosome LC3 protein, which acts as a receptor for ubiquitin binding proteins. For instance, p62 and Nbr1 promote the turnover of polyubiquitinated protein aggregates by selectively binding to K63 ubiquitin chains, which are recognized through a ubiquitin binding domain, while also binding to LC3 to shuttle the substrates to autophagosomes [133]. While

it is clear that a level of reciprocity exists between the autophagy and UPS pathways, a greater appreciation of the protein quality control elements will be needed before we can truly understand how substrates are triaged between these two compartments.

## 1.7 Spatial Protein Quality Control: CytoQ, IPOD, and INQ

Protein aggregation has traditionally been viewed as a last resort when protein quality control is exhausted. More recently however, the perception of spatial sequestration of misfolded proteins has changed, and it is now believed to represent an early event in protein quality control and to occur even under physiological conditions. In *S. cerevisiae*, there are three spatially distinct protein quality control compartments that sequester misfolded or aggregated proteins into inclusions within the cell. These are: the cytosolic quality control compartment (CytoQ), the immobile protein deposit (IPOD), and the intranuclear quality control compartment (INQ). These compartments are not unique to yeast as similar cytoplasmic inclusions have been described in mammalian cells [134, 135].

CytoQ inclusions (also referred to as stress foci or Q-bodies) are found throughout the cytosol and require Hsp42 for their formation following heat stress [136, 137]. Hsp42, along with Hsp26 constitute the cytosolic members of the small heat shock family of molecular chaperones and, like all small heat shock proteins, have a conserved alpha-crystallin C-terminal domain [138, 139]. Functional under stress and non-stress conditions, Hsp42 binds to misfolded proteins to prevent protein aggregation. In addition to being a monomer, Hsp42 can also form barrel like oligomeric structures from hexameric rings of dimers if present at high concentrations. Hsp42 is exclusive to CytoQ and is used as a marker for this compartment.

A single IPOD inclusion is found adjacent to the vacuole and formation is independent of stress [135]. This deposit does not co-localize with proteasomes and contains insoluble non-ubiquitinated proteins as well as amyloid proteins [135]. To date, most attention has been paid to the INQ quality control compartment. Originally thought to associate with the nucleus while remaining in the cytosol, the juxtanuclear quality control compartment (JUNQ) has recently been discovered to

reside within the nucleus in close proximity to the nucleolus and has, as a consequence, been renamed the intranuclear quality control compartment (INQ) [77, 135]. Cytosolic proteins require active transport through the nuclear pore complex to reach INQ and substrate targeting and aggregation is mediated by Sis1 in the cytosol and Btn2 within the nucleus [77, 140]. Sis1 alone however, is not sufficient to target proteins for nuclear import suggesting that other factors remain to be discovered [140]. Sis1 levels are relatively high under both physiological and stress conditions, while Btn2 is barely detectable and must be rapidly induced upon heat shock. Even under stress conditions Btn2 is rapidly degraded and inhibiting its degradation stabilizes INQ deposits underscoring its importance in nuclear inclusion formation [77]. Hsp104 is an AAA-ATPase that associates with aggregates to assist with their disassembly [141]. Hsp104 is used as a general aggregation marker and is conserved in fungi and plants but no metazoan homolog has yet been identified. While not essential for viability, Hsp104 is required for induced thermotolerance in yeast [142]. Ubiquitination was once thought to be the sorting signal dictating protein sorting to the INQ compartment [135]. INQ's association with Hsp104 however, suggests instead that sequestration of misfolded proteins occurs prior to, or independently from, the decision to refold or degrade a misfolded substrate.

## 1.8 Stress Responses

Exposure to a range of intrinsic or extrinsic stressors can precipitate protein misfolding overwhelming the proteostasis capacity of the cell. Depending on the nature of the stress, the cell can elicit a number of cellular responses to ensure survival and restore proteostasis. Common to most of these is the induction of molecular chaperones and other factors required to mitigate the stress as well as a decrease in the transcription, translation, and splicing of all other factors not essential to the stress response [143]. While a number of pathways have been described, the most widely studied are the heat shock and general stress responses.

### 1.8.1 Heat Shock and General Stress Response

Exposure to elevated temperatures results in a highly conserved physiological heat shock response, which is characterized by induced expression of genes including members of the heat shock molecular chaperone family. While the heat shock response is cytoprotective, many of the genes induced are not required for surviving the initial stress, but are instead necessary for surviving subsequent stresses, thereby forming acquired stress resistence [144]. Genes are induced through binding of the heat shock transcription factor Hsf1 to heat shock elements in promoter regions [141]. Vertebrates and plants have four Hsf proteins, with the Hsf1 isoform primarily responsible for the heat shock response [145]. In contrast, invertebrates and yeast have a single Hsf1 protein. Low level Hsf1 activity is essential for yeast viability and is required for basal expression of Hsp70 and Hsp90 chaperones [146]. In higher eukaryotes under non-stress conditions, Hsf1 is maintained in an inactive monomeric form in the cytoplasm through an interaction with Hsp90 proteins. Exposure to stress releases Hsf1 resulting in its trimerization, which is required for DNA binding and gene induction [141].

A broad range of environmental stresses such as heat, nutrient starvation, osmotic shock, and oxidation precipitate a transcriptional response in eukaryotes. This general stress response, resulting in the induction of approximately 200 genes, is mediated by the zinc-finger transcription factors Msn2 and Msn4 which bind to stress response elements (STRE) in the promoter regions of target genes (Figure 1.5) [147]. Originally, the heat shock response was considered to be a subset of the general stress response, but a recent report suggests that, in yeast at least, the heat shock response is largely Hsf1 independent and, instead, the heat shock transcriptional response is predominantly driven by Msn2/4 activity [146]. Msn2 and Msn4 are partially redundant transcription factors that share 41% sequence identity at the amino acid level. Neither gene is essential in yeast and they are not conserved from yeast to metazoans [145]. While Msn4 expression is induced by stress, Msn2 is constitutively expressed and is thought to play the dominant role in stress response as overexpression of *MSN4* can only partially suppress the phenotype of the *msn2*$\Delta$ mutant [148]. Msn2 contains an N-terminal transcriptional activating domain (TAD), a nuclear export sequence (NES), a nuclear localization

sequence (NLS), and a C-terminal zinc finger DNA binding domain (DBD) [149]. Structurally, Msn2 is predicted to be intrinsically disordered with the exception of two structured regions in the TAD domain. The sequences of these structured motifs are highly conserved in yeast and mutations result in decreased Msn2 activity and nuclear localization [149]. Msn2 activity is thought to be regulated by two nutrient sensing pathways: protein kinase A (PKA) and target of rapamycin (TOR) [141]. Under non-stress conditions, cAMP dependent PKA phosphorylation negatively regulates Msn2 by phosphorylating the nuclear localization sequence, thereby retaining Msn2 in the cytoplasm [150]. Nuclear exclusion in the absence of stress is also thought to be mediated by an interaction between Msn2 and the 14-3-3 protein homolog Bmh2, which is enhanced by TOR activity [150]. A second PKA consensus site on Msn2 regulates nuclear export, which requires the Msn5 exportin receptor that controls the nuclear localization of many transcription factors (Figure 1.5) [150, 151]. Msn2 is primarily found in the nucleus under certain conditions such as when TOR activity is inhibited, in *msn5*$\Delta$ cells, or when PKA levels decrease [150–152]. Interestingly, Msn2/4 display oscillatory nucleocytoplasmic shuttling under intermediate stress conditions that is regulated by PKA levels in the case of Msn2, but not for Msn4 [153]. How this oscillatory shuttling relates to transcriptional activity remains unknown. Msn2/4 bind to a five base pair (CCCCT or AGGGG) consensus binding site resulting in a transcriptional response that is both transient and scales with the magnitude of the stress [147]. This is in part the product of a linear relationship between induced gene expression and the concentration of nuclear Msn2, which is produced by low Msn2 binding affinity and a limited number of Msn2 molecules relative to the number of STRE binding sites in the genome [154–156]. The combination of environmental sensing pathways regulating Msn2 localization and activity and the linear relationship between Msn2 concentration and target gene expression means that Msn2/4 can mediate a commensurate homeostatic response to a range of extrinsic stresses.

## 1.9 Diseases

Protein homeostasis networks maintain proteome integrity and are essential for cell viability. Perturbations that disrupt the equilibrium of this system can lead

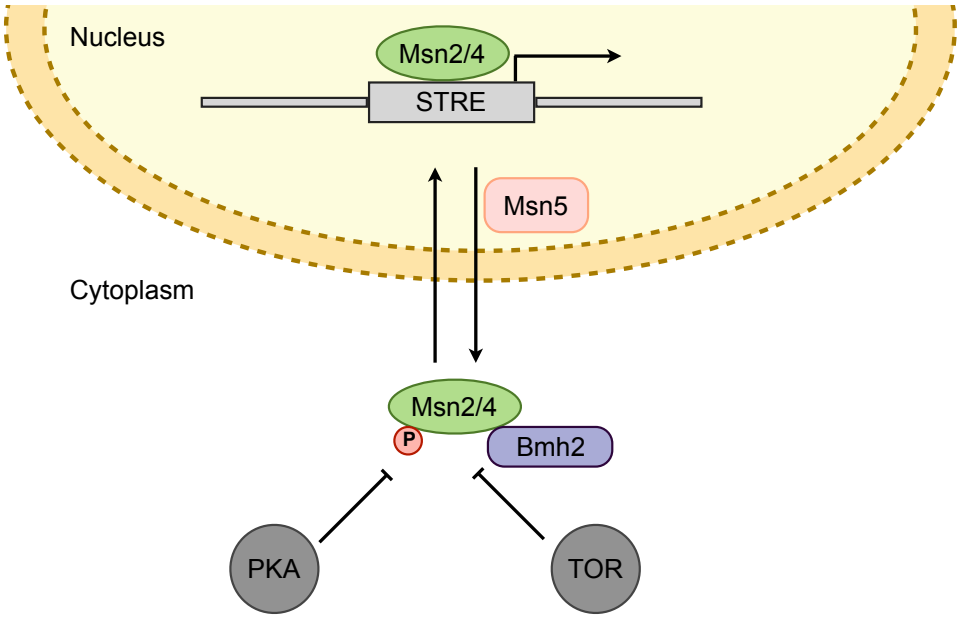


**Figure 1.5:** The general stress response. Under a range of stress conditions the transcription factors Msn2 and Msn4 bind to stress response elements (STREs) in the promoter regions of target genes. Nuclear localization and import is regulated by the PKA and TOR pathways. Nuclear export is mediated by PKA activity and the exportin Msn5.

to a class of diseases known as proteopathies, which range from lysosomal storage diseases to cystic fibrosis and neurodegenerative disorders [157]. Protein misfolding, which can lead to protein aggregation, is characteristic of a number of proteopathies. Moreover, it is thought that an age related decline in the cell's capacity to respond to the presence of misfolded proteins underlies the late onset of neurodegenerative diseases such as Alzheimer's and Parkinson's [12]. The effect of missense mutations on protein stability is of particular interest in the context of disease as missense mutations represent more than half of all mutations in the Human Gene Mutation Database (HGMD) [158]. Sahni and colleagues tested approximately 3000 human disease associated missense alleles and found about one third of the mutations altered protein stability and resulted in an increased engagement with components of the protein homeostasis network [159].

There is currently great interest in the potential for developing therapeutics that target proteostatic imbalance and components of the ubiquitin proteasome system. One such example is Bortezomib, a proteasome inhibitor used to treat relapsed multiple myeloma [160]. The selectivity of proteasome inhibition to kill tumor cells as opposed to normal healthy cells is thought to be attributed to tumor cells being more sensitive to proteasome inhibition due to higher concentrations of abnormal proteins [161]. Recently, selective proteasome inhibition by a compound targeting the kinetoplastid proteasome was shown to clear mice of the parasites responsible for leishmaniasis, sleeping sickness, and Chagas disease, which lead to 50,000 deaths annually and affect more than 20 million people globally [162]. Therapies targeting molecular chaperones are also being developed for the treatment of diseases ranging from cancer to neurodegeneration. For instance, a recombinant human HSP70 therapy was shown to reduce a number of disease associated neurological symptoms in mouse models of lysosomal storage diseases [163]. In addition, the drug Lumacaftor, which acts as a chaperone, was recently approved by the food and drug administration (FDA) to treat patients with the F508Δ mutation in CFTR [164]. Together, these examples highlight the exciting potential targeting protein homeostasis networks have for drug development and clinical applications.

## 1.10 Model Substrates Used to Study Proteostasis

Protein quality control pathways have been identified and characterized using a wide range of model substrates. These substrates are essential components of genetic screens that have been used to probe protein quality control and will continue to be vital if we are to understand what aspects within misfolded proteins are necessary for recognition by molecular chaperones and E3 ubiquitin ligases to target them for degradation. Model substrates used in the study of ER, nuclear, and cytoplasmic protein quality control include: VHL, CPY*, Ura3, Ubc9, and GFP fusions.

VHL is an E3 ligase that acts as a tumor suppressor with mutations leading to a disease of the same name. VHL folding and stability is coupled to its assembly into a complex containing elongin B and C. An absence of the elongin partners, or mutations that disrupt binding, results in VHL being degraded by the

proteasome [165]. Folding defective mutants of VHL were used to examine how different molecular chaperones contribute to the triage decision of whether to fold or degrade misfolded proteins. McClellan and colleagues demonstrated that some chaperones, such as the TRiC chaperonin, were only required for folding, whereas Hsp90 was necessary for VHL degradation, and Hsp70 had a role in both folding and degradation [50].

The vacuolar carboxypeptidase (CPY) encoded by the gene *PRC1*, has been instrumental in the study of ER and cytoplasmic protein quality control. Mutant *prc1-1* (or CPY*) is retained in the ER and targeted for degradation while the wild type protein is located in the vacuole. Genetic screens looking for mutants that are defective in CPY* degradation isolated key factors of the ERAD pathway, including the E3 ligase Hrd1 and E2 conjuating enzymes Ubc6 and Ubc7 [166]. ΔssCPY*, a truncated version of the mutant CPY* protein that has had its signal sequence removed restricting its localization to the cytosol, has been used in the discovery of cytosolic protein quality control pathways [53, 74, 103]. Primarily, ΔssCPY* substrates have been used to delineate the role of Ubr1 and San1 in the degradation of misfolded cytoplasmic proteins [74, 103].

Fused to a model substrate or short peptide, Ura3 is used as a reporter protein in genetic screens to identify protein quality control components. It has been used to screen for mutations in the Type I and II substrate binding sites of Ubr1 and more recently used to generate a new panel of model substrates through fusion with a degron library [98]. Screening this panel of substrates revealed a global requirement for the molecular chaperones Ssa1, 2 and Ydj1 as well as a novel role for Ltn1 in a mechanism distinct from ribosomal quality control [167]. The E3 ligase Doa10 was also identified as the primary ligase required for these substrates.

Ubc9 is essential for yeast viability and is required for cyclin degradation [168]. A temperature sensitive allele of Ubc9 was identified and found to undergo conditional proteasomal degradation [169]. More recently, Ubc9 has been used as a green fluorescent protein (GFP) fusion protein in the study of the INQ and CytoQ pathways [135, 136]. As is the case with Ubc9, the majority of the work presented in this thesis relies upon fusing novel model substrates to GFP to study cytosolic protein quality control. GFP is a 27 kDa protein originally isolated from the jellyfish *Aequorea victoria* that emits green light at a wavelength of 509 nm and can be

used to tag proteins at their N- or C-termini [170]. It forms a cylindrical beta barrel structure consisting of eleven beta strands with a central alpha helix that is covalently bonded to the chromophore. The GFP chromophore is formed through the cyclisation and oxidation of three amino acids (Ser65, Tyr66, and Gly67), which occurs within two to four hours of synthesis [171, 172]. The S65T GFP mutant is more amenable to biological applications as it has a faster maturation time, is more resistant to photobleaching, and its single excitation peak at 490 nm means that it can be used with fluorescein isothiocyanate (FITC) filter sets [173]. The advent of whole proteome GFP tagging collections has meant that it was possible to perform high throughput studies using flow cytometry to identify factors that influence protein stability or abundance and shifted the focus of flow cytometry screens away from single substrates or a small collection of deletion strains. Two methodologies highlight these advances: global protein stability profiling and tandem fluorescent protein timers. Global protein stability (GPS) analysis is a method for analysing protein turnover at the proteome level in mammalian cells [174]. Two fluorescent proteins, an internal control DsRed and an EGFP fusion with a protein of interest, are translated from a single mRNA transcript containing an internal ribosome entry site (IRES). The EGFP/DsRed ratio of a cell represents the stability of the protein of interest as both fluorescent proteins are produced from the same mRNA. Changes to the stability of the GFP fusion protein will therefore be reflected by a change in the EGFP/DsRed ratio. EGFP/DsRed constructs were created for the entire human ORFeome containing approximately 8000 human protein encoding open reading frames (ORFs) and pooled transformed cells are fluorescence activated cell sorted (FACS) into bins based on the GFP/DsRed ratio and then microarray analysis is performed to identify the tagged ORF. This approach was used to successfully identify substrates of the SCF ubiquitin ligase in mammalian cells [175]. The tandem fluorescent protein timer method uses a similar dual fluorescent protein approach, however, in this case, the two proteins are fused and mature with different kinetics. The fluorescence ratio of the two proteins provides a measure of protein age and has been used to identify regulators of the N-end rule pathway in yeast [176].

## 1.11 Research Objective

Protein homeostasis encompasses the network of pathways that influence the fate of proteins from synthesis to degradation for the purpose of maintaining proteome integrity, thereby promoting viability at both the cellular and organism levels. Misfolded proteins challenge the cell's capacity to maintain the proteostatic balance and may divert resources away from essential cellular processes or result in the production of potentially toxic protein aggregates. Consequently, cells have adopted numerous protein quality control pathways to prevent aberrant protein aggregation, promote protein folding, and to target terminally misfolded proteins for degradation. Previous work from the Mayor lab identified a panel of temperature sensitive alleles of essential genes encoding for cytosolic proteins in *S. cerevisiae* that are degraded in a proteasome-dependent manner once shifted to an elevated temperature of 37°C. The protein quality control pathways responsible for the degradation of a number of these alleles, which contain potentially destabilizing missense mutations, are unknown. Recently, there has been renewed interest in the role that missense mutations play in genetic disease as they can induce protein instability which leads to premature and/or increased rates of protein degradation and, as a consequence, loss of function phenotypes. My hypothesis is that a number of quality control pathways, both known and as yet undiscovered, are present within the cytoplasm to aid the cell in the recognition, refolding and/or degradation of proteins destabilized by missense mutations. This thesis is focused on identifying and characterizing cytosolic protein quality control factors that induce proteasome-mediated degradation of thermally unstable model substrates.

### 1.11.1 Specific Aims

1. Develop a flow cytometry based assay to monitor the stability of a GFP-tagged substrate.
2. Use genetic screens to identify protein quality control factors that promote proteasomal degradation of a model substrate.
3. Perform in depth characterization of the factors identified in Aim2.

This work was performed using the model organism *Saccharomyces cerevisiae* with a combination of cell biology, biochemical, and genetic approaches.

# Chapter 2

# Prefoldin Promotes Proteasomal Degradation of Cytosolic Proteins with Missense Mutations by Maintaining Substrate Solubility

## 2.1 Introduction

The protein homeostasis network encompasses systems required by the cell to generate and maintain the correct levels, conformational state, and distribution of its proteome [1]. Misfolded proteins threaten this balance by triggering loss of function phenotypes, diverting resources away from producing essential protein products, or precipitating the production of potentially toxic protein aggregates [4]. The presence of protein aggregates is characteristic of a number of neurodegenerative diseases such as Parkinson's and Alzheimer's disease, and a decrease in the protein homeostasis capacity of the cell is thought to underlie the later stages of cellular ageing [11, 12, 177]. It is, therefore, not surprising that the cell has evolved a number of protein quality control pathways aimed at preventing protein aggregation, promoting protein folding, and targeting terminally misfolded proteins for degradation [178–180]. These pathways triage misfolded proteins, which will face three

main possible fates: to be refolded back to their functional native conformation; to be targeted for degradation; or to be sequestered into spatially distinct quality control compartments.

Proteins are selectively targeted to the eukaryotic ubiquitin proteasome system by the covalent attachment of polyubiquitin chains catalyzed by a cascade of E1 (ubiquitin-activating), E2 (ubiquitin-conjugating), and E3 (ubiquitin ligase) enzymes [62, 181]. Substrate recruitment and specificity is determined by the E3 ubiquitin ligases, either alone or in concert with an E2 conjugating enzyme or other substrate adaptors. A number of subcellular compartment-specific quality control pathways have been identified, each associated with a particular E3 ligase or set of ligases [63, 70, 178]. In yeast, the San1 ligase is responsible for ubiquitinating nuclear misfolded proteins [70]. Experiments have shown that San1 binds misfolded proteins through recognition sequences located in disordered regions of its N- and C-terminal domains [72]. In contrast to the nucleus, a number of ligases have been identified to target cytosolic proteins for degradation in yeast. While initially characterized for its role as the recognin of the N-end rule pathway, Ubr1 has also been shown to target misfolded cytoplasmic proteins for degradation [74, 76, 102–104]. It does so either alone, or in conjunction with other E3 ligases such as Ubr2 in the case of newly synthesized kinases, or with the nuclear San1 where both are required for the complete degradation of the engineered ΔssCPY*-GFP substrate [74, 104]. Hul5, a nuclear protein that relocalizes to the cytoplasm upon heat shock, and Rsp5 have been identified as the two ligases responsible for the marked increase in cytoplasmic protein ubiquitination following heat shock stress [52, 182]. Finally, the ribosome associated ligase Ltn1 targets non-stop polypeptides stalled during translation for degradation [115].

Recently, the importance of spatial organization in protein quality control has gained recognition. Under normal physiological conditions, misfolded proteins can be concentrated into dynamic Q-bodies where they can be refolded by chaperones or degraded [136]. However, if the protein quality control systems become overwhelmed, misfolded proteins can be sequestered into discrete cellular inclusions. The INQ compartment acts to concentrate detergent soluble misfolded proteins capable of being refolded, or degraded, and contains 26S proteasomes and chaperones such as the disaggregase Hsp104 [77, 135]. The IPOD by contrast contains

insoluble non-ubiquitinated proteins; does not co-localize with proteasomes; and is the site of amyloidogenic protein sequestration, perhaps to prevent their toxic interaction with quality control machinery [135]. The IPOD is also postulated to be the site of yeast prion maturation [183].

In this study we performed a screen to identify factors involved in degradative protein quality control of a model substrate that misfolds as the result of destabilizing missense mutations. We show that our model substrate is thermally unstable, undergoes proteasome mediated degradation, and forms Q-body like inclusions. We then identified and characterized the prefoldin chaperone subunit Gim3 as a factor important for maintaining our substrate protein's solubility, and thereby facilitating its degradation.

## 2.2 Materials and Methods

### 2.2.1 Yeast Strains, Plasmids, and Media

All yeast deletion strains used in this study are derived from BY4741 or BY4742 wild type (WT) strains and are listed in Table 2.1. The temperature sensitive alleles were generously provided by Dr. P. Hieter. The Cup1-Deg1-GFP plasmid was a gift from T. Sommer [184]. The Hsp104-mCherry and Hsp42-mCherry strains were constructed by homologous recombination of a PCR product amplified from a plasmid containing a yeast codon optimized mCherry ORF (BPM 866). Guk1 and Guk1-7 GFP-tagged fusion plasmids (BPM 453, BPM 458) were constructed by inserting ORFs amplified from genomic DNA, with primers containing BamHI and XbaI restriction enzyme recognition sequences, into PGPD-GFP(S65T) (BPM 241). Ugp1-3 (BPM 457), Pro3-1 (BPM 507), and Gus1-3 (BPM 500) GFP tagged plasmids were produced in the same fashion using: BamHI and NotI; BamHI and NotI; and NotI and XbaI, respectively. The histidine tagged fusions were produced by cloning PCR amplified inserts into PGPD (BPM 171) using BamHI and SalI (BPM 659, BPM 717). All plasmids used in this study are listed in Table 2.2. Cells were grown in synthetic drop out media following standard procedures.

**Table 2.1:** Yeast strains used in Chapter 2

| Strain ID | Alias | Genotype | Source |
|---|---|---|---|
| YTM 408 | BY4741 | *ura3Δ0, leu2Δ0, his3Δ1, met15Δ0* | Open Biosystems Collection |
| YTM 703 | *ubr1Δsan1Δ* | *his3Δ1, leu2Δ0, met15Δ0, ura3Δ0, san1Δ::His3MX6, ubr1Δ::KanMX* | Khosrow-Khavar *et al.* 2012 |
| YTM 736 | Guk1-7-13myc | *his3Δ1, leu2Δ0, LYS2, met15Δ0, ura3Δ0, guk1-7-13myc::KanMX6::URA3, CAN1* | Khosrow-Khavar *et al.* 2012 |
| YTM 749 | Gus1-3 | *ura3Δ0, leu2Δ0, his3Δ1, LYS, MET, can1Δ::Leu2-MFA1pr::His3, Gus1-3::Ura* | P. Hieter |
| YTM 755 | Pro3-1 | *ura3Δ0, leu2Δ0, his3Δ1, LYS, MET, can1Δ::Leu2-MFA1pr::His3, Pro3-1::Ura* | P. Hieter |
| YTM 758 | Guk1-7 | *ura3Δ0, leu2Δ0, his3Δ1, LYS, MET, can1Δ::Leu2-MFA1pr::His3, Guk1-7::Ura* | P. Hieter |
| YTM 766 | Ugp1-3 | *ura3Δ0, leu2Δ0, his3Δ1, LYS, MET, can1Δ::Leu2-MFA1pr::His3, Ugp1-3::Ura* | P. Hieter |
| YTM 938 | *san1Δ* | *his3Δ1, leu2Δ0, met15Δ0, ura3Δ0, san1Δ::KanMX* | Open Biosystems Collection |
| YTM 981 | *ubr1Δ* | *his3Δ1, leu2Δ0, met15Δ0, ura3Δ0, ubr1Δ::KanMX* | Open Biosystems Collection |
| YTM 1183 | *tda2Δ* | *his3Δ1, leu2Δ0, met15Δ0, ura3Δ0, tda2Δ::KanMX* | Open Biosystems Collection |
| YTM 1184 | *yak1Δ* | *his3Δ1, leu2Δ0, met15Δ0, ura3Δ0, yak1Δ::KanMX* | Open Biosystems Collection |

*Continued on next page*

| Strain ID | Alias | Genotype | Source |
|---|---|---|---|
| YTM 1185 | *rim15*Δ | *his3*Δ*1, leu2*Δ*0, met15*Δ*0, ura3*Δ*0, rim15*Δ*::KanMX* | Open Biosystems Collection |
| YTM 1186 | *gim3*Δ | *his3*Δ*1, leu2*Δ*0, met15*Δ*0, ura3*Δ*0, gim3*Δ*::KanMX* | Open Biosystems Collection |
| YTM 1187 | *YOR364W*Δ | *his3*Δ*1, leu2*Δ*0, met15*Δ*0, ura3*Δ*0, YOR364W*Δ*::KanMX* | Open Biosystems Collection |
| YTM 1290 | *vhr1*Δ | *his3*Δ*1, leu2*Δ*0, met15*Δ*0, ura3*Δ*0, vhr1*Δ*::KanMX* | Open Biosystems Collection |
| YTM 1293 | *sli15*Δ | *his3*Δ*1, leu2*Δ*0, met15*Δ*0, ura3*Δ*0, sli15*Δ*::KanMX* | Open Biosystems Collection |
| YTM 1294 | *fau1*Δ | *his3*Δ*1, leu2*Δ*0, met15*Δ*0, ura3*Δ*0, fau1*Δ*::KanMX* | Open Biosystems Collection |
| YTM 1301 | *gim5*Δ | *his3*Δ*1, leu2*Δ*0, met15*Δ*0, ura3*Δ*0, gim5*Δ*::KanMX* | Open Biosystems Collection |
| YTM 1302 | *gim6*Δ | *his3*Δ*1, leu2*Δ*0, met15*Δ*0, ura3*Δ*0, gim6*Δ*::KanMX* | Open Biosystems Collection |
| YTM 1304 | *gim1*Δ | *his3*Δ*1, leu2*Δ*0, met15*Δ*0, ura3*Δ*0, gim1*Δ*::KanMX* | Open Biosystems Collection |
| YTM 1305 | *gim4*Δ | *his3*Δ*1, leu2*Δ*0, met15*Δ*0, ura3*Δ*0, gim4*Δ*::KanMX* | Open Biosystems Collection |
| YTM 1306 | *gim2*Δ | *his3*Δ*1, leu2*Δ*0, met15*Δ*0, ura3*Δ*0, gim2*Δ*::KanMX* | Open Biosystems Collection |
| YTM 1356 | *rpt6-20* | *his3*Δ*1, leu2*Δ*0, met15*Δ*0, ura3*Δ*0, RPT6::rpt6-20::KanMX* | Boone ts collection |

*Continued on next page*

| Strain ID | Alias | Genotype | Source |
|---|---|---|---|
| YTM 1357 | *pep4Δprb1Δ* | *his3Δ1, leu2Δ0, met15Δ0, ura3Δ0, lys2Δ0, PRB1::KanMX6, PEP4::His3MX6* | Fang *et al.* 2015 |
| YTM 1489 | Gim3-TAP | *his3Δ1, leu2Δ0, met15Δ0, ura3Δ0, gim3::TAP::His3MX* | Open Biosystems Collection |
| YTM 1677 | *tcp1-1* | *his3Δ1, leu2Δ0, met15Δ0, ura3Δ0, TCP1::tcp1-1-KanMAX6* | P. Hieter |
| YTM 1678 | *tcp4-1* | *his3Δ1, leu2Δ0, met15Δ0, ura3Δ0, CCT4::cct4-1-KanMAX6* | P. Hieter |
| YTM 1692 | *bra7Δ* | *his3Δ1, leu2Δ0, met15Δ0, ura3Δ0, bra7Δ::KanMX* | Open Biosystems Collection |
| YTM 1693 | *asp1Δ* | *his3Δ1, leu2Δ0, met15Δ0, ura3Δ0, asp1Δ::KanMX* | Open Biosystems Collection |
| YTM 1694 | *mal11Δ* | *his3Δ1, leu2Δ0, met15Δ0, ura3Δ0, mal11Δ::KanMX* | Open Biosystems Collection |
| YTM 1695 | *mup3Δ* | *his3Δ1, leu2Δ0, met15Δ0, ura3Δ0, mup3Δ::KanMX* | Open Biosystems Collection |
| YTM 1696 | *pol4Δ* | *his3Δ1, leu2Δ0, met15Δ0, ura3Δ0, pol4Δ::KanMX* | Open Biosystems Collection |
| YTM 1697 | *pph22Δ* | *his3Δ1, leu2Δ0, met15Δ0, ura3Δ0, pph22Δ::KanMX* | Open Biosystems Collection |
| YTM 1855 | *ubr1Δgim3Δ* | *his3Δ1, leu2Δ0, met15Δ0, ura3Δ0, ubr1Δ::KanMX, gim3Δ::His3MX6* | This thesis |
| YTM 1901 | Hsp104-mCherry | *his3Δ1, leu2Δ0, met15Δ0, ura3Δ0, Hsp104-mCherry::His3MX6* | This thesis |
| YTM 1902 | Guk1-7-13myc | *gim3Δ, his3Δ1, leu2Δ0, LYS, MET15, Guk1-7-13myc::KanMX6::Ura3, CAN1, gim3Δ::His3MX6* | This thesis |
| YTM 1919 | Hsp42-mCherry | *his3Δ1, leu2Δ0, lys2Δ0, ura3Δ0, Hsp42-mCherry::KanMX6* | This thesis |

**Table 2.2:** Plasmids used in Chapter 2

| Plasmid ID | Name | Auxo-trophic Marker | Plasmid Type | Source |
|---|---|---|---|---|
| BPM 42 | pRS316 | Ura | CEN/ARS | RJD Collection |
| BPM 45 | pRS313 | His | CEN/ARS | RJD Collection |
| BPM 171 | $P_{GPD}$ | His | CEN/ARS | F. Khosrow-Khavar |
| BPM 241 | $P_{GPD}$-GFP(S65T) | His | CEN/ARS | F. Khosrow-Khavar |
| BPM 368 | $P_{Ubr1}$-Ubr1 | Leu | CEN/ARS | R. Hampton |
| BPM 369 | $P_{Ubr1}$-Ubr1(C1220S) | Leu | CEN/ARS | R. Hampton |
| BPM 453 | $P_{GPD}$-Guk1-GFP | His | CEN/ARS | This thesis |
| BPM 457 | $P_{GPD}$-Ugp1-3-GFP | His | CEN/ARS | This thesis |
| BPM 458 | $P_{GPD}$-Guk1-7-GFP | His | CEN/ARS | This thesis |
| BPM 500 | $P_{GPD}$-Gus1-3-GFP | His | CEN/ARS | This thesis |
| BPM 507 | $P_{GPD}$-Pro3-1-GFP | His | CEN/ARS | This thesis |
| BPM 509 | $P_{GPD}$-Guk1(E127K)-GFP | His | CEN/ARS | This thesis |
| BPM 510 | $P_{GPD}$-Guk1(T95A)-GFP | His | CEN/ARS | This thesis |
| BPM 511 | $P_{GPD}$-Guk1(F59H)-GFP | His | CEN/ARS | This thesis |
| BPM 513 | $P_{GPD}$-Guk1(A84T)-GFP | His | CEN/ARS | This thesis |
| BPM 551 | $P_{GPD}$-Gim3 | Ura | CEN/ARS | This thesis |
| BPM 572 | $P_{Ubr1}$-Ubr1 | Ura | CEN/ARS | This thesis |
| BPM 659 | $P_{GPD}$-Guk1::His6 | His | CEN/ARS | This thesis |
| BPM 708 | $P_{Cup1}$-Deg1-cNLS-GFP | Ura | CEN/ARS | T. Sommer |
| BPM 717 | $P_{GPD}$-Guk1-7::His6 | His | CEN/ARS | This thesis |
| BPM 779 | $P_{GPD}$-GFP | Ura | CEN/ARS | This thesis |
| BPM 780 | $P_{GPD}$-Guk1-GFP | Ura | CEN/ARS | This thesis |
| BPM 781 | $P_{GPD}$-Guk1-7-GFP | Ura | CEN/ARS | This thesis |
| BPM 866 | pFA6a-mCherry-KanMX6 | KanMX | CEN/ARS | This thesis |
| BPM 894 | $P_{Guk1}$-Guk1-GFP | His | CEN/ARS | This thesis |
| BPM 895 | $P_{Guk1}$-Guk1-7-GFP | His | CEN/ARS | This thesis |

### 2.2.2 Stability Effect of Guk1-7 Mutations

The predicted thermodynamic stability changes of mutations in Guk1-7 were computed using FoldX (version 3.0). The protein structure of Guk1 was downloaded from the Protein Data Bank (PDB accession 1EX7) and was optimized using the repair function of FoldX. Structures corresponding to each of the single point mutations and all four point mutants combined were generated. The predicted effect of mutations on protein structural stability was expressed as the predicted free energy change ($\Delta\Delta G$) and was obtained by subtracting the energy values of the mutant structures from that of the wild type.

### 2.2.3 Cellular Thermal Shift Assay (CETSA)

A 50 mL yeast culture grown at 25°C was collected at log phase and harvested by centrifugation. Cells were then lysed with glass beads in 200 $\mu$L of native lysis buffer (20 mM HEPES, pH 7.5, 0.5% NP-40, 200 mM NaCl, 1X protease inhibitor mix (Roche), 1 mM 1,10 phenanthroline, 1 mM EDTA). The soluble fraction was collected by centrifugation (16,000 g, 10 min, 4°C) and protein concentration was determined by the DC Protein Assay (BioRad). Samples were normalized to 2 $\mu$g/$\mu$L and 50 $\mu$L aliquots were distributed into PCR strip tubes and run on a PCR machine with the following program: 25°C, 3:00; Gradient 30–50°C, 10:00; 25°C, 1:00. The soluble fraction was once again collected by centrifugation (16,000 g, 10 min, 4°C). Equal volumes were resolved by SDS-PAGE. Membranes were immunoblotted with mouse anti-HIS6 (Ablab, 1:2,500) and secondary antibodies (Mandel Scientific, 1:10,000) and then quantified using an Odyssey Infrared Imaging System.

### 2.2.4 Solubility Assay

Yeast cells were grown to log phase at 25°C and then incubated for 20 min at either 25°C or 37°C. Cells were lysed with glass beads in native lysis buffer (20 mM HEPES, pH 7.5, 0.5% NP-40, 200 mM NaCl, 1X protease inhibitor mix, 1 mM 1,10 phenanthroline, 1 mM EDTA) and then precleared by centrifugation at 2,000 g for 5 min at 4°C. Sample protein concentrations were measured by the DC Protein Assay (BioRad) and normalized. Samples were further fractionated into

soluble and pellet fractions by centrifugation at 16,000 g for 10 min at 4°C. The pellet fractions were then washed twice with lysis buffer. Equal volumes of total cell lysate, soluble, and pellet fractions were resolved by SDS-PAGE. Samples were analyzed by mouse anti-GFP (Roche, 1:2,500) and rabbit anti-Pgk1 antibodies (Acris Antibodies, 1:10,000) as a loading control.

### 2.2.5 Microscopy

Cells were grown in synthetic dropout media lacking histidine to log phase (OD600 = 0.8–1.0) at 25°C and then collected at the indicated time points following incubation at 25°C or 37°C with our without 100 $\mu$g/mL cycloheximide (CHX), as noted. Samples were fixed in 3.7% formaldehyde for 15 minutes at room temperature and then rinsed in 0.1 M potassium phosphate containing 1 M sorbitol before being permeabilized with 0.1% Triton X-100 for ten minutes. Nuclei staining was performed by incubating permeabilized cells in Hoechst 33342 (25 $\mu$g/mL) for 10 minutes before mounting cells on slides in mounting media (2% N-Propylgallate, 80% glycerol, 0.02% sodium azide in 1X PBS). Cells were imaged with a Zeiss Axio observer inverted microscope equipped with a 63x oil-immersion objective and a digital camera. Images were analyzed with Zeiss Axiovision software.

### 2.2.6 Degradation Assay

Cells were grown to log phase in synthetic drop out media at 25°C and cycloheximide was added to a final concentration of 100 $\mu$g/mL. Cells were then incubated at either 25°C or 37°C, and at the indicated time points cells were collected by centrifugation. The cells were then resuspended in modified Laemmli buffer (50 mM Tris-HCl, pH 6.8, 2% SDS, 10% glycerol), and lysed with glass beads. Protein concentration was assessed by the DC Protein Assay (BioRad). Equal amounts of protein were resolved by SDS-PAGE following the addition of 10X 2-mercaptoethanol (20%) and dye to each sample. Immunoblots were performed with a mouse anti-GFP primary antibody (Millipore, 1:2,500) and a rabbit anti-Pgk1 (1:10,000, Acris Antibodies) as a loading control. Infrared secondary antibodies were used (Mandel Scientific, 1:10,000) and membranes were scanned and analyzed with an Odyssey Infrared imaging system (LI-COR).

### 2.2.7 Flow Cytometry

Yeast cells were grown in synthetic drop out media to log phase before the addition of 100 $\mu$g/mL cycloheximide and incubated at 25°C or 37°C as indicated. Samples were run on a BD FACSCalibur instrument (BD Biosciences) with a 488 laser and GPF was detected with a 530/30 filter. 50,000 events were collected. Analysis was performed with FlowJo (FlowJo Data Analysis Software, LLC). For multi-hour CHX chase experiments median GFP fluorescence values were normalized to that of the first time point. FACS sorting was performed with a BD Influx instrument by the UBC Flow facility.

### 2.2.8 GFP Pulldown

Gim3-TAP yeast cells transformed with a control empty vector (BPM 42), PGPD-GFP (BPM 779), PGPD-Guk1-GFP (BPM 780), or PGPD-Guk1-7-GFP (BPM 781) were grown to log phase and then lysed with glass beads and native lysis buffer (20 mM HEPES, pH 7.5, 0.5% NP-40, 200 mM NaCl, 1X protease inhibitor mix, 1 mM 1,10 phenanthroline, 1 mM EDTA, 10 mM iodoacetamide). To pull-down GFP-tagged proteins, lysates were incubated for 2 hours at 4°C with 20 $\mu$L GFP-Trap coupled agarose beads (Chromotek). Beads were washed three times in lysis buffer before samples were eluted with 3X SDS sample buffer. Nitrocellulose membranes were probed with mouse anti-GFP (Roche, 1:2,500), rabbit anti-Pgk1 (Acris Antibodies, 1:10,000), rabbit anti-TAP (Fisher, 1:2,500), and mouse anti-ubiquitin (Millipore, 1:2,500) primary antibodies.

### 2.2.9 Proteasome Function

Yeast cultures were grown to saturation in synthetic drop out media overnight at 30°C and then diluted to OD600 = 0.2 and left to grow for 3 hours at 30°C. 100 $\mu$M copper sulphate was added to the culture and incubated at 30°C for 4 hours. An initial sample was removed and then cycloheximide was added to the culture to a final concentration of 100 $\mu$g/mL. Samples were collected at the indicated time points. Cells were lysed with glass beads and lysis buffer (1% Tx-100, 0.1% SDS, 150 mM NaCl, 5 mM EDTA, 50 mM Tris-HCl, pH 7.5, 1 mM PMSF, 1X protease inhibitor mix). Protein concentrations were assessed using the DC Protein Assay

(BioRad) and equal amounts were resolved by SDS-PAGE.

### 2.2.10 Statistical Analysis

Unpaired two tailed Student's t-tests were used to assess significance of differences between wild type and *gim3*Δ or *ubr1*Δ strains. One-way ANOVA with post-hoc Tukey HSD (honest significant difference) was used to assess significance of differences between multiple deletion strains.

## 2.3 Results

### 2.3.1 Guk1-7 is Thermally Unstable

Our lab previously identified a panel of temperature sensitive alleles of essential genes encoding for cytosolic proteins in *Saccharomyces cerevisiae* [101]. A large fraction of mutant proteins underwent proteasome-mediated degradation when incubated at the restrictive temperature of 37°C, whereas the wild type proteins were stable. While approximately one third of the unstable alleles were found to be substrates of the E3 ubiquitin ligase Ubr1 [101], the protein quality control pathways responsible for the proteasomal degradation of the remaining mutant proteins are unknown. To screen for other proteins involved in proteasome mediated degradation of thermosensitive mutant proteins, we sought to establish an assay based on fluorescence intensity to facilitate the quantification of a model quality control substrate fused to GFP. For this study, we selected the Guk1-7 allele that contains four missense mutations generated by random PCR-based mutagenesis [101, 185, 186]. Guk1 is a member of the nucleoside monophosphate kinase (NMP) family and converts GMP to GDP [187]. Similar to other members of the NMP family, Guk1's structure contains a core, a lid, and a dynamic NMP-binding domain [188]. Mutants of Guk1 are defective in mannose chain elongation, have higher cell wall porosity, and are hypersensitive to larger molecular weight antibiotics [189]. We first predicted the structural stability effects of the missense mutations found in Guk1-7 using FoldX (Figure 2.1A) [190]. The predicted free energy changes ($\Delta\Delta G$) between the single point mutants and the wild type protein were modest, whereas the combined effect of all the mutations found in Guk1-7

was much larger (∼7 kcal/mol). While this value is higher than that predicted for missense mutations in transmembrane domains of disease-associated proteins such as cystic fibrosis transmembrane conductance regulator (CFTR) and rhodopsin (1.5 and 1.9 kcal/mol, respectively), it is in line with those predicted for mutations in phenylalanine hydroxylase (PAH) associated with mild or severe forms of phenylketonuria (5.7 and 14.2 kcal/mol, respectively) [191, 192]. We then compared the thermodynamic stability of ectopically expressed wild type Guk1 with Guk1-7 in cellular lysates by a cellular thermal shift assay (CETSA) [193]. In agreement with its predicted lower stability, Guk1-7 was less stable than the wild type Guk1 at incubation temperatures above 38°C (Figure 2.1B). We further examined the solubility of Guk1 and Guk1-7 proteins in cells incubated at the normal growth temperature of 25°C and following a short 20 minute incubation at 37°C. Guk1 was found predominantly in the soluble form while Guk1-7 was enriched in the NP-40 insoluble fraction at 25°C and 37°C (Figure 2.1C). Together these data suggest that Guk1-7 is much less stable than the wild type protein and misfolds forming NP-40 insoluble aggregates.

### 2.3.2 Fluorescence-Based Assay to Assess Protein Stability

To determine whether the ectopically expressed mutant protein was also degraded when fused to GFP, we first examined fluorescence levels by microscopy. Guk1-7-GFP fluorescence was on average 58% lower than that of Guk1-GFP at 25°C (n = 101, 108), and was nearly undetectable with an average 87% loss of fluorescence following a two hour incubation at 37°C in the presence of the translation inhibitor cycloheximide (n = 168) (Figure 2.2A, Figure 2.12A). By contrast, the fluorescence of the wild type Guk1-GFP only slightly decreased by 29% between 37°C and 25°C (n = 120). To verify that the loss of fluorescence was due to proteolysis and not misfolding of GFP, we examined levels of Guk1 and Guk1-7 by Western blot in a cycloheximide chase assay. While Guk1-GFP levels remained relatively unchanged, the level of Guk1-7-GFP decreased by 30% after a four hour incubation at 25°C, and decreased by 70% after the same period at 37°C (Figure 2.2B). We then verified whether adding a GFP tag alters Guk1 or Guk1-7 solubility. Three times as much Guk1-7 as Guk1 was found in the NP-40 insoluble

pellet fraction at 25°C, and this rose to nine times more upon the short incubation at 37°C (Figure 2.2C). Although Guk1-7-GFP is less insoluble than Guk1-7-His6, presumably due to stabilization conferred by the GFP moiety, the GFP tagged mutant was both less soluble and more degraded than the wild type protein, and could therefore be employed as a model substrate.

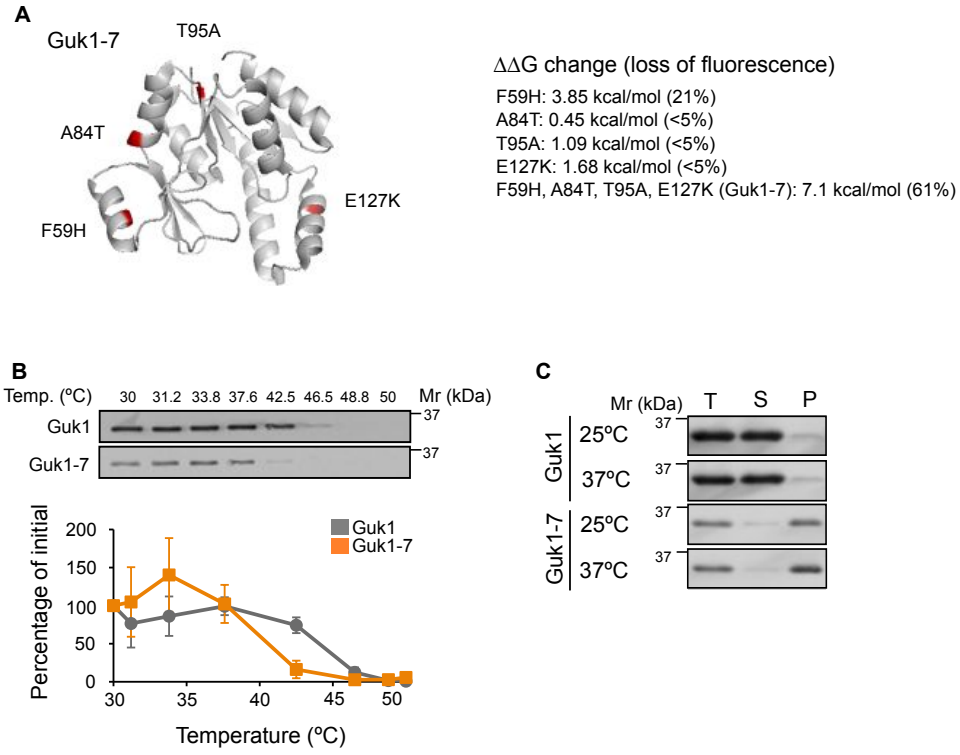


**Figure 2.1:** Guk1-7 is thermally unstable. (A) Ribbon structure of Guk1 (PDB 1EX7). Positions of the four missense mutations and predicted $\Delta\Delta G$ values are indicated. Loss of fluorescence measured by flow cytometry after a two hour incubation at 37°C with cycloheximide is indicated in brackets. (B) Cellular thermal shift assay of Guk1 and Guk1-7 fused to a six histidine tag in lysates derived from cells grown at 25°C. One representative anti-His Western Blot is shown. The graph represents the means and standard deviations of Guk1 levels from three independent experiments. (C) Guk1 and Guk1-7 fused to a six histidine tag were expressed in cells grown at 25°C or shifted to 37°C for 20 min. Total cell lysate (T), soluble (S), and pellet fractions (P) were immunoblotted with anti-His antibodies.

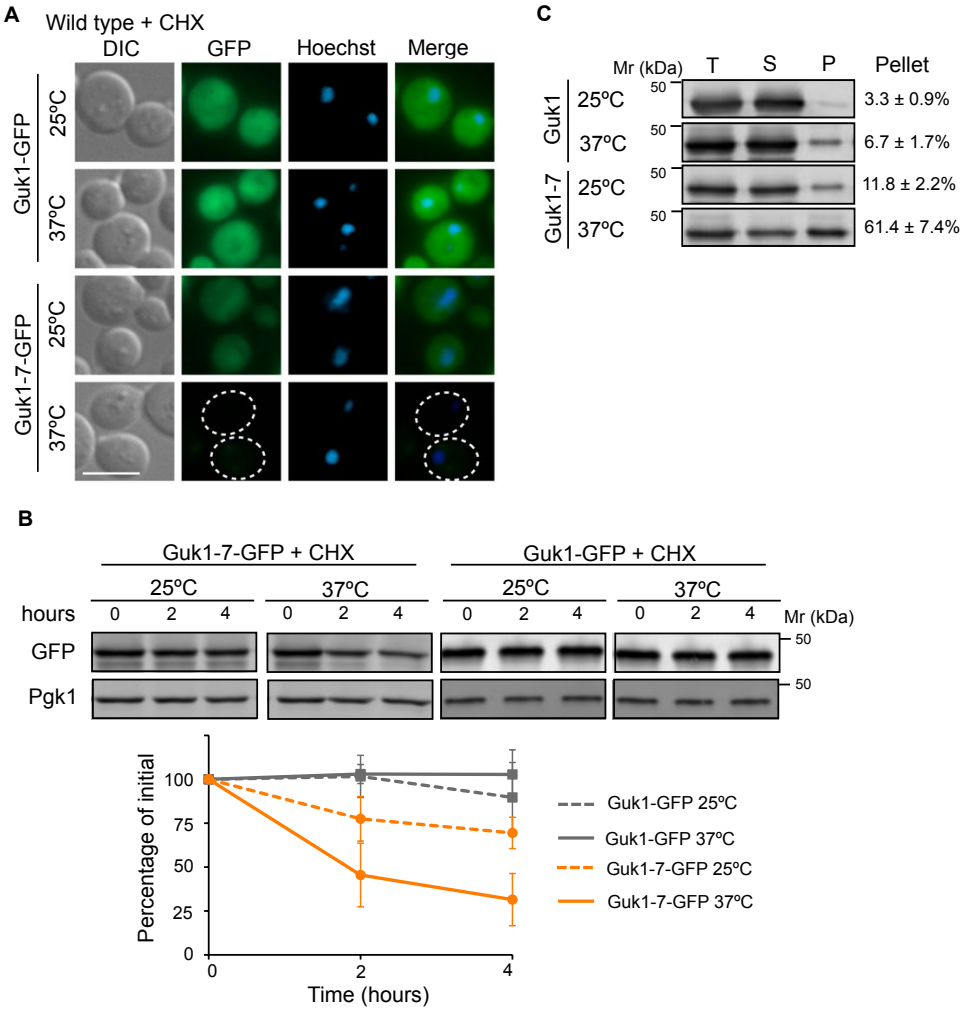


**Figure 2.2:** Misfolded Guk1-7 is degraded at the non-permissive temperature.

**Figure 2.2:** (Previous page) Misfolded Guk1-7 is degraded at the non-permissive temperature. (A) Wild type cells expressing ectopic Guk1-GFP or Guk1-7-GFP were grown at 25°C and then incubated in the presence of the translation inhibitor cycloheximide (CHX) at 25°C or 37°C for 2 hours prior to fixation and imaging. Scale bar represents 5 $\mu$m. (B) Cycloheximide chase assay. Wild type cells expressing ectopic Guk1-GFP or Guk1-7-GFP were incubated with CHX for 4 hours at 25°C or 37°C and samples were collected at the indicated time points. Guk1-GFP and Guk1-7-GFP was immunoblotted with anti-GFP antibodies and a representative blot is shown. GFP levels were normalized to Pgk1 levels and shown in the graph below with results representing the means and standard deviations of three independent experiments. (C) Guk1-GFP and Guk1-7-GFP were ectopically expressed in wild type cells grown at 25°C or shifted to 37°C for 20 min. Total cell lysate (T), soluble (S), and pellet fractions (P) were immunoblotted with anti-GFP antibodies. The ratio of the pellet fraction to total cell lysate is noted and represents the mean and standard deviation of three independent experiments.

In order to use Guk1-7-GFP as a model substrate to screen for factors important in maintaining cytosolic protein homeostasis, we established a flow cytometry assay to monitor protein stability. Cultures were incubated at 25°C or 37°C in the presence of cycloheximide for two hours and then the GFP fluorescence intensity from single cells was measured by flow cytometry. The relative difference in median intensity values between 37°C and 25°C was used as a measure of protein stability. In a wild type strain at 25°C Guk1-7-GFP fluorescence intensity is lower than that of the wild type allele, suggesting that the model substrate is inherently unstable even at lower temperatures. After shifting the cells to 37°C in the presence of CHX for two hours, GFP intensity levels remained nearly constant for Guk1-GFP (5% loss) but decreased for Guk1-7-GFP (60% loss; Figure 2.3A). These data are consistent with our previous fluorescence microscopy and CHX-chase observations (Figure 2.2A, 2.2B). The data obtained from flow cytometry measurements was comparable to that acquired using traditional Western blotting techniques (Figure 2.3B).

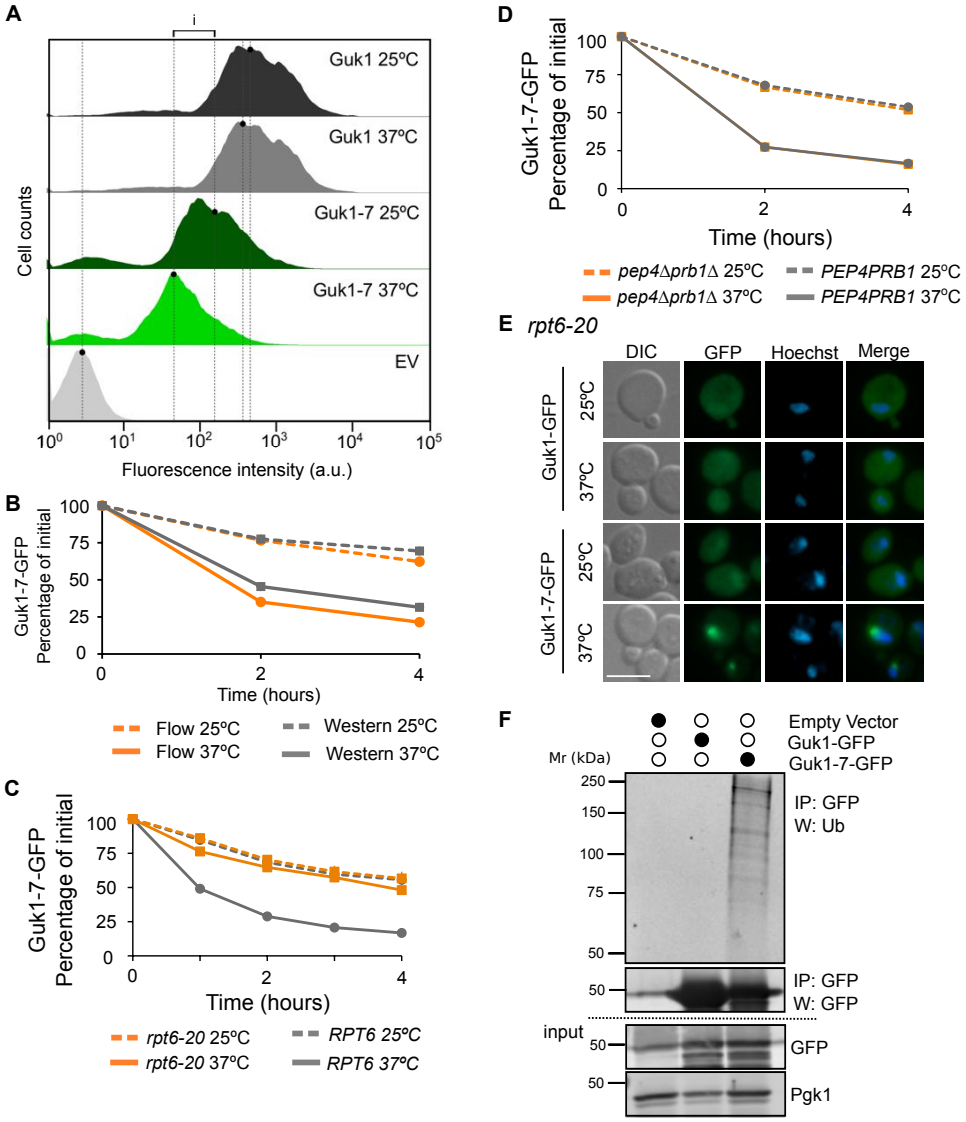


**Figure 2.3:** Guk1-7 degradation is proteasome dependent.

**Figure 2.3:** (Previous page) Guk1-7 degradation is proteasome dependent. (A) Flow cytometry profiles of wild type cells expressing Guk1-GFP or Guk1-7-GFP were incubated at 25°C or 37°C for two hours in the presence of CHX. Fluorescence in cells with the control empty vector (EV) are also shown. Lines demark median GFP fluorescence values and i denotes the difference in median intensity values used to measure protein stability. (B) Comparison of quantitation of Guk1-7 levels in a CHX chase assay by Western blot or flow cytometry. (C) Wild type and *rpt6-20* cells expressing Guk1-7-GFP were incubated with CHX at 25°C or 37°C and samples were analysed by flow cytometry at the indicated time points. The results represent the means and standard deviations of three independent experiments. (D) Guk1-7-GFP expressing wild type or pep4Δprb1Δ cells were incubated at 25°C or 37°C in the presence of CHX and samples were analyzed by flow cytometry at the indicated time points. The results represent the means and standard deviations of three independent experiments. (E) *rpt6-20* cell expressing Guk1-GFP or Guk1-7-GFP were grown at 25°C and then shifted to 37°C for 1 hour prior to their fixation and imaging. Scale bar represents 5 $\mu$m. (F) Guk1-GFP and Guk1-7-GFP expressing cells were incubated at 25°C and cell lysates were immunoprecipitated using GFP-Trap beads and then immunoblotted with anti-ubiquitin, anti-GFP, and anti-Pgk1 antibodies.

The Guk1 and Guk1-7 constructs used in this report are ectopically expressed from the constitutive GPD promoter. To ensure that the overexpression from a plasmid does not influence the stability of our model substrate, we expressed both Guk1-GFP and Guk1-7-GFP from their endogenous locus and promoters, and performed a cycloheximide assay. Consistent with our previous CHX chase observations, Guk1-GFP levels remained relatively constant and Guk1-7-GFP levels decreased by approximately 30% after four hours at 25°C and by 60% when incubated at 37°C (Figure 2.12B). Together, this data suggested that the flow cytometry assay was suitable for monitoring protein levels and for screening purposes.

### 2.3.3 Guk1-7 Degradation is Proteasome Dependent

We next verified that degradation of the ectopically expressed model GFP-fusion substrate was proteasome-dependent. When we assayed levels of Guk1-7 at 37°C in the temperature sensitive proteasome mutant *rpt6-20* [52], degradation of the

mutant protein was largely stopped (Figure 2.3C). Conversely, no difference in Guk1-7-GFP stability was seen between the wild type strain or a double mutant of the two main lysosomal proteases (Figure 2.3D). These results suggest that loss of Guk1-7-GFP fluorescence is primarily caused by proteasomal degradation. Fluorescence microscopy revealed that Guk1-GFP was evenly distributed with no inclusions in *rpt6-20* cells at both 25°C and 37°C, as was the case for Guk1-7-GFP at 25°C (n = 126, 104, 118, respectively) (Figure 2.3E). Guk1-7-GFP inclusions were detected in 69% of the cells incubated at 37°C (n = 120), of which 94% of cells contained a single inclusion and 5% contained two. These data indicate that non-degraded Guk1-7-GFP was prone to aggregation at the non-permissive temperature. Finally, we asked whether the difference in protein stability between Guk1-GFP and Guk1-7-GFP was also reflected by their respective ubiquitination levels. We found that Guk1-7-GFP, but not Guk1-GFP, was ubiquitinated at 25°C (Figure 2.3F). In this case, we collected cell lysates from cultures incubated at the lower growth temperature, as we encountered issues with our model substrate being mostly lost to the insoluble pellet fraction when cultures were grown at higher temperatures. Together these experiments suggest that misfolded Guk1-7 is targeted for degradation by the ubiquitin proteasome system.

### 2.3.4 FACS-Based Screen for Protein Homeostasis Factors

To identify novel factors involved in targeting proteins destabilized by missense mutations for degradation, we performed a genome-wide screen based on flow cytometry using the Guk1-7-GFP allele. A schematic of the screen is depicted in Figure 2.4A. First, we pooled and bulk transformed the yeast non-essential knockout collection with a low copy number plasmid containing Guk1-7-GFP (Figure 2.4A i). Growth prior to and after transformation was limited, to avoid under representation of slow growing strains. Pooled transformants were grown in selective media at 25°C and then subjected to an initial FACS presort to obtain a narrow fluorescence range, which reduces cell-to-cell variability of GFP fusion expression (Figure 2.4A ii; compare grey and green profiles for before and after presort, respectively). Presorted cells were then incubated at 37°C in the presence of CHX for two hours (Figure 2.4A iii) and then sorted again, selecting for cells with GFP

fluorescence in the top 10% range (Figure 2.4A iv). Samples were collected over a short fifteen minute period to minimize shifting of the population during the handling time. Cells were recovered in selective liquid media and the screen was repeated two more times for a total of three rounds of enrichment (Figure 2.4A v). Following the final FACS sorting, cells were collected on solid selective media plates (Figure 2.4A vi).

We selected 170 colonies, which had been isolated using the FACS screen described above, for validation using the flow cytometry assay. In approximately two thirds of the colonies tested, Guk1-7-GFP was more stable than in the wild type cells (Figure 2.4B). The yeast knockout collection was created by replacing each yeast open reading frame with a KanMX module (conferring resistance to the antibiotic geneticin) and a unique 20 base pair nucleotide sequence, referred to as a molecular barcode. Universal priming sites located upstream and downstream of the barcodes are used for PCR amplification of the barcode region. Sequencing or microarray of the resulting amplicon can be used to reveal the identity of the corresponding yeast deletion strain. We therefore selected fifty colonies at random, spanning the range of Guk1-7-GFP stabilities, and their corresponding gene knockouts were identified by Sanger sequencing of the unique strain-specific barcodes. From these fifty colonies, we identified fifteen different gene deletions (Table 2.3). Next, to ensure that the phenotype (*i.e.*, stabilization of Guk1-7) was not acquired during the screening process, we assessed the stability of Guk1-7-GFP for each of the fifteen gene deletions we identified through Sanger sequencing. To do so, we individually retransformed the Guk1-7-GFP containing plasmid into each knockout strain from our pre-pooled knockout collection. Results of this phenotypic validation were considered positive (denoted as P in Table 2.3) if Guk1-7-GFP was at least 15% more stable in the deletion strain than in wild type cells (Figure 2.12C). Strains that did not meet this criterion were classified as negative (denoted as N in Table 2.3). Surprisingly, we failed to observe any stabilization of our model substrate in our most frequently identified hits (*e.g.*, *tda2*$\Delta$), which may have been susceptible to the acquisition of secondary mutations (Table 2.1). Among the validated hits, we identified the N-end rule E3 ligase Ubr1, which was previously shown to target cytosolic misfolded proteins for degradation [74, 76, 101–104], and the prefoldin chaperone subunit Gim 3 (Table 2.3, Figure 2.12C).

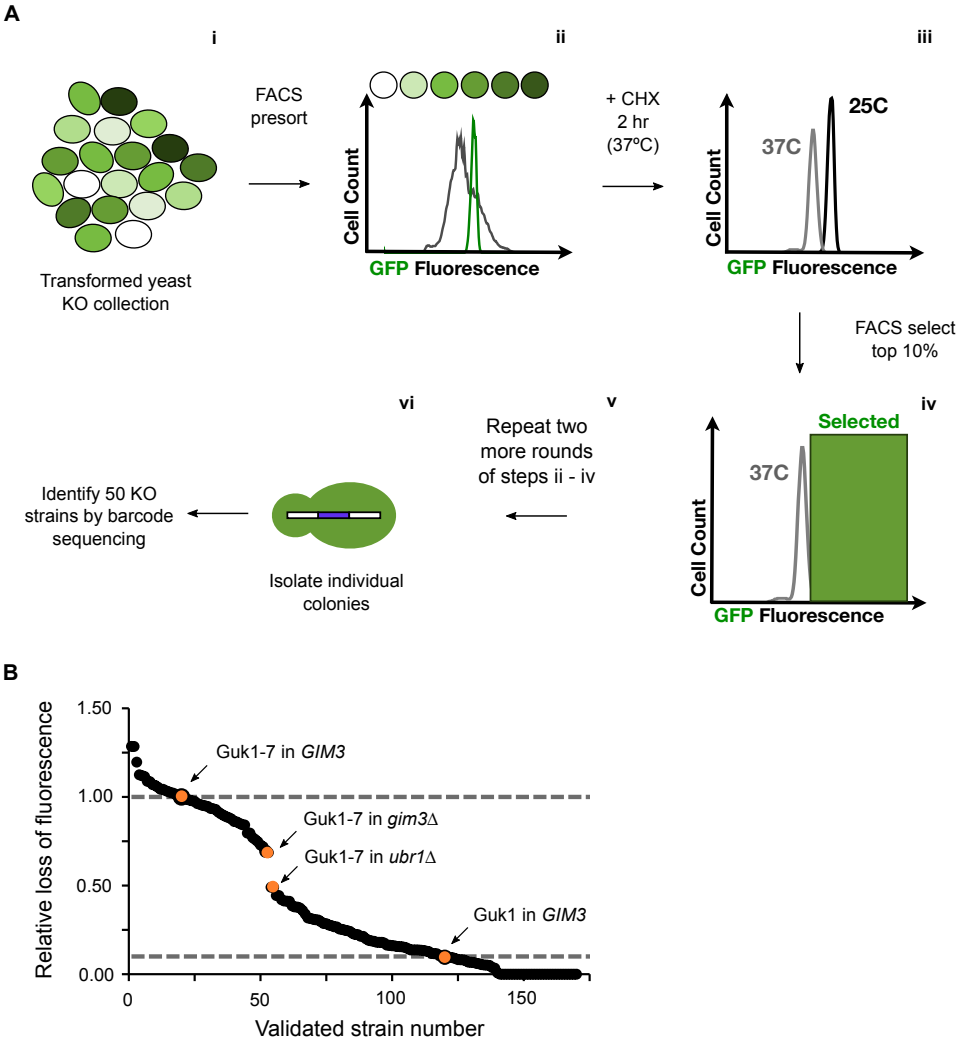


**Figure 2.4:** FACS-based screen. (A) Schematic of FACS-based screen. (B) Flow cytometry validation of 170 colonies isolated from the FACS screen. Relative loss of fluorescence of Guk1-GFP or Guk1-7-GFP in wild type cells is noted as a comparison.

**Table 2.3:** Summary of FACS screen validation

| Standard Name | Systematic Name | Number of Times Barcode Identified by Sanger Sequencing | Result of Phenotypic Validation[†] |
|---|---|---|---|
| TDA2 | YER071C | 22 | N |
| YAK1 | YJL141C | 10 | N |
| RIM15 | YFL033C | 5 | P |
| UBR1 | YGR184C | 2 | P |
| YOR364W | YOR364W | 1 | P |
| GIM3 | YNL153C | 1 | P |
| SLI15 | YBR156C | 1 | N |
| FAU1 | YER183C | 1 | N |
| VHR1 | YIL056W | 1 | N |
| BRA7 | YER056C | 1 | P |
| ASP1 | YDR321W | 1 | N |
| MAL11 | YGR289C | 1 | N |
| MUP3 | YHL036W | 1 | P |
| POL4 | YCR014C | 1 | N |
| PPH22 | YOL188C | 1 | N |

[†]P: positive
N: negative

### 2.3.5 Ubr1 Stabilizes Guk1 Missense Mutant

We identified the E3 ubiquitin ligase Ubr1 in our screen for factors responsible for degradative protein quality control of misfolded cytosolic proteins destabilized by missense alleles. In addition to its role as the E3 ligase of the N-end rule pathway, Ubr1 has also been shown to target misfolded cytoplasmic proteins for degradation [74, 101, 102]. In CHX chase experiments, Guk1-7-GFP levels were approximately 10% higher in *ubr1*Δ cells compared to wild type (P = 0.0008) at two hours

and remained significantly higher after four hours (P = 0.00003) (Figure 2.5A). To confirm that the stability observed was directly caused by the loss of Ubr1, we performed addback experiments whereby the wild type Ubr1 was expressed from a plasmid in *ubr1*Δ cells. We observed that Guk1-7-GFP levels were similar between the *UBR1* cells containing a control empty vector and *ubr1*Δ cells with the Ubr1 expressing plasmid, confirming that the phenotype observed could be attributed to the absence of Ubr1 (Figure 2.5B). To further validate our findings, we performed the same addback experiments but this time included a mutant form of Ubr1, which contains a point mutation in the RING domain producing an inactive ligase [74]. Guk1-7-GFP levels in the Ubr1 (C1220S) expressing cells were indistinguishable from those with a control plasmid, lending further support to Ubr1 having a direct role in controlling Guk1-7 stability (Figure 2.5C). We next assessed the importance of Ubr1 on a second unstable allele of Guk1 (T290G, hereinafter referred to as Guk1-11) that contained a single missense mutation. This mutant was generated by site directed mutagenesis and was selected based on its instability, as a two hour incubation at 37°C in the presence of cycloheximide typically resulted in approximately 60% loss of fluorescence. Consistent with our previous results, an absence of *UBR1* led to a significantly reduced clearance of this second model substrate (P = 0.00035) (Figure 2.5D). The relative fluorescence of Guk1-GFP was not significantly different between wild type and *ubr1*Δ cells (Figure 2.13A). These results indicate Ubr1 participates in the clearance of these model misfolded substrates, although other factors are also involved.

Ubr1 has been shown to act in concert with the nuclear E3 ligase San1 to target misfolded cytoplasmic proteins for degradation [74, 101]. To test whether Ubr1 also acts with San1 in the degradation of Guk1-7-GFP, we performed flow cytometry experiments in the single *ubr1*Δ and *san1*Δ deletion strains along with a double *ubr1*Δ *san1*Δ deletion. Guk1-7-GFP was not markedly more stable upon the deletion of SAN1, although levels were slightly higher in *ubr1*Δ *san1*Δ cells in comparison to *ubr1*Δ cells (Figure 2.13B). These results indicate that San1 does not play a major role in the turnover of Guk1-7. To confirm that our assay was capable of detecting an effect with San1, we ran the same assay using the previously characterized Ubr1 and San1 substrate Pro3-1 [101]. In this case we were able to observe a significant stabilization of Pro3-1 in *san1*Δ cells, which was even more

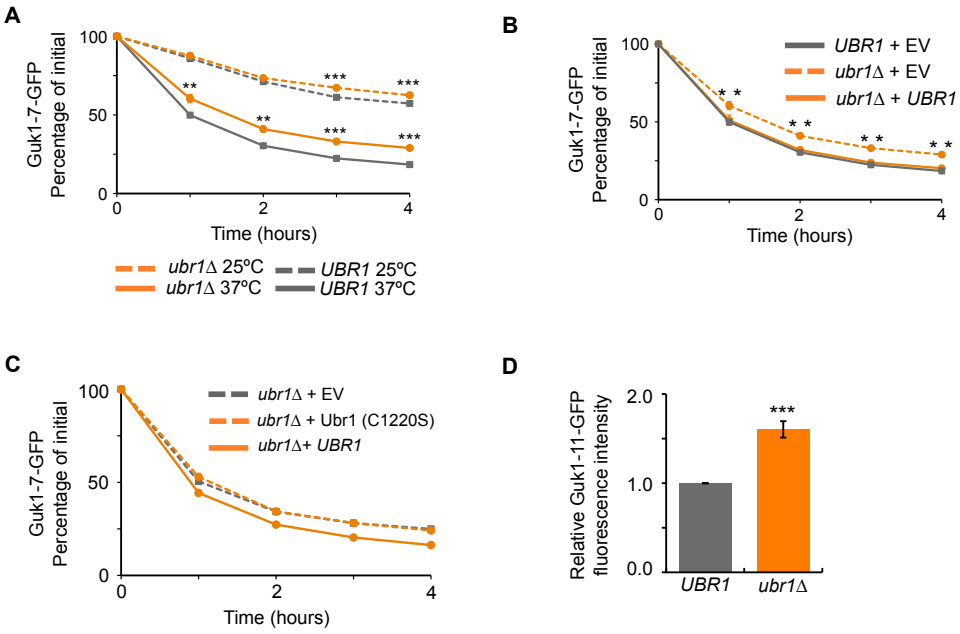


**Figure 2.5:** Ubr1 promotes Guk1-7-GFP degradation. (A) Wild type and *ubr1*Δ cells expressing Guk1-7-GFP were incubated with CHX at 25°C or 37°C and samples were analysed by flow cytometry at the indicated time points. The results represent the means and standard deviations of three independent experiments. P values were calculated with an unpaired Student's t test, *, ** and *** denote $P < 0.05$, 0.005, and 0.0005, respectively. (B) *UBR1* and *ubr1*Δ cells expressing Guk1-7-GFP along with an empty vector (EV) control or *UBR1* were incubated at 37°C and samples were collected at the indicated time points for flow cytometry analysis. Results represent the means and standard deviations of three independent experiments. P values were calculated with a one-way ANOVA and post-hoc Tukey HSD to assess significance, ** denotes $P < 0.005$. (C) *ubr1*Δ cells coexpressing Guk1-7-GFP and an empty vector control or either *UBR1* or *UBR1* (C1220S) were incubated at 37°C with CHX and samples were collected at the indicated time points. (D) Wild type or *ubr1*Δ cells expressing Guk1 (T290G) fused to GFP were incubated with CHX at 37°C for two hours before being analyzed by flow cytometry. The results represent the relative fluorescence intensities from three independent experiments (with standard deviations). P values were calculated with a one-way ANOVA and post-hoc Tukey HSD to assess significance, *** denotes $P < 0.0005$.

pronounced in the double *ubr1*Δ *san1*Δ strain (Figure 2.13C). Together, these data suggest that San1 does not play a role alongside Ubr1 in targeting Guk1-7-GFP for degradation, indicating that other E3 ligases may be involved in the proteasome-mediated degradation of this substrate.

### 2.3.6 Gim3 Impairs Guk1-7-GFP Degradation

Prefoldin is a hetero-oligomeric protein complex composed of six subunits ranging in size from 14–23 kDa [41]. Conserved in archaea and eukaryotes, but absent in prokaryotes, the prefoldin hexamer forms a "jellyfish-like" structure with N- and C-terminal coiled-coil regions of each subunit forming "tentacles" that emanate from a central region [42]. Misfolded substrates are transferred for folding from prefoldin to the TRiC/CCT chaperonin in an ATP-independent manner through direct binding of the two chaperone complexes [41]. In addition to its role in aiding nascent proteins, such as actin and tubulin, to attain their functional conformations, the prefoldin chaperone complex has been shown to prevent huntingtin and alpha-synuclein aggregate formation [43, 44]. Having identified the prefoldin subunit Gim3 in our screen, we decided to further examine its potential role in degradative protein quality control. In CHX chase experiments, Guk1-7-GFP levels were approximately 25% higher in the *gim3*Δ strain compared to wild type (P = 0.0057) (Figure 2.6A). To ensure that the stabilization was specifically caused by the absence of Gim3, we expressed in *gim3*Δ cells the wild-type *GIM3* from a plasmid, which rescued the degradation of the model substrate (Figure 2.6B). While degradation of Guk1-7-GFP is not fully inhibited in *gim3*Δ cells, levels are markedly higher than in the wild type strain, indicating that Gim3 is required for the normal turnover of our model substrate. We next wished to see if Gim3 works together with Ubr1. In this case we preferred a model substrate that is misfolded as the result of a single point mutation (Guk1-11) to eliminate or minimize potential confounding factors caused by multiple destabilizing mutations. The double *ubr1*Δ *gim3*Δ strain showed increased Guk1-11 stability compared to single deletion strains, however the substrate was still degraded by over 50% (Figure 2.6C). This data indicates that potentially other E3 ligases or chaperones are required for complete proteolysis to occur. In addition, this would suggest that Ubr1 and Gim3 work partially in

parallel or in independent pathways to target the assessed misfolded substrate for degradation.

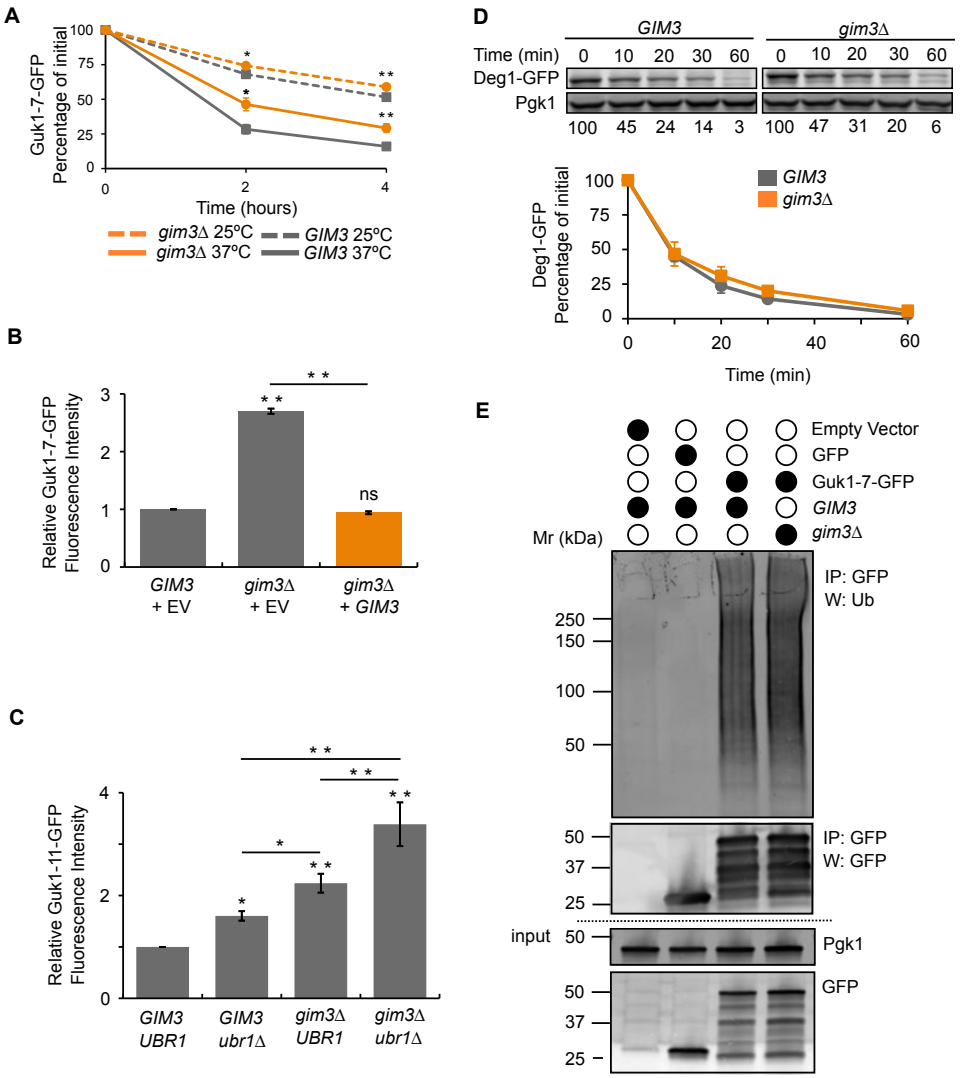


**Figure 2.6:** Absence of Gim3 reduces Guk1-7 turnover.

**Figure 2.6:** (Previous page) Absence of Gim3 reduces Guk1-7 turnover. (A) Wild type and *gim3*Δ cells expressing Guk1-7-GFP were incubated with CHX at 25°C or 37°C and samples were analysed by flow cytometry at the indicated time points. The results represent the means and standard deviations of three independent experiments and the asterix denotes significance of $P < 0.05$. (B) Gim3 addback experiment. *GIM3* or *gim3*Δ cells expressing Guk1-7-GFP and either an empty vector (EV) control or *GIM3*. The results represent the means and standard deviations of three independent experiments of the relative fluorescence intensity after a two hour CHX incubation at 37°C. P values were calculated with a one-way ANOVA and post-hoc Tukey HSD to assess significance, ** denotes $P < 0.005$. (C) Wild type, *ubr1*Δ, *gim3*Δ, and *ubr1*Δ *gim3*Δ cells expressing Guk1 (T290G) fused to GFP were incubated at 37°C with CHX for two hours and then analysed by flow cytometry. P values were calculated with a one-way ANOVA and Holm multiple comparison to assess significance, * and ** denote $P < 0.05$ and 0.01, respectively. (D) Proteasome activity assay. Gim3 or *gim3*Δ cells expressing Deg1-GFP under the Cup1 promoter were incubated at 30°C in the presence of CHX and samples were collected at the indicated time points. Deg1-GFP was immunoblotted with an anti-GFP antibody. The results represent the mean and standard deviation of three independent experiments. (E) *GIM3* or *gim3*Δ cells expressing Guk1-7-GFP, GFP alone, or a control empty vector were grown at 25°C. Guk1-7-GFP was immunoprecipitated with GFP-Trap beads and eluted samples were immunoblotted with anti-ubiquitin and anti-GFP antibodies.

The TRiC/CCT chaperonin cooperates with prefoldin in folding a number of cellular proteins and has been shown to interact with proteasome subunits, suggesting that it may be involved in proteasome maturation [194]. Therefore, one possibility is that the stabilizing effect of Gim3 on Guk1-7 could be indirect, a result of decreased proteasome function. We tested for compromised proteasome function in the *gim3*Δ strain using the constitutive Deg1-GFP proteasome substrate [184]. We found that there was no significant difference in the degradation of Deg1-GFP in *gim3*Δ cells compared to the wild type strain at all time points tested, with the exception of the thirty minute sample ($P = 0.77$, $P = 0.22$, $P = 0.04$, $P = 0.07$ for the 10, 20, 30, and 60 minute time points, respectively) (Figure 2.6D). Hence, the reduced turnover of misfolded protein observed in *gim3*Δ cells is unlikely caused by an impaired proteasome.

We next determined whether an absence of *GIM3* could affect ubiquitination of our misfolded model substrate. GFP tagged Guk1-7 was pulled down from cells grown at 25°C, where it remained mostly soluble, and then ubiquitin levels were detected by immunoblotting. After normalizing the quantity of ubiquitin to that of eluted Guk1-7, ubiquitination levels were essentially unchanged, with under 5% less ubiquitinated model substrate in *gim3*Δ cells compared to wild type (Figure 2.6E). This experiment indicates that the absence of Gim3 did not impair ubiquitination of our model substrate, in agreement with Gim3 functioning independently of Ubr1.

### 2.3.7 Gim3 Facilitates the Clearance of Insoluble Guk1 and Maintains Guk1-7 Solubility

We next sought to evaluate the impact an absence of Gim3 has on Guk1-7 localization. Fluorescence microscopy performed on wild type and *gim3*Δ strains showed that while there was no difference in wild type Guk1-GFP localization between the two strains, Guk1-7-GFP formed cytoplasmic puncta in 93% of *gim3*Δ cells when incubated at 37°C, and additional faint and diffuse cytoplasmic GFP was also visible (n = 200) (Figure 2.7A). Cells contained on average 1.5 puncta, which were typically located next to the nucleus. In contrast, only sixteen percent of wild type cells contained Guk1-7-GFP puncta (n = 200). These puncta were no longer present when we expressed Gim3 from a plasmid in *gim3*Δ cells and the diffuse cytoplasmic GFP signal was also not present, similar to that observed in *GIM3* cells (Figure 2.7B). We decided to examine this phenomenon more closely by performing a time course microscopy experiment incubating cells at 37°C, but in the absence of the translation inhibitor CHX which we had been using up to this point and which may interfere with aggregate formation [195]. Within five minutes numerous Guk1-7-GFP containing puncta were detected within the cytoplasm of *GIM3* cells with those in the *gim3*Δ strain being slightly delayed and visible after 10 minutes (Figure 2.7C). While puntca remained visible in both strains after 45 minutes at 37°C, those in the *gim3*Δ strain appeared to coalesce slower than in *GIM3* (after 15–20 minutes in *GIM3* compared to 20–25 minutes in *gim3*Δ) and remained visibly brighter. Some diffuse cytoplasmic Guk1-7-GFP signal was also present in *gim3*Δ cells up to 25 minutes after shifting to the increased growth tem-

perature, but was only present in the first 10 minutes for *GIM3* cells. While the number of puncta did not differ between Gim3 containing or deleted cells, the intensity of the *gim3*Δ puncta remained brighter for longer. These results suggest that Gim3 may play a role in maintaining Guk1-7-GFP solubility at higher temperatures to facilitate substrate degradation.

These Guk1-7-GFP puncta observed in the time course experiment in both *GIM3* and *gim3*Δ cells are reminiscent of the Q-bodies described by Frydman and colleagues [136]. To determine whether this is indeed the case, we examined Guk1-GFP and Guk1-7-GFP colocalization in *GIM3* cells with two cytosolic aggregate markers: Hsp104 and Hsp42. Hsp104 is an aggregate-specific chaperone that has a diffuse cytoplasmic and nuclear localization pattern at 25°C but forms puncta when incubated at 37°C (Figure 2.8A, enlarged Figure 2.8C). Hsp104-mCherry and Guk1-7-GFP puncta colocalized in 100% of cells at 37°C (n = 100). We then examined Guk1-7-GFP colocalization with the small heat shock protein Hsp42, which is required for peripheral aggregate formation during physiological heat stress [137]. As with Hsp104, Hsp42-mCherry formed puncta when incubated at 37°C, but not at 25°C (Figure 2.8B, enlarged Figure 2.8D). Guk1-7-GFP colocalized in all Hsp42-mCherry puncta. However, in 34% of the cells examined (n = 100), we find an average of 1.4 Guk1-7-GFP puncta per cell that do not colocalize with Hsp42. Overall, Hsp42-free Guk1-7-GFP puncta represented 9% of all puncta observed in the one hundred cells examined. Together, the Hsp104 and Hsp42 colocalization data suggest that at 37°C Guk1-7-GFP forms cytosolic inclusions similar to Q-bodies.

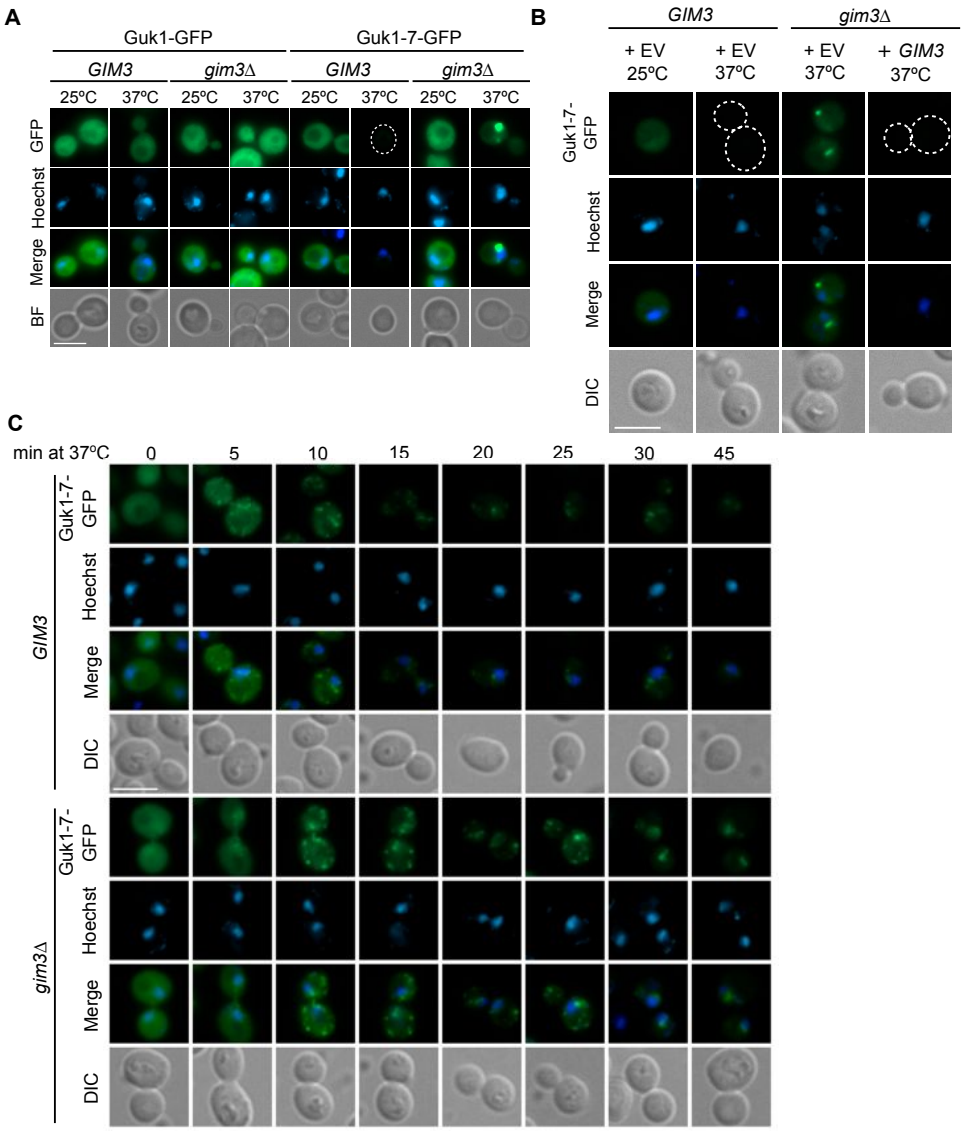


**Figure 2.7:** Gim3 facilitates clearance of insoluble Guk1-7.

**Figure 2.7:** (Previous page) Gim3 facilitates clearance of insoluble Guk1-7. (A) *GIM3* or *gim3*Δ cells expressing Guk1-7-GFP were grown at 25°C and then incubated at either 25°C or 37°C for 2 hours in the presence of CHX before fixation and imaging. (B) *GIM3* and *gim3*Δ cells expressing Guk1-7-GFP along with an empty vector control or *GIM3* were incubated at 25°C or 37°C for two hours in the presence of CHX before fixation and imaging. (C) *GIM3* or *gim3*Δ cells expressing Guk1-7-GFP were incubated at 25°C and then shifted to 37°C. Samples were collected at the indicated time points and then fixed before imaging. For all images, the scale bar represents 5 $\mu$m and dotted lines demark cell boundaries.

To verify the importance of Gim3 in maintaining Guk1-7 solubility, we examined the sedimentation of the mutated protein after centrifugation. Twice as much Guk1-7 is found in the NP-40 insoluble pellet fraction at 25°C in *gim3*Δ cells compared to wild type *GIM3* cells (Figure 2.9A). There was also more Guk1-7 in the pellet of *gim3*Δ than wild type cells after incubating cells at 37°C. We then performed immunoprecipitation experiments to test whether Gim3 could directly interact with Guk1-7 as a potential mechanism for maintaining Guk1-7 solubility. From cell extracts incubated at 25°C, Guk1-7-GFP can pull down a TAP-tagged form of Gim3 whereas no interaction was detected between Gim3-TAP and Guk1-GFP (Figure 2.9B). We verified this interaction in an independent experiment (Figure 2.14A). Once again, a lower temperature was used for pulldown experiments to avoid losing Guk1-7 in the insoluble pellet fraction. These results suggest that Gim3 could maintain Guk1-7 in a more soluble state through physical interaction, potentially acting as a holdase. Holdases are a type of molecular chaperone that bind to misfolded proteins in an ATP-independent manner to prevent protein aggregation, but they do not directly refold their substrates [47]. Consistent with these findings, we tested the viability of the guk1-7 strain over a range of temperatures (25°C to 37°C), in the presence or absence of *GIM3*, and found that in both cases viability largely decreased between 32°C and 33°C with no growth at temperatures of 34°C or above (Figure 2.14B). These results indicate that, whereas degradation of poorly soluble Guk1-7 was delayed, temperature-dependent lethality is not rescued in *gim3*Δ cells.

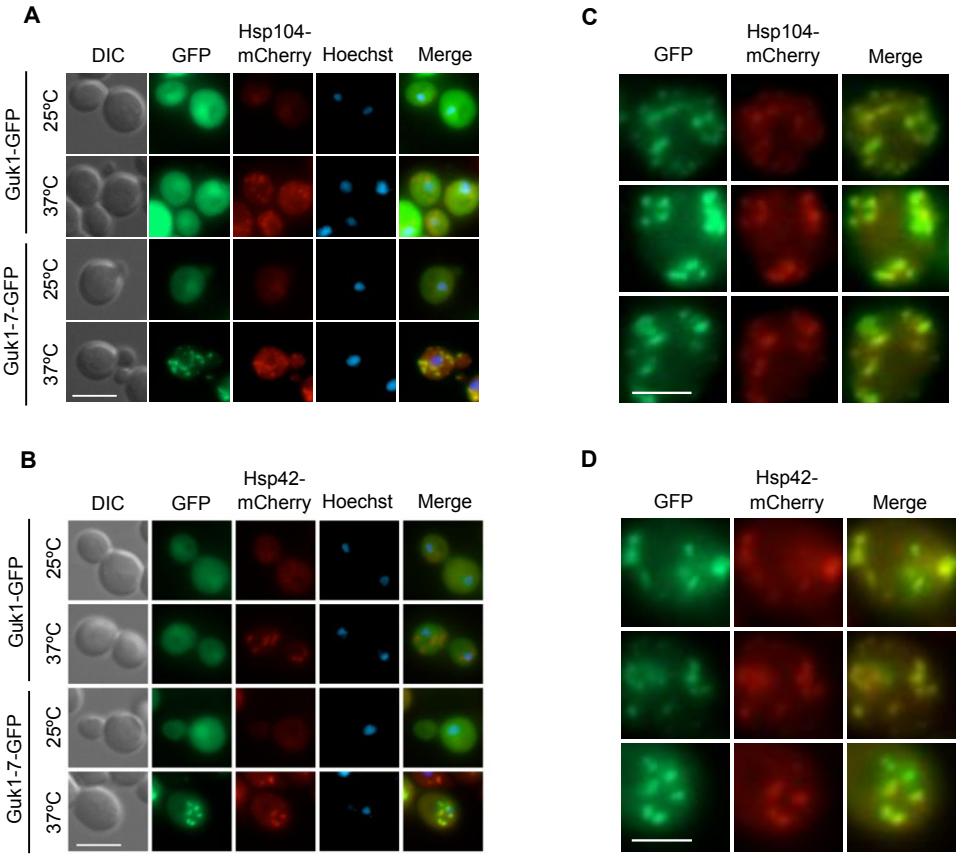


**Figure 2.8:** Guk1-7-GFP puncta colocalize with Q-body markers. (A) Cells with Hsp104 endogenously tagged with mCherry and ectopically expressing Guk1-GFP or Guk1-7-GFP were grown at 25°C and then incubated at 25°C or 37°C for 30 minutes before fixation and imaging. Scale bar represents 5 $\mu$m. (B) Hsp42-mCherry cells ectopically expressing Guk1-GFP or Guk1-7-GFP were grown at 25°C prior to incubation at 25°C or 37°C for 30 minutes. Cells were then fixed before imaging. The scale bar represents 5 $\mu$m. (C) Enlarged images from cells collected as in A. Scale bar represents 2.5 $\mu$m. (D) Enlarged images from cells collected as in B. Scale bar represents 2.5 $\mu$m.

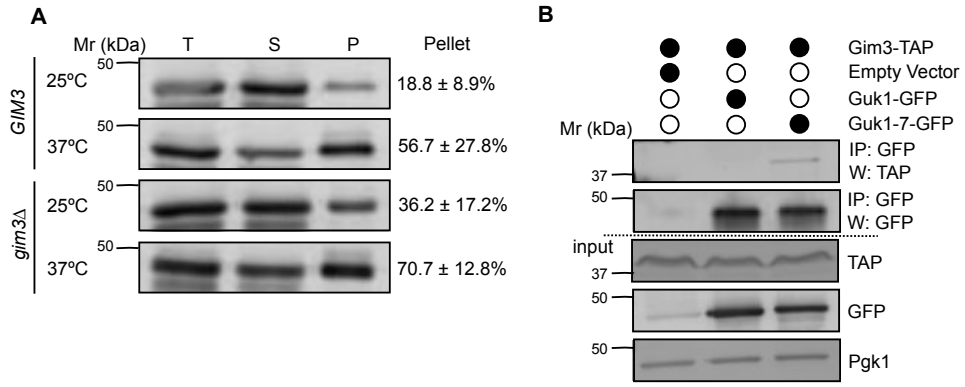


**Figure 2.9:** Gim3 helps maintain Guk1-7 solubility. (A) *GIM3* or *gim3*Δ Guk1-7-GFP expressing cells were grown at 25°C or shifted to 37°C for 20 min. The ratio of the pellet fraction to total cell lysate is noted and represents the mean and standard deviation of three independent experiments. (B) Guk1-7-GFP was immunoprecipitated from Gim3-TAP expressing cells incubated at 25°C and then immunoblotted with anti-TAP, anti-GFP, or anti-Pgk1 antibodies.

### 2.3.8 Gim3 Has a General Effect Towards Thermally Destabilized Proteins

To see if the effect of Gim3 on Guk1-7 solubility was specific to this prefoldin subunit, or common to all prefoldin subunits, we performed fluorescence microscopy with the other prefoldin mutant strains. Guk1-7-GFP puncta were visible in all of the prefoldin deletions, albeit to varying degrees, suggesting that they all play a role in Guk1-7 solubility (Figure 2.10A). Fifty-six per cent of *gim1*Δ cells contained puncta, whereas only 26% of *gim4*Δ did (n = 50, each). While the number of puncta per cell only differed slightly between prefolin strains, either faint or no cytoplasmic Guk1-7-GFP was visible in *gim2*Δ, *gim4*Δ, *gim5*Δ, and *gim6*Δ strains while markedly present in *gim1*Δ and *gim3*Δ cells. To better quantify the effect, we measured Guk1-7 levels by flow cytometry and found that only deletions of *GIM1* and *GIM3*, and to a lesser extent *GIM5*, retarded the degradation of the model substrate (Figure 2.10B). Not surprisingly, *gim1*Δ and *gim3*Δ were the only strains that, in addition to puncta, also had a diffuse cytoplasmic Guk1-7-GFP signal visible by fluorescence microscopy. All together, these results suggest that while deletion of

individual members of the prefoldin complex impacted degradation of the model substrate, some (*i.e.*, Gim1 and Gim3) may play a more important role.

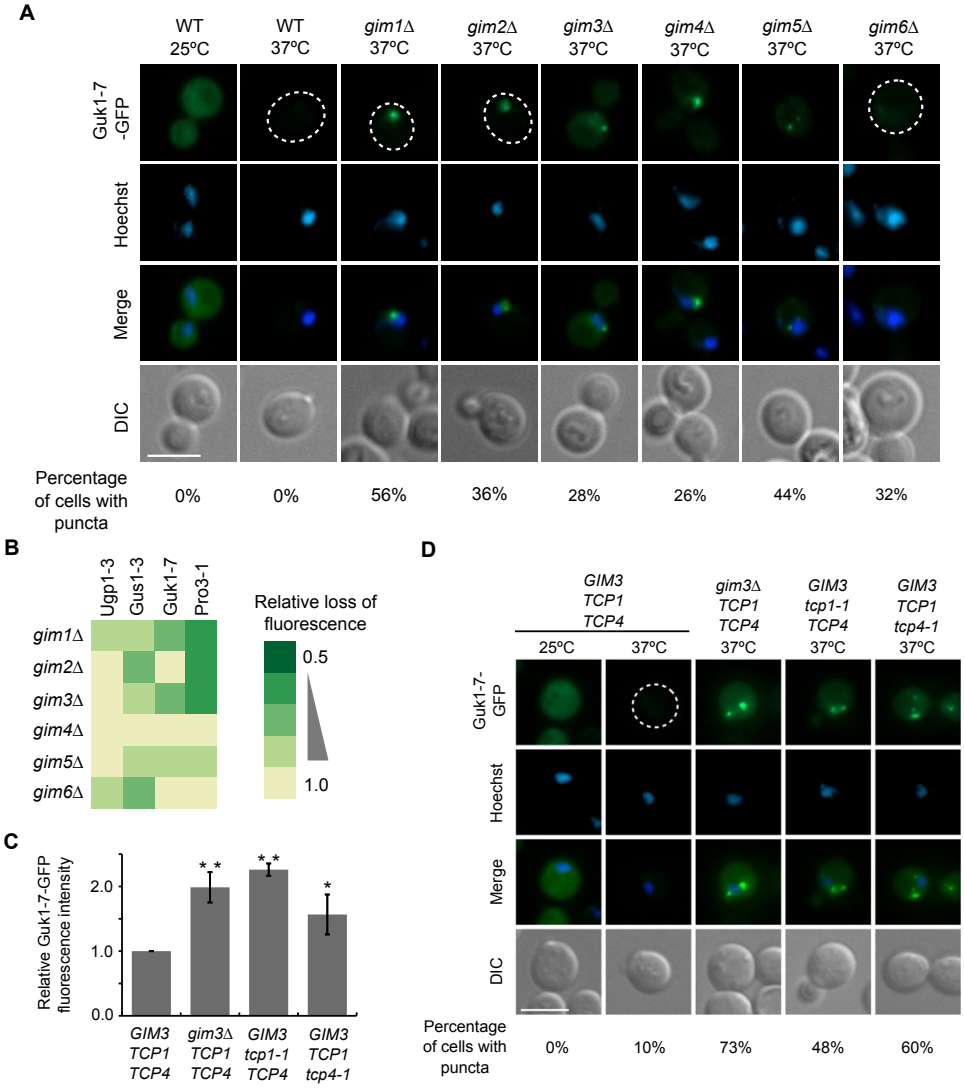


**Figure 2.10:** Thermosensitive alleles are stabilized by prefoldin subunits.

**Figure 2.10:** (Previous page) Thermosensitive alleles are stabilized by prefoldin subunits. (A) Individual prefoldin subunit mutants expressing Guk1-7-GFP were incubated at 37°C in the presence of CHX for 2 hours. The percentage of cells with puncta was calculated from 30–50 GFP positive cells. Scale bar represents 5 $\mu$m. (B) Four thermosensitive alleles were expressed as GFP fusion proteins in the six prefoldin deletion strains. Cells were incubated with CHX at 25°C and 37°C for 2 hours and fluorescence intensity was measured by flow cytometry. (C) Guk1-7-GFP was expressed in wild type, *gim3*Δ, *tcp1-1*, or *tcp4-1* cells and incubated with CHX for two hours at either 25°C or 37°C before flow cytometry analysis. (D) Wild type, *gim3*Δ, *tcp1-1*, and *tcp4-1* cells expressing Guk1-7-GFP were incubated with CHX for 2 hours at 25°C or 37°C prior to fixation and imaging. Scale bar represents 5 $\mu$m.

We next wished to explore whether prefoldin can stabilize additional proteins that are destabilized by missense mutations other than Guk1-7. We selected a number of cytoplasmic thermosensitive alleles, which we have previously shown to be degraded in a proteasome dependent manner, and created C-terminal GFP fusions to test by flow cytometry [101]. Ugp1 is the UDP-glucose pyrophophorylase in *S. cerevisiae* and is involved in the oxidative stress response [196, 197]. The Ugp1-3 allele contains two silent and two missense mutations and temperature sensitive lethality can be restored by Ubr1 deletion [101]. Ugp1-3-GFP was only modestly stabilized by all prefoldin deletions (including *gim3*Δ) with the largest effect seen in *gim1*Δ and *gim6*Δ strains (Figure 2.8B). Glutamyl tRNA synthetase (Gus1) attaches amino acids to cognate tRNA and the Gus1-3 allele contains seven missense mutations [101, 198, 199]. Unlike Guk1-7, Gus1-3 was most stabilized by *gim2*Δ and *gim6*Δ strains. Delta 1-pyrroline-5-carboxylate reductase (Pro3) converts delta 1-pyrroline-5-carboxylate to proline in the final step of the proline biosynthesis pathway [200]. Pro3-1 has four missense mutations and its temperature sensitive lethality is restored in a double deletion of Ubr1 and San1 [101]. Of all the alleles tested, Pro3-1 was the most stabilized by the prefoldin deletions, with *gim1*Δ, *gim2*Δ, and *gim3*Δ strains having the largest effect. Gim5 also stabilized Pro3-1, but to a lesser extent. The *gim4*Δ strain had the smallest effect on substrate stabilization of all the deletions tested. These data suggest that while individual

prefoldin subunit deletions may differentially affect substrate stability, they can stabilize a range of substrates misfolded due to missense mutations.

Given that the TRiC/CCT chaperonin folds client proteins delivered to it by the prefoldin complex, we sought to see if it also had a role in stabilizing our Guk1-7-GFP substrate. Using temperature sensitive alleles of the TRiC/CCT subunits Tcp1 and Tcp4, we performed CHX chase experiments and found Guk1-7-GFP levels to be significantly higher compared to wild type, similar to those found in *gim3*Δ cells (Figure 2.10C). Fluorescence microscopy showed that Guk1-7-GFP forms cytoplasmic puncta in 48% of *tcp1-1* cells (n = 100) and 60% of *tcp4-1* cells (n = 100) when incubated at 37°C (Figure 2.10D). In cells where puncta were observed, an average of 1.8, 2.4, and 1.3 puncta per cell were found for the *gim3*Δ, *tcp1-1*, and *tcp4-1* strains, respectively. These data would suggest a possible role for TRiC/CCT chaperonin in addition to prefoldin in maintaining the solubility of our Guk1-7-GFP model substrate.

## 2.4 Discussion

Classically, degradative quality control pathways have been identified and characterized using model substrates. In this study, we have established Guk1-7 as a novel model protein quality control substrate whose stability is temperature dependent and is degraded by the proteasome. The mutant protein also forms Q-body like inclusions when shifted to the non-permissive temperature that co-localize with Hsp104, as well as Hsp42. We developed a flow cytometry assay to assess protein stability and then performed a FACS-based screen to isolate factors important for cytosolic protein homeostasis. We identified the E3 ubiquitin ligase Ubr1 and the prefoldin chaperone subunit Gim3. Gim3 promotes Guk1-7-GFP degradation and influences its solubility, but not ubiquitination. We also showed that in addition to Guk1-7, prefoldin can stabilize a number of temperature sensitive proteins that misfold as the result of missense mutations.

Protein degradation is generally assayed by pulse-chase metabolic labelling, or by using protein synthesis inhibitors coupled with downstream biochemical analysis [201]. More recently, fluorescently tagged proteins have been used to monitor protein stability [74, 174]. This development means that it is now feasible to per-

form high-throughput genome-wide screens using flow cytometry to identify factors that influence protein stability or abundance. Flow cytometry confers a number of advantages compared to stability assays using endogenous or ectopically expressed fluorescently tagged substrates as the method is quantitative, measurements are performed in vivo, thousands of cells can be analyzed in under an hour, and for most purposes no additional processing or cell lysis is required. While temperature sensitive alleles have been used in suppressor screens to identify protein quality control components such as San1 and Ubr1, these screens require that the model substrate be functional at the restrictive temperature [70, 101]. Perhaps most importantly, in addition to the relative speed and precision flow cytometry provides over Western blotting methods, the assay is sensitive enough to discern partial effects (*e.g.*, stabilization of Guk1-7 in *ubr1*$\Delta$) that might not be detected by traditional Western blotting methods and can be used as a screening tool that does not rely on protein function.

Limiting the damaging effects of misfolded proteins appears to have influenced protein evolution as the most conserved proteins are those with the highest translation rate and as a result face the greatest risk of incurring mistranslation errors [2]. As missense mutations represent more than half of all mutations in the HGMD and mistranslation-induced misfolding is a potential mechanism for pathologies independent of genomic alterations, we anticipate that understanding the protein quality control pathways that recognize and triage proteins misfolded as the result of missense mutations will gain in importance [158]. A recent study by Sahni *et al.* [159] found two-thirds of the disease associated missense alleles they tested to have disrupted protein-protein interactions compared to the wild type allele, and approximately 30% of mutant proteins displayed increased binding to components of the protein homeostasis network. While nascent polypeptides that misfold during translation are rapidly degraded, our model substrate has a half life of over four hours at the permissive temperature of 25°C and approximately 90 minutes at 37°C. Our lab has previously reported a panel of temperature sensitive alleles of essential cytosolic genes in *S. cerevisiae* and showed that just under half of these alleles have half lives of three hours or less [101]. At the non-permissive temperature of 37°C, Guk1-7's half life is similar to that of the cytoplasmic model substrate $\Delta$ssCPY* ($\sim$1 hr) and GFP-Ubc9-2 ($\sim$40 min) [74, 136]. Interestingly, by contrast, nuclear

temperature sensitive proteins such as Cdc68-1, Sir4-9, Cdc13-1 and Sir3-8, all recognized by the E3 ubiquitin ligase San1, have significantly shorter half lives than the cytoplasmic alleles we have identified [70]. There are a number of potential explanations for why a slower turnover rate is observed. First, the cytoplasmic proteins used in our study and that of Escusa-Toret *et al.* [136] are constitutively expressed at high levels compared to the low abundance endogenously expressed nuclear proteins examined by Gardner *et al.* [70]. As a single protein in the cell is represented by a spectrum of folding states, it may be that highly abundant proteins prone to misfolding may only have a fraction of their cellular pool misfolded in such a state as to be recognized and degraded at one time. Second, temperature sensitive alleles of natural proteins, as opposed to engineered model substrates, have evolved in a cellular context replete with chaperones and protein homeostasis machinery. Given that most chaperones are cytoplasmic, our model substrates have the potential to be recognized and interact with a number of chaperones undergoing refolding cycles before being targeted for degradation. This would be reflected by a slower turnover rate. Finally, we identified the ubiquitin E3 ligase Ubr1 in our screen. Ubr1 alone, or as a double mutant in combination with Gim3 or San1, was not sufficient to completely stop degradation of our model substrate. This would suggest that some misfolded proteins require the activity of a number of E3 ligases for their disposal.

While performing fluorescence microscopy we observed that the model substrate Guk1-7-GFP forms Q-body like inclusions in the cytoplasm. A similar phenomenon was described for the temperature sensitive Ubc9-2 allele by Escusa-Toret *et al.* [136]. They speculate that Q-body formation is a rapid early response deployed by the cell to manage misfolded proteins. It would be interesting to see if this inclusion formation can explain the longer half life of our misfolded substrate. A major question is whether proteins sequestered in Q-bodies get redirected to the nucleus for degradation with the help of San1 (as in the case of Pro3-1), or do proteasomes co-localize to Q-bodies as they do with JUNQ inclusions providing a means for substrate disposal in the cytoplasm.

In addition to Ubr1, we identified the prefoldin chaperone subunit Gim3 in our screen. We demonstrate that Gim3 was necessary for maintaining Guk1-7 solubility and interacted with our missense allele, but not the wild type protein.

In contrast to other reports, we did not find Gim3 to influence ubiquitination of our model substrate, suggesting that it acts independent of substrate ubiquitination (Figure 2.11). This discrepancy could be explained as being due to previous studies being performed under conditions of proteasome inhibition, or due to the nature of the substrate [202]. Previous reports have demonstrated that knocking down prefoldin subunits results in increased ubiquitination of alpha-synuclein and large inclusion formation, as well as aggregation of huntingtin, an amyloidogenic IPOD substrate [43, 44, 135, 136]. Whereas Abe *et al.* [202]examined the ubiquitination status of the proteome either in the soluble or pellet fraction under proteasome inhibition, we focused our attention to the soluble fraction of a single substrate.

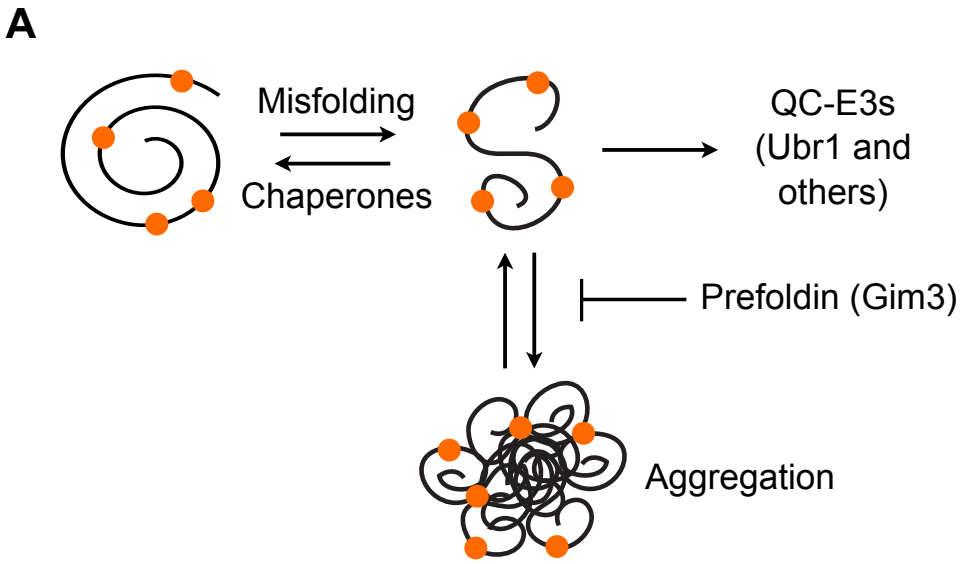


**Figure 2.11:** Model for stabilization of temperature sensitive alleles by Gim3. (A) Proposed model for how Gim3 promotes degradation of temperature sensitive alleles destabilized by missense mutations.

As the structure of the prefoldin complex has no evidence for a nucleotide binding site and therefore lacks ATP-regulated functionality, it is tempting to speculate that prefoldin may act as a holdase [42]. Interestingly, only the mutated and not wild type Guk1 requires Gim3 to remain soluble. In addition, mutations that affect chaperonin components also impaired Guk1-7 degradation. These results

indicate that in addition to maintaining misfolded proteins soluble, prefoldin also handed them to the chaperonin for refolding. More work will be required to clearly demonstrate whether Gim3 acts as a holdase to prevent protein aggregation to enhance substrate accessibility for ubiquitin-proteasome mediated degradation. Several other chaperone or co-chaperone proteins have been shown to be important for promoting the degradation of cytosolic misfolded proteins in yeast. Sse1 was shown to help mediate the degradation of the tumor suppressor VHL and is required for the recognition of misfolded proteins by Ubr1 [50, 74]. The Ydj1 J-domain containing Hsp40 mediates both the degradation of ER proteins with exposed misfolded cytosolic domains and the Rsp5 mediated degradation of cytosolic proteins after heat shock [52, 53]. In contrast Sis1, another J-domain containing Hsp40, was shown to be important for the relocalization of cytosolic misfolded proteins to the nucleus [75]. Fes1, an Hsp70 nucleotide exchange factor, was also shown to be important for the degradation of cytosolic misfolded proteins and does so by interacting with the misfolded proteins bound to Hsp70 and triggering their release [54, 167, 203]. By demonstrating a role for Gim3 in substrate solubility, our work adds to a growing body of evidence suggesting that prefoldin is important for preventing potentially toxic protein aggregation [44, 204, 205]. In addition to our temperature sensitive alleles, prefoldin has been shown to inhibit human amyloid-beta fibrillation and prevents aggregation of huntingtin [44, 204]. This underscores the potential importance the prefoldin chaperone complex has in maintaining protein homeostasis.

## 2.5 Supplemental Data

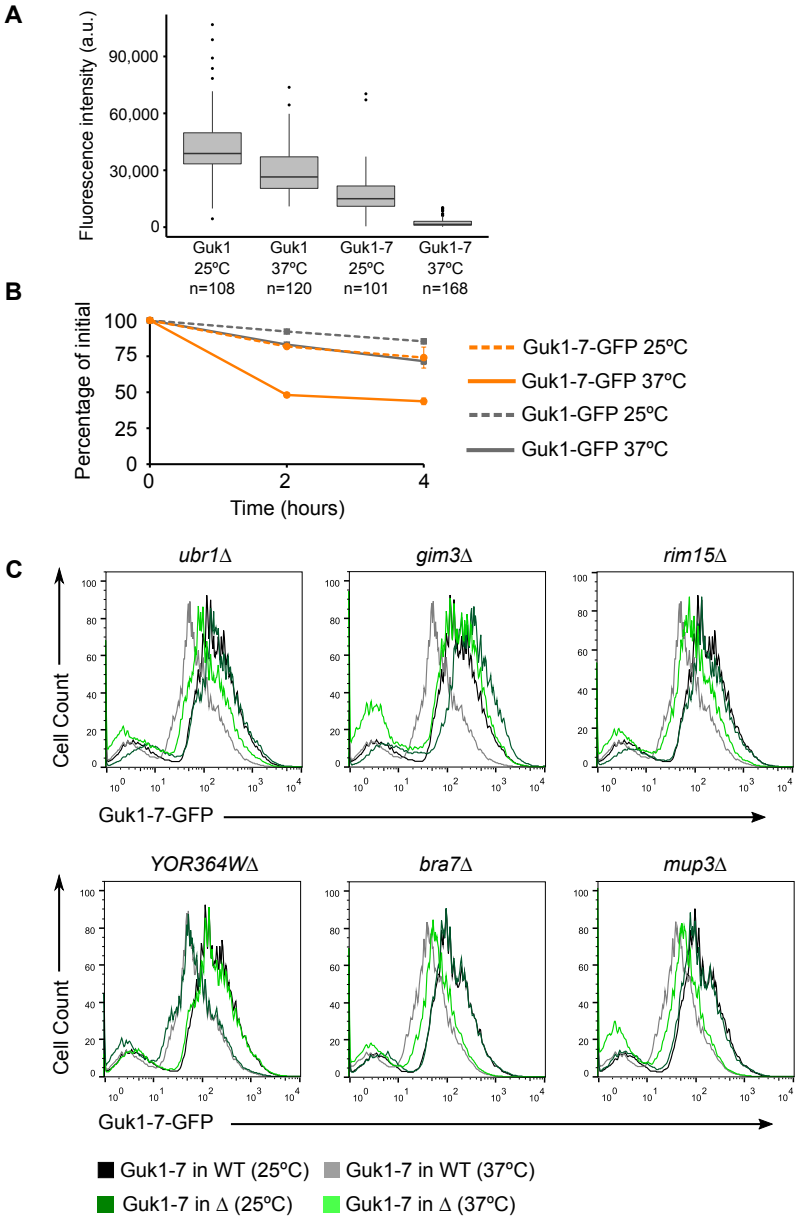


**Figure 2:12:** Guk1-7-GFP flow cytometry.

**Figure 2.12:** (Previous page) Guk1-7-GFP flow cytometry. (A) Box plot of quantification for fluorescence microscopy images in Figure 2.2A. Corrected total cell fluorescence was calculated by subtracting the mean fluorescence of background readings from the integrated density. n = 108, 120, 101, and 168 for Guk1 25°C, Guk1 37°C, Guk1-7 25°C, and Guk1-7 37°C, respectively. (B) Wild type cells expressing Guk1-GFP or Guk1-7-GFP on a plasmid and expressed from their endogenous promoters were incubated at 25°C or 37°C with CHX. Samples were collected at the indicated time points and analyzed by flow cytometry. (C) Flow cytometry validation experiments for the deletion strains identified by barcode sequencing. Cells expressing Guk1-7-GFP were incubated with CHX at 25°C or 37°C for two hours prior to flow cytometry analysis. Note that expression of *YOR364W* and *RIM15* from a plasmid (*i.e.*, add back experiments) failed to rescue the phenotype indicating that an additional mutation may have caused stabilization of the model substrate. Deletions of *UBR1* and *GIM3* were further analyzed in this work but not MUP3 and BRA7.

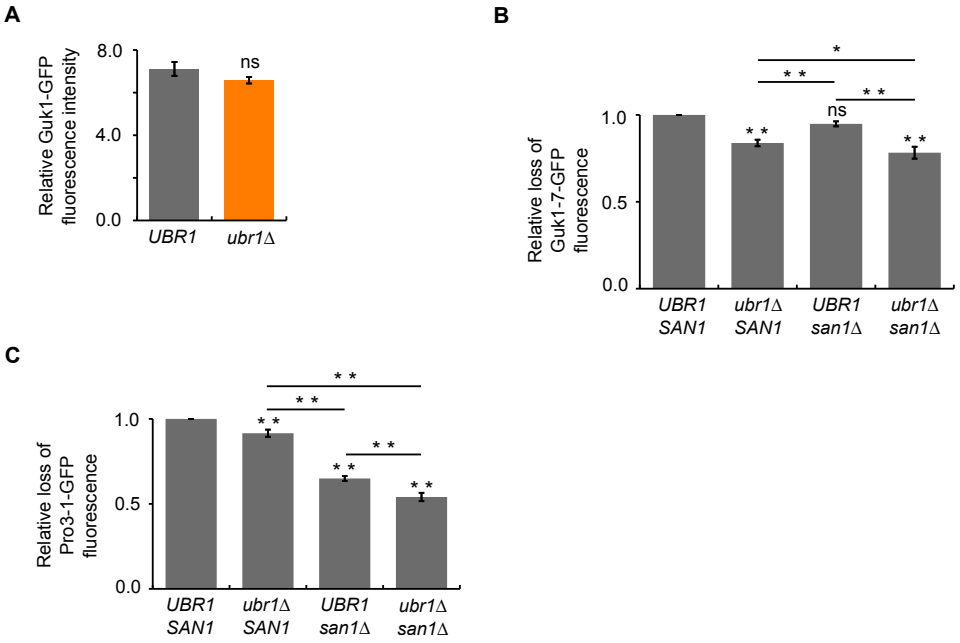


**Figure 2.13:** Ubr1 does not act with San1 in the degradation of Guk1-7-GFP. (A) Guk1-GFP was expressed in wild type or *ubr1*Δ cells and incubated with cycloheximide for 2 hours at 25°C or 37°C prior to performing flow cytometry. The results represent the relative fluorescence intensities and standard deviations from three independent experiments. Statistical significance was tested using an unpaired two tailed Student's t-test. (B) Guk1-7-GFP was expressed in wild type, *ubr1*Δ, *san1*Δ, and *ubr1*Δ*san1*Δ cells and incubated with cycloheximide for 2 hours at 25°C or 37°C prior to performing flow cytometry. The results represent the average and standard deviations from three independent experiments. Statistical significance was tested using a one-way ANOVA and a Tukey HSD post-hoc test. *, **, and ns denote $P < 0.05$, $P < 0.01$, and not significant, respectively. (C) Pro3-1-GFP expressing cells were grown and treated as in B. Samples were analysed using a one-way ANOVA followed by Tukey's post hoc test, ** denotes $P < 0.01$.

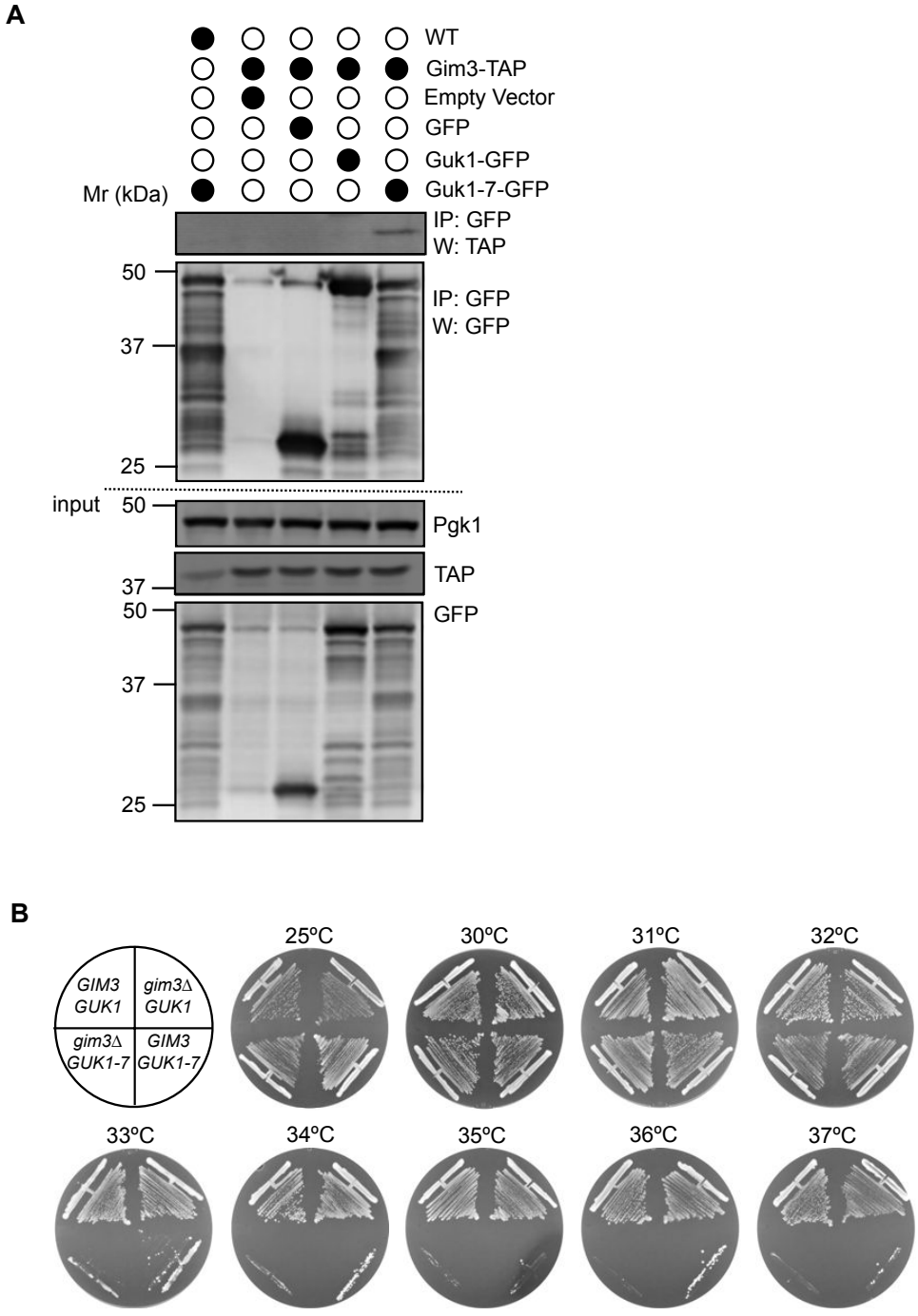


**Figure 2.14:** Guk1-7-GFP Gim3 interaction and viability assay.

**Figure 2.14:** (Previous page) Guk1-7-GFP Gim3 interaction and viability assay. (A) Guk1-7-GFP was immunoprecipitated from wild type or Gim3-TAP expressing cells incubated at 25°C and then immunoblotted with anti-TAP, anti-GFP, or anti-Pgk1 antibodies. (B) Viability assay. Wild type, *gim3*Δ, guk1-7, or double guk1-7, *gim3*Δ cells were streaked on rich media plates and incubated for two days at the indicated temperatures.

# Chapter 3

# Recurrent Background Mutations in *WHI2* Alter Proteostasis and Impair Degradation of Cytosolic Misfolded Proteins in *Saccharomyces cerevisiae*

## 3.1 Introduction

Protein homeostasis (proteostasis) is maintained by an extensive protein quality control network that promotes and mediates protein folding by molecular chaperones and prevents the accumulation of misfolded proteins by targeting them for degradation via the ubiquitin proteasome system or autophagy [1]. The proteostatic balance can be challenged by exposure to a range of intrinsic or extrinsic stressors, which require the cell to mount an adequate response, most notably by regulating the expression of protein quality control network elements in a concerted manner. Inadequate management of misfolded proteins can have deleterious consequences,

such as aggregation, which is characteristic of some neurodegenerative diseases that include Alzheimer's, Parkinson's, and ageing [11].

Proteasomal degradation of misfolded cytosolic proteins is mediated by several quality control E3 ubiquitin ligases, which typically work in concert with other chaperone proteins to recognize their substrates [178, 203]. For instance, Hsp110 Sse1, which acts as a nucleotide exchange factor, was shown to promote ubiquitination by the Ubr1 E3 ligase in yeast [74]. As well, we proposed that the Ydj1 Hsp40 co-chaperone acts as a substrate adaptor for the Rsp5 E3 ligase upon acute heat stress [52]. In other cases, chaperone proteins are also required to promote proteolysis. The Hsp40 co-chaperone Sis1 for example, is necessary for the translocation of misfolded cytosolic proteins to the nucleus where most proteasomes reside [140]. We also recently showed that the yeast prefoldin subunit Gim3 is required to promote proteolysis of cytosolic proteins misfolded due to missense mutations by preventing their aggregation [206]. Therefore, although chaperone proteins primarily promote polypeptide folding and assembly, they may also play a key role in the clearance of misfolded proteins. Understandably, the relationship between the folding and degradation machineries is complex. For example, the structurally related chaperone regulatory proteins Bag1 and Bag2, respectively promote and inhibit the degradation of cytosolic misfolded proteins by the CHIP E3 quality control ligase [85, 86, 207]. Therefore, a major challenge is to understand how changes in the intricate protein quality control network can perturb proteostasis, for instance by shifting the balance between folding and proteolysis.

Temperature sensitive alleles of essential genes in *S. cerevisiae* are invaluable model substrates that can be employed to characterize components of the protein quality control machinery [70, 101, 135, 136, 146, 206]. We previously identified the E3 ubiquitin ligase Ubr1 from a genetic screen for factors involved in degradative protein quality control of Guk1-7, a thermally unstable mutant allele of the guanylate kinase Guk1 [206]. Ubr1 activity alone, however, was not sufficient to account for the bulk of substrate degradation. Therefore, we performed a targeted flow cytometry based screen using a panel of E3 mutant strains. Using this approach, we identified a surprising number of yeast strains with impaired degradation. However, following whole genome sequencing we identified numerous secondary mutations in the stress response gene *WHI2*, which were responsible

for the impaired proteolysis of the misfolded model substrate. We linked this phenotype to a deficiency of the Msn2/Msn4 transcription factor response that altered the cell's capacity to adeptly degrade cytosolic misfolded proteins.

## 3.2 Methods

### 3.2.1 Yeast Strains, Media, and Growth Conditions

The *S. cerevisiae* strains used in this study are listed in Table 3.1 and Table 3.2. Yeast strains were cultured in synthetic media with 2% dextrose (lacking the appropriate amino acids for plasmid selection) or YPD (1% yeast extract, 2% peptone, 2% dextrose) and grown at 25°C with shaking unless indicated otherwise. When not specified otherwise, cultures in log phase were obtained by diluting overnight saturated cultures grown at 25°C to an OD600 = 0.2 and grown for 4–6 hours until log phase OD600 = 0.8–1.0 was reached.

**Table 3.1:** Yeast strains used in Chapter 3

| Strain ID | Alias | Genotype | Source |
|---|---|---|---|
| YTM 408 | BY4741 | *his3Δ1, leu2Δ0, ura3Δ0, met15Δ0* | Open Biosystems Collection |
| YTM 409 | BY4742 | *his3Δ1, leu2Δ0, ura3Δ0, lys2Δ0* | Open Biosystems Collection |
| YTM 445 | *ssa1-45* | *his3Δ11, leu2Δ3, ura3Δ52, trp1Δ1* | T. Mayor |
| YTM 639 | *rsp5-1* | *his3Δ1, leu2Δ, ura3Δ0, met15Δ0, RSP5::rsp5-1-KanMX* | T. Mayor |
| YTM 660 | *ydj1Δ* | *his3Δ1, leu2Δ, ura3Δ0, ydj1Δ::KanMX* | T. Mayor |
| YTM 1867 | *asi1Δ* Tetrad 3a | *his3Δ1, leu2Δ0, ura3Δ0, MET15, LYS2, asi1Δ::KanMX4, whi2-1* | This thesis |
| YTM 1868 | *asi1Δ* Tetrad 3b | *his3Δ1, leu2Δ0, ura3Δ0, met15Δ0, lys2Δ0, asi1Δ::KanMX4, WHI2* | This thesis |
| YTM 1869 | *ASI1* Tetrad 3c | *his3Δ1, leu2Δ0, ura3Δ0, MET15, LYS2, whi2-1* | This thesis |

*Continued on next page*

| Strain ID | Alias | Genotype | Source |
|---|---|---|---|
| YTM 1870 | *ASI1* Tetrad 3d | *his3Δ1, leu2Δ0, ura3Δ0, met15Δ0, lys2Δ0, WHI2* | This thesis |
| YTM 1857 | *ASI1* Tetrad 1a | *his3Δ1, leu2Δ0, ura3Δ0, MET15, lys2Δ0, whi2-1* | This thesis |
| YTM 1856 | *ASI1* Tetrad 4c | *his3Δ1, leu2Δ0, ura3Δ0, MET15, lys2Δ0, WHI2* | This thesis |
| YTM 1871 | *asi1*Δ Tetrad 3a / BY4741 | *his3Δ1/his3Δ1, leu2Δ0/leu2Δ0, ura3Δ0/ura3Δ0, met15Δ0/MET15, LYS2/lys2Δ0, asi1Δ::KanMX4/ASI1, whi2-1/WHI2* | This thesis |
| YTM 1872 | *asi1*Δ Tetrad 3a / *asi1*Δ | *his3Δ1/his3Δ1, leu2Δ0/leu2Δ0, ura3Δ0/ura3Δ0, met15Δ0/MET15, LYS2/lys2Δ0, asi1Δ::KanMX4/asi1Δ::KanMX4, whi2-1/whi2-1* | This thesis |
| YTM 1873 | *asi1*Δ Tetrad 3a / *das1*Δ | *his3Δ1/his3Δ1, leu2Δ0/leu2Δ0, ura3Δ0/ura3Δ0, met15Δ0/MET15, LYS2/lys2Δ0, asi1Δ::KanMX4/ASI1, DAS1/das1Δ::KanMX4, whi2-1/whi2-2* | This thesis |
| YTM 1874 | *asi1*Δ Tetrad 3a / *fap1*Δ | *his3Δ1/his3Δ1, leu2Δ0/leu2Δ0, ura3Δ0/ura3Δ0, met15Δ0/MET15, LYS2/lys2Δ0, asi1Δ::KanMX4/ASI1, FAP1/fap1Δ::KanMX4, whi2-1/whi2-3* | This thesis |
| YTM 1875 | *asi1*Δ Tetrad 3a / *hrt3*Δ | *his3Δ1/his3Δ1, leu2Δ0/leu2Δ0, ura3Δ0/ura3Δ0, met15Δ0/MET15, LYS2/lys2Δ0, asi1Δ::KanMX4/ASI1, HRT3/hrt3Δ::KanMX4, whi2-1/whi2-4* | This thesis |
| YTM 1876 | *asi1*Δ Tetrad 3a / *hul5*Δ | *his3Δ1/his3Δ1, leu2Δ0/leu2Δ0, ura3Δ0/ura3Δ0, met15Δ0/MET15, LYS2/lys2Δ0, asi1Δ::KanMX4/ASI1, HUL5/hul5Δ::KanMX4, whi2-1/whi2-5* | This thesis |
| YTM 1877 | *asi1*Δ Tetrad 3a / *ufd2*Δ | *his3Δ1/his3Δ1, leu2Δ0/leu2Δ0, ura3Δ0/ura3Δ0, met15Δ0/MET15, LYS2/lys2Δ0, asi1Δ::KanMX4/ASI1, UFD2/ufd2Δ::KanMX4, whi2-1/whi2-6* | This thesis |

*Continued on next page*

| Strain ID | Alias | Genotype | Source |
|---|---|---|---|
| YTM 1878 | *asi1*Δ Tetrad 3a / *ufd4*Δ | *his3Δ1/his3Δ1, leu2Δ0/leu2Δ0, ura3Δ0/ura3Δ0, met15Δ0/MET15, LYS2/lys2Δ0, asi1Δ::KanMX4/ASI1, UFD4/ufd4Δ::KanMX4, whi2/whi2-7* | This thesis |
| YTM 1879 | *asi1*Δ Tetrad 3b / BY4741 | *his3Δ1/his3Δ1, leu2Δ0/leu2Δ0, ura3Δ0/ura3Δ0, met15Δ0/MET15, LYS2/lys2Δ0, asi1Δ::KanMX4/ASI1, WHI2/WHI2* | This thesis |
| YTM 1880 | *asi1*Δ Tetrad 3b / *asi1*Δ | *his3Δ1/his3Δ1, leu2Δ0/leu2Δ0, ura3Δ0/ura3Δ0, met15Δ0/MET15, LYS2/lys2Δ0, asi1Δ::KanMX4/asi1Δ::KanMX4, WHI2/whi2-1* | This thesis |
| YTM 1881 | *asi1*Δ Tetrad 3b / *das1*Δ | *is3Δ1/his3Δ1, leu2Δ0/leu2Δ0, ura3Δ0/ura3Δ0, met15Δ0/MET15, LYS2/lys2Δ0, asi1Δ::KanMX4/ASI1, DAS1/das1Δ::KanMX4, WHI2/whi2-2* | This thesis |
| YTM 1882 | *asi1*Δ Tetrad 3b / *fap1*Δ | *his3Δ1/his3Δ1, leu2Δ0/leu2Δ0, ura3Δ0/ura3Δ0, met15Δ0/MET15, LYS2/lys2Δ0, asi1Δ::KanMX4/ASI1, FAP1/fap1Δ::KanMX4, WHI2/whi2-3* | This thesis |
| YTM 1883 | *asi1*Δ Tetrad 3b / *hrt3*Δ | *his3Δ1/his3Δ1, leu2Δ0/leu2Δ0, ura3Δ0/ura3Δ0, met15Δ0/MET15, LYS2/lys2Δ0, asi1Δ::KanMX4/ASI1, HRT3/hrt3Δ::KanMX4, WHI2/whi2-4* | This thesis |
| YTM 1884 | *asi1*Δ Tetrad 3b / *hul5*Δ | *his3Δ1/his3Δ1, leu2Δ0/leu2Δ0, ura3Δ0/ura3Δ0, met15Δ0/MET15, LYS2/lys2Δ0, asi1Δ::KanMX4/ASI1, HUL5/hul5Δ::KanMX4, WHI2/whi2-5* | This thesis |
| YTM 1885 | *asi1*Δ Tetrad 3b / *ufd2*Δ | *his3Δ1/his3Δ1, leu2Δ0/leu2Δ0, ura3Δ0/ura3Δ0, met15Δ0/MET15, LYS2/lys2Δ0, asi1Δ::KanMX4/ASI1, UFD2/ufd2Δ::KanMX4, WHI2/whi2-6* | This thesis |
| YTM 1886 | *asi1*Δ Tetrad 3b / *ufd4*Δ | *his3Δ1/his3Δ1, leu2Δ0/leu2Δ0, ura3Δ0/ura3Δ0, met15Δ0/MET15, LYS2/lys2Δ0, asi1Δ::KanMX4/ASI1, UFD4/ufd4Δ::KanMX4, WHI2/whi2-7* | This thesis |

*Continued on next page*

| Strain ID | Alias | Genotype | Source |
|---|---|---|---|
| YTM 1744 | *msn2*Δ | *his3*Δ*1, leu2*Δ*0, ura3*Δ*0, met15*Δ*0, msn2*Δ*::KanMX4* | Open Biosystems Collection |
| YTM 1745 | *msn4*Δ | *his3*Δ*1, leu2*Δ*0, ura3*Δ*0, met15*Δ*0, msn4*Δ*::KanMX4* | Open Biosystems Collection |
| YTM 1691 | *whi2*Δ | *his3*Δ*1, leu2*Δ*0, ura3*Δ*0, met15*Δ*0, whi2*Δ*::KanMX4* | Open Biosystems Collection |
| YTM 1690 | *glo4*Δ | *his3*Δ*1, leu2*Δ*0, ura3*Δ*0, met15*Δ*0, glo4*Δ*::KanMX4* | Open Biosystems Collection |

### 3.2.2 Plasmids

Plasmids used in this study are listed in Table 3.3. Guk1-GFP (BPM453), Guk1-7-GFP (BPM458), and Guk1-7-$His_6$ (BPM717) expressed from the GPD1 promoter in pRS313 were generated in a previous study [206]; Guk1-7-GFP was subcloned with ApaI and SacI sites in pRS315 to generate BPM609 and with XhoI and SacII sites in pRS316 to generate BPM781. To generate the E3 ligase addback plasmids (BPM748, *ASI1*; BPM749, *DAS1*; BPM750, *FAP1*; BPM751, *HRT3*; BPM752, *HUL5*; BPM753, *UFD2*; BPM754, *UFD4*), the open reading frames and approximately 500 bp of both endogenous 5' and 3'UTR was PCR amplified from genomic DNA (BY4741) and inserted in pRS316 using XhoI and XmaI sites for all but *HUL5* where SacII and XhoI sites were used. The *WHI2* (BPM863, BPM914) addback plasmids were generated as for the E3 ligases except ligated into pRS315 or pRS316 using SacI and XmaI sites, respectively.

### 3.2.3 Flow Cytometry

Cells in log phase were treated with 100 $\mu$g/mL cycloheximide and incubated at either 25°C or 37°C as indicated. GFP fluorescence was measured for 50,000 cells using a FACSCalibur flow cytometer. Median GFP fluorescence values were obtained using FlowJo software. For chase experiments, percentage remaining values

**Table 3.2:** E3 ligase collection used for screening

| Systematic Name | Standard Name | Well No. | Systematic Name | Standard Name | Well No. |
|---|---|---|---|---|---|
| YMR258C | ROY1 | A1 | YHL010C | ETP1 | D1 |
| YOL013C | HRD1 | A2 | YLR368W | MDM30 | D2 |
| YOL054W | PSH1 | A3 | YER116C | SLX8 | D3 |
| YML068W | ITT1 | A4 | YLR352W | n/a | D4 |
| YDR049W | VMS1 | A5 | YAL002W | VPS8 | D5 |
| YDR131C | n/a | A6 | YDR360W | TFB3 | D6 |
| YDR143C | SAN1 | A7 | YLR024C | UBR2 | D7 |
| YHR115C | DMA1 | A8 | YMR119W | ASI1 | D8 |
| YKL010C | UFD4 | A9 | YNL008C | ASI3 | D9 |
| YKL034W | TUL1 | A10 | YGL003C | CDH1 | D10 |
| YJL149W | DAS1 | A11 | YMR247C | RKR1 | D11 |
| YLR247C | IRC20 | A12 | YNL023C | FAP1 | D12 |
| YNL230C | ELA1 | B1 | YJL157C | FAR1 | E1 |
| YKR017C | HEL1 | B2 | YDL013W | SLX5 | E2 |
| YDR265W | PEX10 | B3 | YBR203W | COS111 | E3 |
| YDR306C | n/a | B4 | YKL059C | MPE1 | E4 |
| YDR313C | PIB1 | B5 | YER068W | NOT4 | E5 |
| YIL001W | n/a | B6 | YMR026C | PEX12 | E6 |
| YCR066W | RAD18 | B7 | YJL210W | PEX2 | E7 |
| YJR036C | HUL4 | B8 | YOR191W | ULS1 | E8 |
| YDL190C | UFD2 | B9 | YDR255C | RMD5 | E9 |
| YBR062C | n/a | B10 | YGL131C | SNT2 | E10 |
| YNL116W | DMA2 | B11 | YLR005W | SSL1 | E11 |
| YBR280C | SAF1 | B12 | YDR103W | STE5 | E12 |
| YIL030C | DOA10 | C1 | YDR266C | HEL2 | F1 |
| YBR114W | RAD16 | C2 | YOL138C | RTC1 | F2 |
| YDR457W | TOM1 | C3 | YBR158W | AMN1 | F3 |
| YGL141W | HUL5 | C4 | YJR052W | RAD7 | F4 |
| YGR184C | UBR1 | C5 | YDR132C | n/a | F5 |
| YDL074C | BRE1 | C6 | YLR108C | n/a | F6 |
| YLR224W | n/a | C7 | YMR080C | NAM7 | F7 |
| YLR097C | HRT3 | C8 | YPL046C | ELC1 | F8 |
| YNL311C | SKP2 | C9 | YJR090C | GRR1 | F9 |
| YDR219C | MFB1 | C10 | YJL204C | RCY1 | F10 |
| YLR427W | MAG2 | C11 | | | |
| YOR080W | DIA2 | C12 | | | |

**Table 3.3:** Plasmids used in Chapter 3

| Plasmid ID | Name | Auxotrophic Marker | Plasmid Type | Source |
|---|---|---|---|---|
| BPM 42 | pRS316 | Ura | CEN/ARS | RJD Collection |
| BPM 45 | pRS313 | His | CEN/ARS | RJD Collection |
| BPM 49 | pRS315 | Leu | CEN/ARS | RJD Collection |
| BPM 390 | $P_{YDJ1}$-YDJ1 | Ura | CEN/ARS | E. Craig |
| BPM 453 | $P_{GPD}$-Guk1-GFP | His | CEN/ARS | T. Mayor |
| BPM 458 | $P_{GPD}$-Guk1-7-GFP | His | CEN/ARS | T. Mayor |
| BPM 559 | $P_{SSA1}$-SSA1 | Ura | CEN/ARS | T. Mayor |
| BPM 573 | $P_{RSP5}$-RSP5 | Ura | CEN/ARS | T. Mayor |
| BPM 575 | $P_{RSP5}$-RSP5(C777A) | Ura | CEN/ARS | T. Mayor |
| BPM 609 | $P_{GPD}$-Guk1-7-GFP | Leu | CEN/ARS | T. Mayor |
| BPM 708 | $P_{CUP1}$-Deg1-GFP | Ura | CEN/ARS | T. Mayor |
| BPM 718 | $P_{GPD}$-Guk1-7-GFP | Ura | CEN/ARS | T. Mayor |
| BPM 748 | $P_{ASI1}$-ASI1 | Leu | CEN/ARS | This thesis |
| BPM 749 | $P_{DAS1}$-DAS1 | Leu | CEN/ARS | This thesis |
| BPM 750 | $P_{FAP1}$-FAP1 | Leu | CEN/ARS | This thesis |
| BPM 751 | $P_{HRT3}$-HRT3 | Leu | CEN/ARS | This thesis |
| BPM 752 | $P_{HUL5}$-HUL5 | Leu | CEN/ARS | This thesis |
| BPM 753 | $P_{UFD2}$-UFD2 | Leu | CEN/ARS | This thesis |
| BPM 754 | $P_{UFD4}$-UFD4 | Leu | CEN/ARS | This thesis |
| BPM 914 | $P_{WHI2}$-WHI2 | Ura | CEN/ARS | This thesis |

were calculated by normalizing the median GFP fluorescence intensity values for each time point to the initial t = 0 measurement. To calculate the relative loss of fluorescence for single time-point measurements, the difference of GFP fluorescence values for samples incubated at 25°C and 37°C was normalized to that of the 25°C sample. To perform multiple strain comparisons, the relative loss of fluorescence values (as calculated above) for each strain was normalized to that of the wild type BY4741 strain.

### 3.2.4 Sequencing

Whole-genome sequencing and library preparation was performed at the NextGen Sequencing facility at the Biodiversity Research Centre of the University of British Columbia. Yeast cells were grown overnight to saturation in YPD at 25°C and genomic DNA was extracted using standard protocols [208]. Barcoded libraries for each strain were created according to Illumina protocols (Illumina 2011, all rights reserved) and 100 bp paired end fragments were sequenced by pooling all six libraries and run on a single lane of an Illumina HiSeq2000. The short-read aligner BWA was used to map sequence reads to the yeast reference genome S288C version R64 (Saccharomyces Genome Database, SDG) [209]. Single-nucleotide variants (SNVs) were identified using the SAMtools toolbox and then each SNV was annotated with a custom-made Perl script using gene data downloaded from SDG on January 21, 2014 [210]. IGV viewer was used to visually inspect read alignments in the regions of candidate SNVs [211, 212].

### 3.2.5 *WHI2* Plate Assay

Yeast cultures were grown overnight at 25°C in 5 mL YPD to OD600 = 1–2 and then diluted to OD600 = 0.2 in 5 mL YPD and left to grow for 2 hours at 25°C. 1 mL was kept as an untreated control and the remaining 4 mL of culture was treated with 200 mM acetic acid for 4 hours at 25°C. Treated and untreated cultures were serially diluted fivefold in 1X PBS and plated on solid media. Plates were incubated at 30°C for 2 days before being imaged with a Gel Doc XR+ System (Bio-Rad).

### 3.2.6 Turnover Assay

Cells transformed with a Deg1-GFP containing plasmid were grown to saturation overnight at 30°C, diluted to OD600 = 0.2 and then incubated for 3 hours at 30°C. Deg1-GFP expression was induced for 4 hours at 30°C with 100 $\mu$M copper sulphate and then 100 $\mu$g/mL cycloheximide was added with samples collected at the indicated time points. Cells were lysed with glass beads in lysis buffer (50 mM Tris-HCl, pH 7.5, 1% Tx-100, 0.1% SDS, 150 mM NaCl, 5 mM EDTA, 1 mM PMSF, 1X protease inhibitor mix (Roche)). Protein concentrations were measured using the DC Protein Assay (Bio-Rad) and normalized prior to resolving equal volumes by SDS-PAGE. Membranes were immunoblotted with mouse anti-GFP (Roche, 1:2,500) and rabbit anti-Pgk1 (Acris Antibodies, 1:10,000) primary antibodies and secondary antibodies (Mandel Scientific, 1:10,000). Membranes were scanned and analyzed with an Odyssey Infrared imaging system (LI-COR).

### 3.2.7 Solubility Assay

Cells expressing Guk1-7-GFP in log phase were incubated at either 25°C or 37°C for 20 minutes. Cells were lysed with glass beads in native lysis buffer (20 mM HEPES, pH 7.5, 0.5% NP-40, 200 mM NaCl, 1X protease inhibitor mix (Roche), 1 mM 1,10 phenanthroline, 1 mM EDTA) and centrifuged at 2,000 g for 5 minutes at 4°C. Protein concentrations were determined using the DC Protein Assay (Bio-Rad) and normalized to 0.5 $\mu$g/$\mu$L. Samples were then fractionated into soluble and pellet fractions by centrifuging at 16,000 g for 10 minutes at 4°C. The pellet fraction was washed twice with native lysis buffer prior to being resuspended in 1X SDS buffer (50 mM Tris-HCl, pH 6.8, 2% SDS, 3% glycerol). Equal volumes of total cell lysate, soluble, and pellet fractions were resolved by SDS-PAGE. Membranes were immunoblotted with mouse anti-GFP (Roche, 1:2,500) and secondary antibodies (Mandel Scientific, 1:10,000).

### 3.2.8 Guk1-7-GFP Ubiquitination

Cells expressing ectopic Guk1-7-GFP, Guk1-GFP, or a control empty vector (pRS313), were grown to log phase and then lysed with glass beads in native lysis buffer (20 mM HEPES, pH 7.5, 0.5% NP-40, 200 mM NaCl, 1X protease

inhibitor mix (Roche), 1 mM 1,10 phenanthroline, 1 mM EDTA, 10 mM iodoacetamide). GFP-tagged Guk1-7 was pulled down with GFP-Trap coupled agarose beads (Chromotek; 10 $\mu$L per 3 mg of lysate) for 2 hours at 4°C. Beads were washed three times in lysis buffer before samples were eluted with 3X SDS buffer. Equal volumes of samples were resolved by SDS-PAGE. Membranes were immunoblotted with mouse anti-GFP (Roche, 1:2,500), rabbit anti-Pgk1 (Acris Antibodies, 1:10,000), and mouse anti-ubiquitin (Millipore, 1:2,500) primary antibodies and secondary antibodies (Mandel Scientific, 1:10,000).

### 3.2.9 Cellular Thermal Shift Assay (CETSA)

Cells expressing Guk1-7-$His_6$ were grown to log phase and then lysed with glass beads in 200 $\mu$L native lysis buffer. The soluble fraction was collected by spinning at 16,000 g for 10 minutes at 4°C on a benchtop centrifuge. Protein concentration was determined by the DC Protein Assay (Bio-Rad) and samples were normalized to 2 $\mu$g/mL in native lysis buffer and 50 $\mu$L aliquots were distributed into PCR strip tubes. Samples were heated using a CETSA PCR Program (25°C, 3:00; 30–50°C gradient, 10:00; 25°C, 1:00) on a thermocycler. The resulting soluble fraction was collected by centrifugation at 16,000 g for 10 minutes at 4°C and one third volume of 3X SDS buffer was added to samples prior to resolving equal volumes by SDS-PAGE. Membranes were immunoblotted with a mouse anti-His primary antibody (Ablab, 1:2,500) and a secondary antibody (Mandel Scientific, 1:10,000).

### 3.2.10 Statistical Analysis

Data are presented as mean $\pm$ SD unless otherwise stated. Comparisons were made using the two-tailed Student's t-test and differences were considered significant at a p-value of $< 0.05$. When indicated, multiple strains were compared with a one-way ANOVA and post-hoc Tukey HSD to assess significance.

## 3.3 Results

### 3.3.1 Multiple Strains From the Yeast Knockout Collection Display Impaired Proteostasis

To monitor the stability of the Guk1-7 mutant by flow cytometry in yeast cells, we previously generated a C-terminal GFP fusion protein ectopically expressed from the constitutive GPD promoter [206]. As we reported, Guk1-7-GFP levels are ∼50% and ∼85% lower after incubating cells at 37°C in the presence of the translation inhibitor cycloheximide for two and four hours, respectively (Figure 3.1A). To identify another E3 ubiquitin ligase responsible for the degradation of the Guk1-7-GFP model substrate, we screened a collection of 70 non-essential E3 ligase deletion strains that were individually transformed with a CEN/ARS plasmid encoding the Guk1-7-GFP fusion. Cultures were grown at 25°C and then divided and incubated in the presence of CHX for two hours at 25°C and 37°C before performing flow cytometry analysis (Figure 3.1B). For each deletion strain, the relative difference in median GFP fluorescence intensities from samples incubated at 25°C and 37°C was normalized to that of the wild type strain, to calculate a relative loss of Guk1-7-GFP fluorescence (Figure 3.1B). The collection was screened twice and strains that had a relative loss of Guk1-7-GFP fluorescence value of 0.75 or lower in at least one of the two rounds were selected for further validation. A total of 20 strains met this criterion and were further analysed by flow cytometry in three independent experiments (Figure 3.1C). In agreement with our previous findings, deleting *UBR1* led to a 25% lower averaged loss of Guk1-7-GFP fluorescence compared to that of wild type cells [206]. Surprisingly, we identified twelve E3 ligase deletion strains with a greater impairment in Guk1-7-GFP degradation than that observed in *ubr1*Δ cells. Of these, seven strains had an averaged relative loss of Guk1-7-GFP fluorescence value of 0.5 or lower. These results indicate that an unusually high number of strains from our yeast knockout collection have a reduced capacity to eliminate misfolded cytosolic proteins.

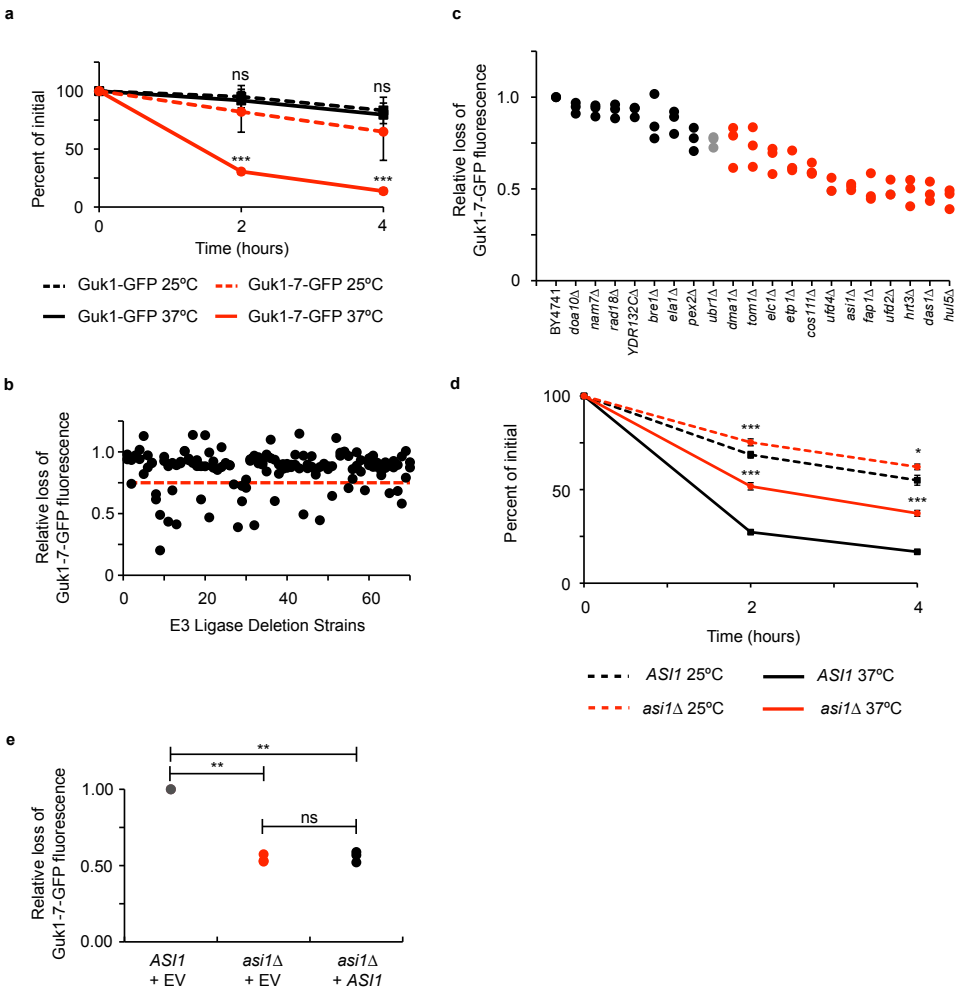


**Figure 3.1:** Flow cytometry based screen for E3 ligases targeting Guk1-7-GFP for degradation.

**Figure 3.1:** (Previous page) Flow cytometry based screen for E3 ligases targeting Guk1-7-GFP for degradation. a) CHX chase assay. Wild type cells expressing ectopic Guk1-GFP or Guk1-7-GFP were incubated with CHX for 4 hours at 25°C or 37°C and samples were collected at the indicated time points. Results represent the mean and standard deviation of three independent experiments. *** and ns denote $p < 0.005$ and not significant, respectively. b) E3 ligase screen. Seventy non-essential E3 ligase deletion strains expressing Guk1-7-GFP were incubated with CHX at 25°C or 37°C for 2 hours and then analyzed by flow cytometry. Red line demarks strains with a relative loss of fluorescence value of 0.75 or lower. c) Triplicate validation. The top 20 strains were selected for further validation by flow cytometry with experiments performed as in b. Data points in red correspond to strains displaying Guk1-7-GFP stabilization levels higher than that of *ubr1*Δ. d) Cycloheximide chase assay. Wild type or *asi1*Δ cells expressing Guk1-7-GFP were incubated with CHX at 25°C and 37°C for two hours prior to flow cytometry analysis. Results represent the mean and standard deviation of three independent experiments. * and *** denote $p < 0.05$ and $p < 0.005$, respectively. e) Wild type and *asi1*Δ cells co-expressing Guk1-7-GFP and an empty vector (EV) or *ASI1* were treated as in d. ns and ** denote not significant and $p < 0.01$, respectively.

### 3.3.2 A Secondary Mutation in *WHI2* Co-Segregates with Increased Guk1-7-GFP Stability

We confirmed the results of our screen by performing CHX chase experiments with cells lacking *ASI1*, a member of the nuclear inner membrane Asi ubiquitin ligase complex (Figure 3.1D) [213]. To determine whether the impaired turnover of the model substrate was caused by the absence of *ASI1*, we co-expressed Guk1-7-GFP with *ASI1* under its endogenous promoter or with a control empty vector (EV). Addition of the wild type *ASI1* did not re-establish normal model substrate degradation levels (Figure 3.1E). We obtained similar results with the six remaining E3 ligase deletions that displayed stabilization values comparable with *ASI1* (*DAS1*, *FAP1*, *HRT3*, *HUL5*, *UFD2*, and *UFD4*) (Figure 3.2 and Figure 3.3). This data implied that the decrease in Guk1-7-GFP degradation conferred by these strains could not be attributed to the absence of the assessed E3 ubiquitin ligase, but rather to that of

another factor, such as a background mutation or potentially an epigenetic factor. Similarly, we previously isolated several hits in a genome wide screen for factors involved in degradative protein quality control (*e.g.*, YER071C and YJL141C) that we could not confirm after addback experiments expressing the deleted gene from a plasmid, indicating that this phenomenon was not limited to E3 ligase mutant cells [206].

We next sought to determine whether the observed phenotype was caused by a single background mutation. Therefore, we performed tetrad analysis on the haploid spores obtained from backcrossing the MATa *asi1*$\Delta$ strain to wild type MATalpha BY4742 cells. No discernable difference in growth rate was seen across the dissected spores. We then expressed Guk1-7 in seven sets of tetrads for further analysis. While both the KanMX deletion cassette, conferring kanamycin resistance, and the impaired degradation phenotype measured by flow cytometry segregated in the expected 2:2 ratio, the two did not appear to be linked, as is shown by a representative tetrad set (Figure 3.4A). We obtained similar data with *das1*$\Delta$ cells (Figure 3.5). Data from CHX chase experiments confirmed that Guk1-7-GFP levels were significantly higher in tetrad c (*ASI1*) compared to those in the parental wild type and tetrad d strains after a two hour ($p = 0.001$ and $p = 0.0023$) and four hour ($p = 0.025$ and $p = 0.028$) incubation at 37°C (Figure 3.4B). These experiments indicate that the stabilization phenotype in the *asi1*$\Delta$ strain was likely due to background mutations at a single locus.

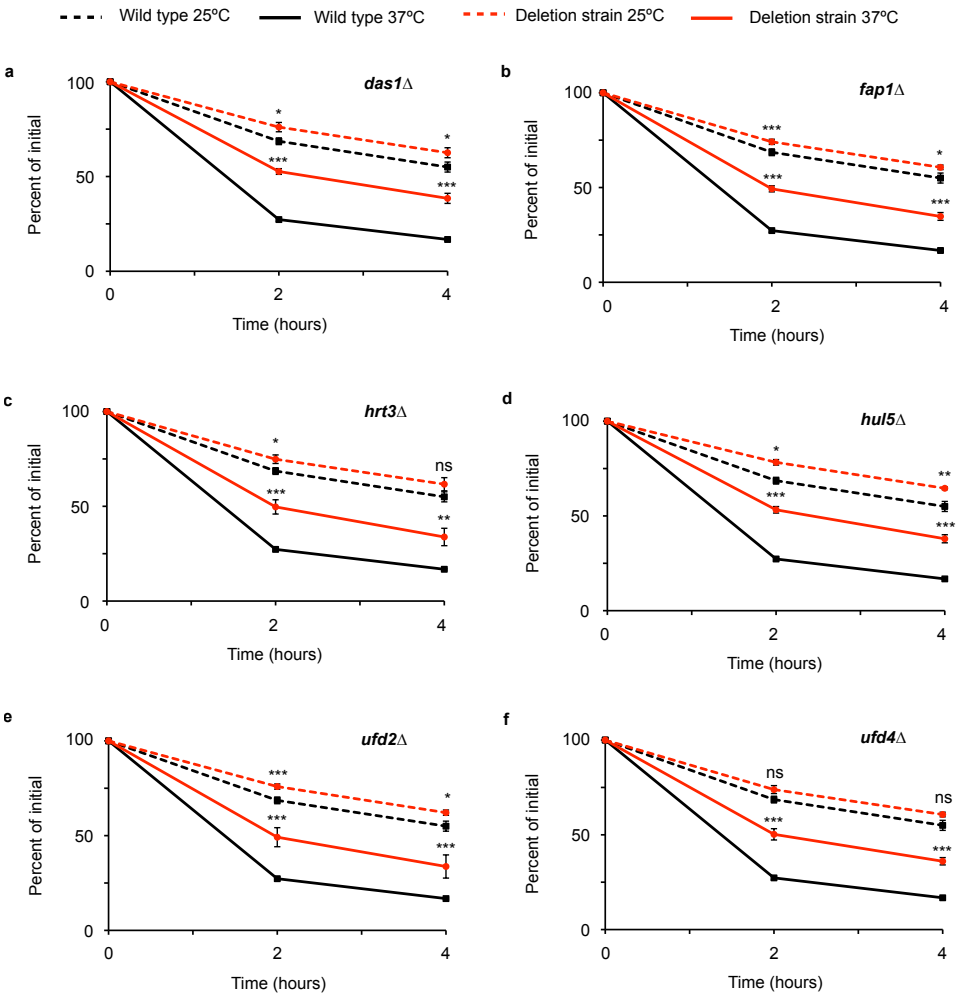


**Figure 3.2:** Guk1-7-GFP degradation in E3 ligase deletion strains. Cycloheximide chase assay. Wild type or the corresponding E3 ligase deletion strain expressing ectopic Guk1-7-GFP were incubated in the presence of CHX at either 25°C or 37°C for four hours and samples were analysed by flow cytometry at the indicated time points. Results represent the mean and standard deviation of three independent experiments. P values were calculated with a two-tailed unpaired Student's t-test (*, **, ***, and ns denote $p < 0.05$, 0.01, 0.005, and not significant, respectively). a) *das1*Δ, b) *fap1*Δ, c) *hrt3*Δ, d) *hul5*Δ, e) *ufd2*Δ, f) *ufd4*Δ.

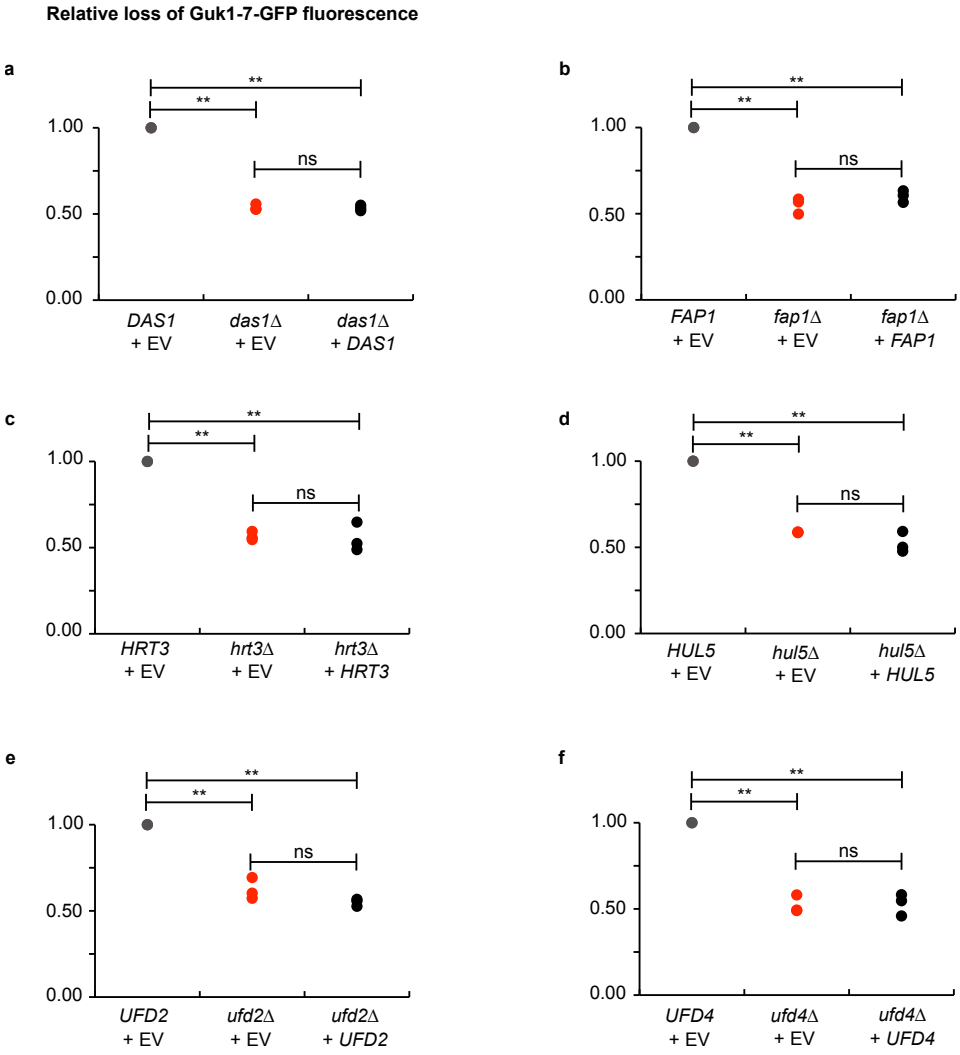


**Figure 3.3:** Guk1-7-GFP stability is not a direct effect of E3 ligase deletion. Wild type and E3 ligase deletion strains expressing Guk1-7-GFP along with an empty vector (EV) control or corresponding E3 gene under its endogenous promoter and terminator were incubated with CHX at 25°C and 37°C for two hours prior to flow cytometry analysis. Results represent three independent experiments. P values were calculated with a one-way ANOVA and post-hoc Tukey HSD to assess significance (** and ns denotes $p < 0.01$ and not significant, respectively). a) *das1*Δ b) *fap1*Δ c) *hrt3*Δ d) *hul5*Δ e) *ufd2*Δ f) *ufd4*Δ.

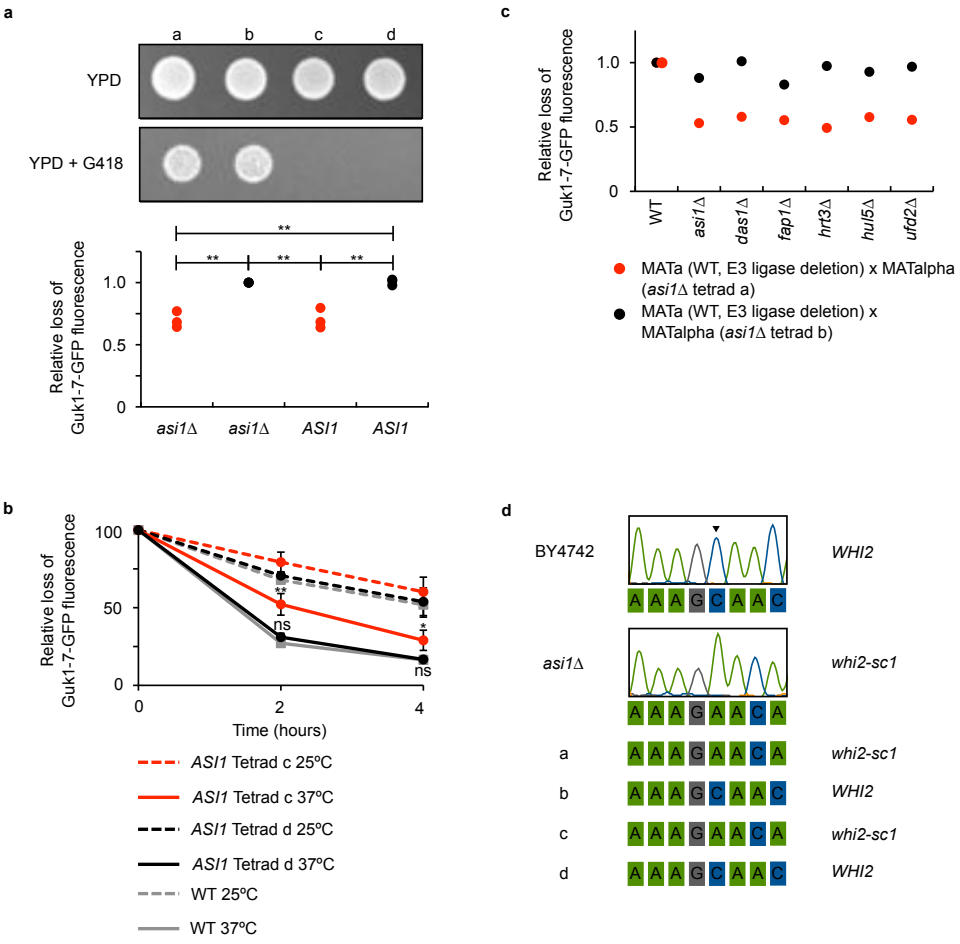


**Figure 3.4:** Mutations in *WHI2* segregate with the Guk1-7-GFP stability phenotype.

**Figure 3.4:** (Previous page) Mutations in *WHI2* segregate with the Guk1-7-GFP stability phenotype. a) Backcross and phenotypic segregation. The MATa *asi1*Δ strain was backcrossed with the wild type MATalpha BY4742 to produce sets of tetrads. Growth was assessed by culturing cells on YPD and 2:2 KanMX deletion marker segregation was observed by spotting onto YPD+G418 plates. This segregation pattern was compared to tetrads expressing Guk1-7-GFP and analyzed by flow cytometry following incubation with CHX at 25°C and 37°C for 2 hours. Results represent three independent experiments and p values were calculated with a one-way ANOVA and post-hoc Tukey HSD to assess significance, ** denotes $p < 0.01$. b) CHX chase assay. Tetrad c and d, produced from the *asi1*Δ backcross, expressing Guk1-7-GFP were incubated with CHX at 25°C and 37°C four hours. Samples were analysed by flow cytometry at the indicated time points. The results represent the mean and standard deviation of three independent experiments. P values were calculated with a two-tailed unpaired Student's t-test (*, **, and ns denote $p < 0.05$, 0.01, and not significant, respectively). c) Complementation test. MATa E3 ligase deletion strains were mated with MATalpha wild type BY4742 and *asi1*Δ cells from tetrad a and b. The resulting diploids expressing Guk1-7-GFP were incubated with CHX for two hours at 25°C and 37°C and analysed by flow cytometry. d) Whole genome sequencing of wild type, *asi1*Δ, and four *asi1*Δ backcross tetrad strains revealed a single base pair deletion in the coding sequence of *WHI2* co-segregates with the Guk1-7-GFP stability phenotype. Arrow head denotes nucleotide base deleted in the *asi1*Δ strain and derivatives.

Next, we performed a complementation test to determine whether the secondary mutations responsible for the stability phenotype observed in the seven E3 ligase deletion strains are in the same locus, or different loci. Heterozygous diploids were produced by mating a wild type strain (BY4742) and each of the seven E3 ligase deletions to two haploids, derived from the *asi1*Δ backcross shown: one, contained the secondary mutation (tetrad a) and the other, did not (tetrad b). Guk1-7-GFP levels were indistinguishable between heterozygous diploids produced from mating tetrad a and BY4741 and diploids produced from crossing tetrad b with any of the E3 deletion mutants, or the wild type BY4741 (Figure 3.4C). Conversely, all heterozygous diploids derived from mating E3 ligase deletions with tetrad a (harbouring the secondary mutation) demonstrated increased

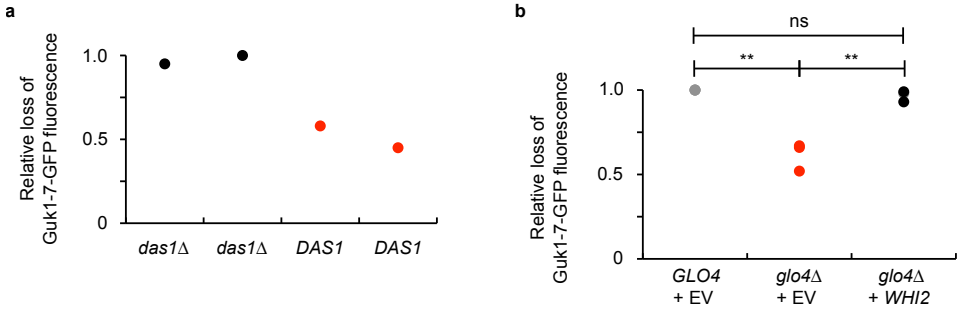


**Figure 3.5:** *das1*Δ tetrad analysis and *WHI2* addback. a) Analysis of one tetrad obtained from backcrossing the MATa *das1*Δ strain with the wild type MATalpha BY4742. Tetrad spores expressing Guk1-7-GFP were incubated with CHX at 25°C and 37°C for two hours prior to flow cytometry analysis. b) Wild type and *glo4*Δ cells co-expressing Guk1-7-GFP and an empty control vector (EV) or *WHI2* were incubated with CHX at 25°C and 37°C for two hours and then analysed by flow cytometry. Results represent three independent experiments and p values were calculated with a one-way ANOVA and post-hoc Tukey HSD to assess significance (** and ns denote $p < 0.01$ and not significant, respectively).

Guk1-7-GFP stability, thereby indicating that they belong to the same complementation group, and suggests that the secondary mutations present in each strain are in the same gene.

To identify the locus containing the secondary mutation, we performed whole-genome sequencing on four haploid tetrads and their parental wild type and *asi1*Δ strains. Secondary mutations in the genes *GLO4* and *WHI2*, which are approximately 3000 bp apart on chromosome fifteen, co-segregated with the strains harbouring the increased Guk1-7-GFP stability phenotype. Interestingly, secondary mutations in the general stress response gene *WHI2* have been identified previously in yeast knockout collections and genome evolution studies [214–216]. We identified a single nucleotide deletion in the coding sequence of *WHI2*. This mutation, hereinafter referred to as *whi2-sc1*, produces a frameshift introducing a premature stop codon and likely results in a loss of *WHI2* function (Figure 3.4D). In contrast, the coding sequence of *GLO4*, a mitochondrial glyoxalase, contained a single missense mutation.

### 3.3.3 Guk1-7-GFP Degradation is Impaired Owing to Secondary Mutations in *WHI2*

To determine whether the mutation in *WHI2* caused the observed stabilization, we expressed the wild type ORF from a plasmid in cells derived from the backcross. Whereas the addition of an empty vector did not rescue the phenotype, addition of *WHI2* re-established normal Guk1-7-GFP degradation levels (Figure 3.6A). Moreover, we observed a similar impairment in the degradation of the Guk1-7-GFP model substrate in *whi2*Δ cells, that could be rescued by the expression of *WHI2* (Figure 3.6B). Intriguingly, we found that *glo4*Δ cells had a similar reduction in Guk1-7-GFP degradation (Figure 3.5B). Subsequent Sanger sequencing of a PCR product amplified from the *WHI2* locus of *glo4*Δ cells identified two point mutations that produce a premature stop codon. These results suggest that the effect observed in glo4Δ cells is attributed to a loss of *WHI2* function, not of *GLO4*, and that loss of *WHI2* function is sufficient to strongly impair degradation of a misfolded cytosolic model substrate.

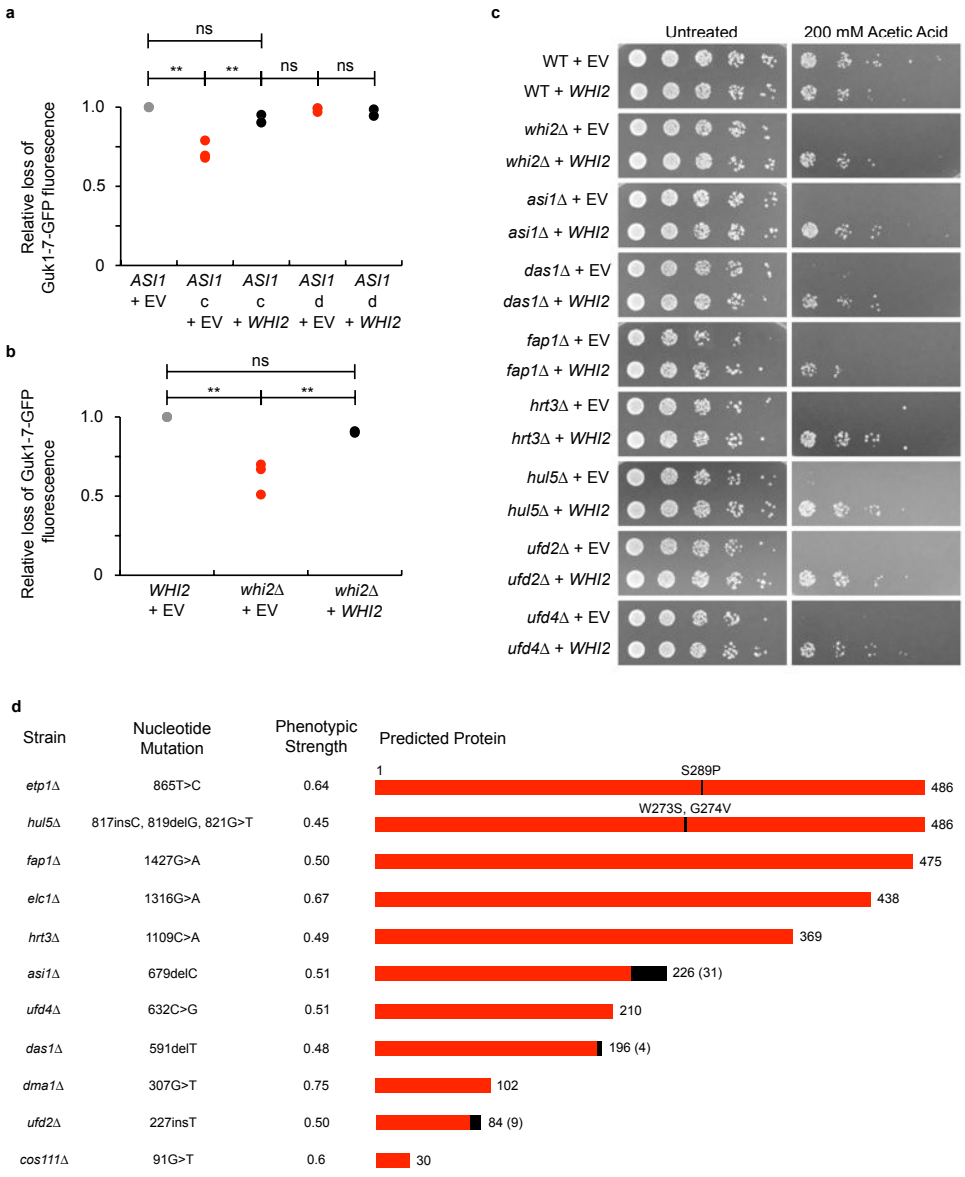


**Figure 3.6:** Absence of *WHI2* leads to Guk1-7-GFP stability.

**Figure 3.6:** (Previous page) Absence of *WHI2* leads to Guk1-7-GFP stability. a) *ASI1* tetrads c and d co-expressing Guk1-7-GFP and a control empty vector (EV) or *WHI2* were incubated with CHX at 25°C and 37°C for two hours and then analysed by flow cytometry. Results represent three independent experiments and p values were calculated with a one-way ANOVA and post-hoc Tukey HSD to assess significance (ns and ** denote not significant and $p < 0.01$, respectively). b) Wild type and *whi2*Δ cells expressing Guk1-7-GFP along with an empty vector (EV) control or *WHI2* were treated and analysed as in a. c) *WHI2* function assay. Diluted overnight cultures of wild type or E3 ligase deletion strains expressing either an empty control vector or *WHI2* were treated with 200 mM acetic acid for four hours prior to serial dilution and spotting onto synthetic drop out plates. Images were taken after two days of growth at 30°C. d) Mutations in *WHI2* were identified by Sanger sequencing of a PCR amplicon spanning 100 bp up and downstream of the start and stop codons. For each strain, the mutations identified are as listed and, the predicted protein length is depicted in red. Black boxes denote the C-terminal mismatch extensions.

We next sought to confirm that *WHI2* was also mutated in the other E3 ligase mutant strains in which Guk1-7-GFP degradation was impaired. Mutations in *WHI2* sensitize cells to exposure to acetic acid, which lends itself to a convenient assay for Whi2 function [214]. The *whi2*Δ and all seven E3 ligase deletion strains were sensitive to acetic acid treatment (Figure 3.6C). Expressing *WHI2* from a plasmid under its endogenous promoter restored cell viability in all strains, confirming data from the complementation test suggesting that all strains contain secondary mutations in the same locus (Figure 3.4C). We proceeded to sequence the entire *WHI2* gene, including approximately one hundred base pairs upstream and downstream of the start and stop codons, in all twenty of the top E3 ligase deletion strains from our screen. Whereas the *ubr1*Δ and six other strains had no apparent mutations, we identified *WHI2* mutations in a total of eleven strains (Figure 3.6D). These consist of: *dma1*Δ, *elc1*Δ, *etp1*Δ, *cos111*Δ, and all seven strains that failed in addback experiments: *asi1*Δ, *das1*Δ, *fap1*Δ, *hrt3*Δ, *hul5*Δ, *ufd2*Δ, and *ufd4*Δ. In two cases, *pex2*Δ and *tom1*Δ, we were unable to obtain unambiguous sequencing results after two independent genomic extractions and sequencing runs. Of the *WHI2* mutations identified, nine are predicted to produce truncated proteins result-

ing from the introduction of a premature stop codon. Three of the nine also contain additional C-terminal extensions (ranging from 4 to 31 amino acids in length) as the result of frameshift mutations. The mutations are relatively evenly dispersed along the length of the protein with the exception of a mutation free region, seventy amino acids in length, found approximately three quarters of the way into the protein. Whereas the different *WHI2* mutations led to varying degrees of impaired Guk1-7-GFP degradation, we did not see a clear correlation between the severity of the Guk1-7-GFP stabilisation phenotype and the predicted Whi2 length in these strains (Figure 3.6D).

### 3.3.4 Reduced Proteostasic Capacity in *WHI2* Mutants is Linked to Msn2

Exposure to stressors such as heat, oxidative or osmotic shock, and nutrient starvation results in the transcriptional activation of approximately 200 genes in yeast [146]. Activation of this general stress response is mediated by binding of the partially-redundant zinc finger transcription factors Msn2 and Msn4 to STREs in the promoters of stress-response genes [146, 217]. Under non-stress conditions, Msn2 is sequestered in the cytoplasm and upon exposure to stress, Msn2 translocates to the nucleus [218, 219]. To determine whether Guk1-7-GFP stability in *WHI2* mutants is linked to reduced Msn2/Msn4 activity, we assessed Guk1-7-GFP levels in single deletions. An absence of *MSN2*, but not *MSN4*, led to a significant increase in Guk1-7-GFP compared to wild type ($p = 0.003$) with levels similar to those seen in *whi2*Δ cells (Figure 3.7A). These data would therefore suggest that decreased Guk1-7-GFP degradation is associated to a general impairment of stress response factors acting downstream of Msn2.

Intriguingly, while performing *WHI2* addback experiments we noticed a pronounced decrease in Guk1-7-GFP stability when adding a second plasmid bearing the auxotrophic marker leucine. To further investigate this observation, we transformed wild type and *whi2-sc1* cells with a plasmid expressing Guk1-7-GFP that contained one of the following selection markers: histidine, uracil, or leucine. Consistent with our previous data, loss of Guk1-7-GFP fluorescence was 53% lower in *whi2-sc1* cells compared to wild type when the histidine marker was used (Figure 3.7B). However, when *whi2-sc1* cells containing the leucine selection marker

were grown in synthetic media without additional leucine, Guk1-7-GFP degradation was mostly impaired and levels were approximately two fold higher. As well, uracil selection resulted in an intermediate phenotype. Leucine was previously shown to activate the TORC1 kinase complex that can also inhibit Msn2/4 [220–222]. One possibility is that Whi2 is only required to maintain Msn2 active when TORC1 is stimulated in the presence of high levels of exogenous leucine. In support of this view, the addition of increasing amounts of leucine restored the impaired Guk1-7-GFP degradation in *whi2-sc1* cells (Figure 3.7C). These data suggest that mutations in *WHI2* only impair proteostasis in conditions where Whi2 is required to maintain Msn2 active.

### 3.3.5 Mutant *WHI2* Impairs Guk1-7-GFP Degradation by Reducing Substrate Ubiquitination

To determine how an absence of *WHI2* results in increased Guk1-7-GFP stabilization we first needed to clarify what aspect of protein quality control is altered in the mutants. We first compared the thermodynamic stability of ectopically expressed Guk1-7 in cellular lysates by CETSA. Solubility decreased rapidly at temperatures above 42°C in extracts from both wild type and *whi2-sc1* strains (Figure 3.8A). While not marked, slightly more Guk1-7 remained soluble in *whi2-sc1* lysates compared to wild type at 46.5°C and 48.8°C ($p = 0.04$ and $p = 0.032$). By contrast, Guk1-7 was slightly, but not significantly, less soluble in *whi2-sc1* cells grown at 25°C or following a short twenty-minute incubation at 37°C ($p = 0.18$ and $p = 0.07$) (Figure 3.8B). Together these data suggest that Whi2 does not markedly influence Guk1-7-GFP degradation by increasing its thermal stability or inducing its aggregation.

It is possible that mutations in *WHI2* might generally alter the ubiquitin proteasome system. However, using the known proteasome substrate Deg1-GFP, we found no significant difference in degradation in *whi2-sc1* cells compared to wild type ($p = 0.31$, 0.4, 0.7, 0.52 for 10, 20, 30, and 60 minute time points, respectively) (Figure 3.8C). We next asked whether an absence of *WHI2* could affect Guk1-7-GFP ubiquitination. Ubiquitin levels were measured following pulldown of Guk1-GFP and Guk1-7-GFP from cultures grown at 25°C. Normalizing the ubiquitin signal to the amount of GFP tagged substrate eluted revealed approxi-

mately 30% less ubiquitinated Guk1-7-GFP in *whi2-sc1* cells compared to wild type (Figure 3.8D). Together these data suggest that mutated *WHI2* could impair Guk1-7-GFP degradation by decreasing substrate ubiquitination.

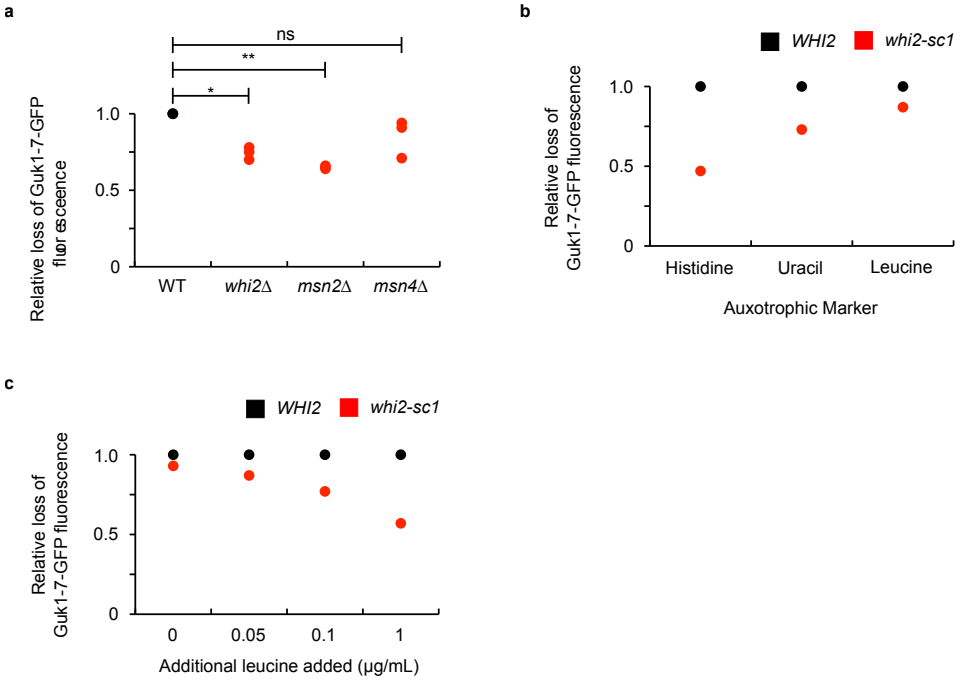


**Figure 3.7:** Msn2 is linked to reduced proteostatic capacity in *WHI2* mutants. a) Wild type, *whi2*Δ, *msn2*Δ, and *msn4*Δ cells expressing Guk1-7-GFP were analysed by flow cytometry following a two hour incubation at 25°C and 37°C in the presence of CHX. P values were calculated with a one-way ANOVA and post-hoc Tukey HSD to assess significance (*, **, and ns denote $p < 0.05$, 0.01, and not significant, respectively). b) Guk1-7-GFP was expressed from CEN/ARS plasmids with histidine, uracil, or leucine auxotrophic markers in wild type or *whi2-sc1* cells. Cultures were incubated with CHX for two hours at 25°C or 37°C before being analysed by flow cytometry. c) Wild type and *whi2-sc1* cells were co-transformed with Guk1-7-GFP and pRS315 (LEU2). Cultures were grown in synthetic drop out media containing different amounts of leucine and then incubated for two hours in the presence of CHX at 25°C and 37°C before flow cytometry analysis.

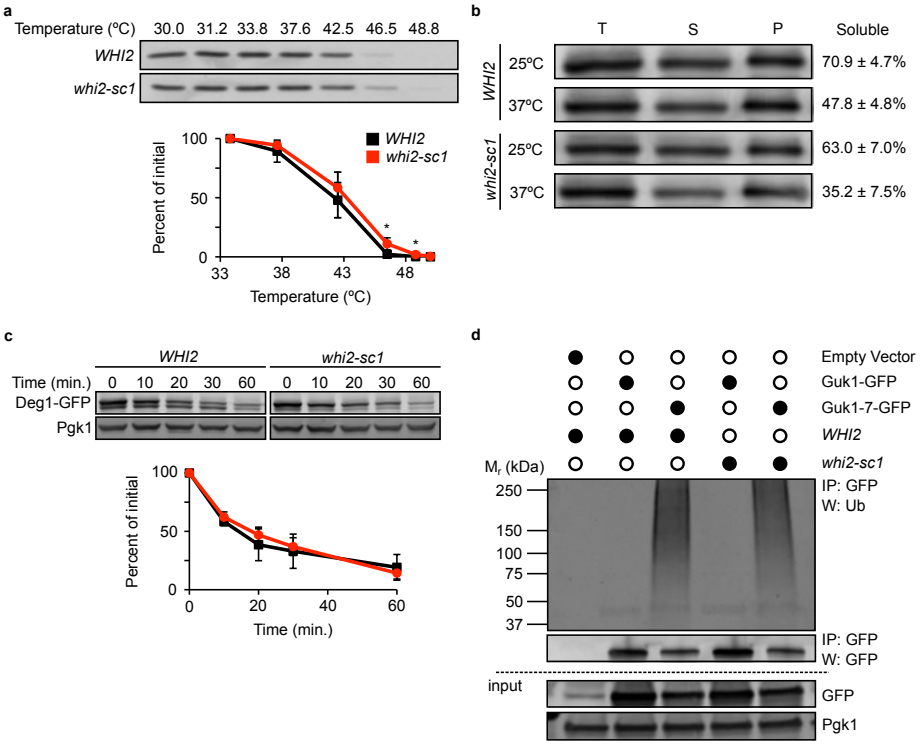


**Figure 3.8:** *whi2*Δ promotes Guk1-7-GFP stability through reduced ubiquitination. a) Cellular thermal shift assay of Guk1-7 fused to a six histidine tag in lysates of *WHI2* and *whi2-sc1* cells grown at 25°C. One representative anti-His western blot is shown. The graph represents the means and standard deviations of Guk1-7 levels from three independent experiments. b) *WHI2* and *whi2-sc1* cells expressing Guk1-7-GFP were grown at 25°C or shifted to 37°C for 20 min. Total cell lysate (T), soluble (S), and pellet fractions (P) were immunoblotted with an anti-GFP antibody. One representative blot is shown and the ratio of soluble fraction to total cell lysate is noted and represents the mean and standard deviation of three independent experiments. c) Proteasome degradation assay. *WHI2* and *whi2-sc1* cells expressing Deg1-GFP under the Cup1 promoter were incubated with CHX at 30°C and samples were collected at the indicated time points. Membranes were immunoblotted with an anti-GFP antibody and an anti-Pgk1 antibody as a loading control. The graph represents the mean and standard deviation of three independent experiments. d) Guk1-GFP or Guk1-7-GFP were immunoprecipitated with GFP-Trap beads from lysates of *WHI2* or *whi2-sc1* cells grown at 25°C and expressing a control empty vector, Guk1-GFP, or Guk1-7-GFP. Samples were eluted and immunoblotted with anti-ubiquitin, anti-GFP, and anti-Pgk1 antibodies.

### 3.3.6 Essential E3 Ligase Rsp5 and Molecular Chaperones Ydj1 and Ssa1 are Required for Guk1-7-GFP Degradation

Considering that the majority of E3 ligase mutants we tested had negligible effects on Guk1-7-GFP degradation, we wanted to know what other quality control factors might play a role in addition to Ubr1. One limitation of the targeted screen is that it was restricted to non-essential genes encoding for known or putative E3 ligases. The essential E3 ligase Rsp5 is required for the increase in ubiquitination observed following acute heat stress and confers increased thermotolerance when overexpressed [52, 223]. Thus, we next sought to determine whether Rsp5 could also play a role in the degradation of cytosolic proteins misfolded due to missense mutation in mild heat shock conditions. We performed cycloheximide chase assays to test whether the temperature sensitive mutant allele *rsp5-1* had an effect on Guk1-7-GFP stability. Guk1-7-GFP levels were significantly higher in *rsp5-1* cells compared to wild type cells after two and four hours at 37°C ($p = 0.002$ and $p = 0.001$, respectively) (Figure 3.9A). To confirm that this enhanced stabilization was the direct consequence of a loss of *RSP5* function, we performed addback experiments whereby wild type *RSP5*, or a catalytically inactive form (C777A), was expressed from a plasmid in *rsp5-1* cells. Following a four hour incubation at 37°C, Guk1-7-GFP levels in *rsp5-1* cells expressing Rsp5 were similar to wild type cells containing a control empty plasmid. Likewise, *rsp5-1* cells containing an empty vector control or expressing the catalytically inactive Rsp5 (C777A) mutant had nearly equivalent Guk1-7-GFP levels that were significantly higher than those observed in the wild type strain ($p = 0.003$ and $p = 0.006$, respectively) (Figure 3.9B). These data confirm that the reduced turnover in *rsp5-1* cells could be directly attributed to the absence of Rsp5 and indicate that Rsp5 has a role in promoting the degradation of Guk1-7-GFP. It is also possible that the role of Rsp5 is indirect as Rsp5 is required for Msn2/4 and Hsf1 mRNA export or mRNA processing during some stress conditions [224, 225].

We next assessed whether Ydj1, which is an Hsp40 chaperone known to associate with Rsp5 to ubiquitinate misfolded proteins following heat shock, may also participate in the turnover of the model substrate [52]. An absence of *YDJ1* resulted in Guk1-7-GFP levels 42% higher than wild type ($p = 0.001$) (Figure 3.9C). An addback experiment expressing *YDJ1* from a plasmid in *ydj1*Δ cells resulted

in Guk1-7-GFP levels comparable to those in the wild type strain. Strikingly, the impairment of the model substrate turnover was more pronounced in *ydj1*Δ than in *rsp5-1*. Therefore, an absence of *YDJ1* is likely causing a broader impact than just impairing Rsp5 function. We next asked whether Ssa1, a member of the Hsp70 family of molecular chaperones shown to be required for the degradation of model cytosolic proteins, was also required for Guk1-7-GFP degradation [203]. Loss of Guk1-7-GFP fluorescence was strikingly low in *ssa1-45* cells, a temperature sensitive mutant of *SSA1*, compared to that observed in wild type cells after a two hour incubation at 37°C ($p = 0.001$) (Figure 3.9D). *ssa1-45* cells expressing a wild type copy of *SSA1* had Guk1-7-GFP levels similar to those of wild type cells suggesting that Ssa1 has a role in promoting Guk1-7-GFP degradation. Together, these data suggest that Hsp70 and Hsp40 chaperones play a part in promoting Guk1-7-GFP degradation.

## 3.4 Discussion

Temperature sensitive alleles have proven to be fruitful model substrates used to elucidate the existence and function of protein quality control pathways. In this study, we set out to identify the E3 ubiquitin ligase, or ligases, responsible for the temperature dependent degradation of the thermally unstable model protein quality control substrate Guk1-7. Screening a yeast deletion collection using a flow cytometry based approach resulted in the identification of a number of putative E3 ligase hits. Further validation, however, suggested that the phenotype observed was produced by an indirect effect. Subsequent complementation analysis and whole genome sequencing revealed secondary mutations in the general stress response factor encoded by the *WHI2* gene that account for the observed increase in Guk1-7-GFP stability. *WHI2* promotes Guk1-7-GFP degradation via substrate ubiquitination with no effect on solubility or thermal stability.

We previously identified the E3 ubiquitin ligase Ubr1 from a genetic screen for factors involved in degradative protein quality control of Guk1-7 [206]. Ubr1 activity alone, however, was not sufficient to account for the bulk of substrate degradation. In some cases, the nuclear E3 ligase San1 and cytosolic ligase Ubr1 have been shown to act in parallel to degrade cytosolic substrates [74, 101]. We found

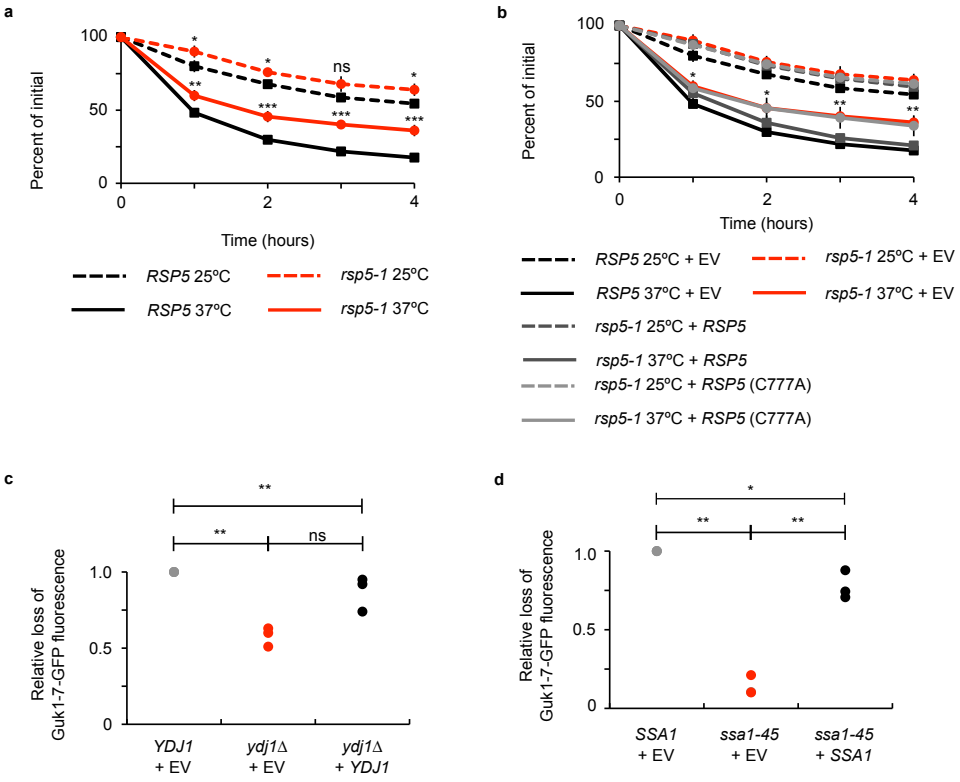


**Figure 3.9:** A role for essential E3 ligases and molecular chaperones in Guk1-7-GFP degradation. a) *RSP5* and *rsp5-1* cells expressing Guk1-7-GFP were incubated with CHX for a total of four hours with samples collected at the indicated time points. P values were calculated using a two-tailed unpaired Student's t-test (*, **, ***, ns denotes $p < 0.05$, 0.01, 0.005, and not significant, respectively). b) *RSP5* cells expressing Guk1-7-GFP and a control empty vector as well as *rsp5-1* cells expressing Guk1-7-GFP and either a control empty vector, *RSP5*, or *RSP5* (C777A) were incubated with CHX and grown for four hours at 25°C and 37°C. Samples were collected at the indicated time points and analysed by flow cytometry. c) *ydj1*Δ cells co-expressing Guk1-7-GFP and an empty vector control or *YDJ1* were incubated at 37°C with CHX for two hours before being analysed by flow cytometry. P values were calculated with a one-way ANOVA and post-hoc Tukey HSD to assess significance (** and ns denote $p < 0.01$ and not significant, respectively). d) *SSA1* and *ssa1-45* cells expressing Guk1-7-GFP were analysed by flow cytometry after being incubated with CHX at 25°C and 37°C for two hours. P values were calculated with a two-tailed unpaired Student's t-test (*** denotes $p < 0.005$).

no role for San1, and no additive effect with the double *ubr1*Δ *san1*Δ mutant in the degradation of the Guk1-7 substrate. Therefore, in this study we wanted to identify the E3 ubiquitin ligases, in addition to Ubr1, that are responsible for the proteasomal degradation of Guk1-7. We identified a number of potential hits in our screen which included: *ASI1*, *DAS1*, *FAP1*, *HRT3*, *HUL5*, *UFD2*, and *UFD4*. Asi1 is a RING domain family member localized to the inner nuclear membrane and is part of the Asi complex that acts as a branch of the ERAD degradation pathway independent from Hrd3 and Doa10 [80, 226]. Both Das1 and Hrt3 are putative F-box SCF ubiquitin ligases [227, 228]. A homologue of the human transcription factor NF-X1, Fap1 also confers resistance to rapamycin by acting as a ligand for FKBP12 [229]. Hul5 is a member of the HECT ubiquitin ligase family. Involved in cytoplasmic protein quality control of short-lived misfolded proteins, Hul5 is also necessary for the increased ubiquitination observed as part of the heat shock quality control response [109]. Ufd2 is both an E3 and E4 enzyme with mutants being hypersensitive to protein misfolding stressors [230]. Finally, Ufd4, like Hul5, is also a member of the HECT family of E3 ligases and physically interacts with Ubr1 to increase processivity of ubiquitin chain formation in the N-end rule pathway [231]. Guk1 is found in both the cytoplasmic and nuclear compartments of yeast cells as assessed by GFP tagging and fluorescence microscopy [154, 206]. It was, therefore, not entirely unexpected for some hits to be nuclear proteins. However, based on the ascribed functions for some of the ligases, and the nature of our substrate, it was puzzling to have identified *DAS1*, *FAP1*, and *HRT3* in our screen. While an absence of seven genes resulted in a significant stabilization our model substrate, we were surprised to have identified so many of them in our screen. Accordingly, the rescue experiments we performed indicated that deletions of these E3 ligases were not the cause of the observed phenotype (Guk1-7-GFP stabilization), which was likely caused by another background mutation.

We found compelling evidence that the impairment of the degradation of the misfolded reporter was caused by mutations in the background of the assessed strains that belong to the same complementation group (Figure 3.4C). Indeed, we identified secondary mutations in the coding sequence of the general stress response gene *WHI2* in eleven of twenty E3 ligase deletion strains tested ($\sim$15% of the E3 mutant stains we assessed) (Figure 3.6D). Mutations in *WHI2* have been

reported in laboratory based evolution studies and are speculated to provide a favorable fitness advantage under certain environments or in combination with other compensatory mutations [215, 232]. However, we did not observe striking differences when comparing growth of haploid cells following tetrad analysis. To our knowledge, ours is the first report of *WHI2* mutations among E3 ubiquitin ligase deletion strains. Nevertheless, the presence of *WHI2* mutations is unlikely restricted to E3 ligase mutant cells. Accordingly, three other studies have reported the presence of secondary mutations in the *WHI2* locus of strains from the yeast deletion collection [216, 233, 234]. In the most recent study, approximately $\sim$30% of all strains sequenced carried unique mutations in *WHI2* and/or five other genes. Most of the mutations identified were frameshift or nonsense mutations suggesting a loss of function phenotype. Finally, it was found that serially passaging *whi2*$\Delta$ strains under conditions with a prolonged stationary phase resulted in an increased abundance of the deletion strain relative to a wild type control. This suggests that secondary mutations in these genes might be found at higher frequencies as the result of selecting for mutants that delay the onset of the stationary phase under laboratory growth conditions.

As part of the general stress response, Whi2 forms a complex with the plasma membrane phosphatase Psr1 and zinc finger transcription factor Msn2 [235]. Upon exposure to stress, Msn2 translocates to the nucleus where it can bind to STRE in the promoters of stress responsive genes [147]. We found that like *WHI2*, an absence of *MSN2* led to reduced turnover of Guk1-7-GFP. This finding suggests that the increase in Guk1-7-GFP stability observed in *WHI2* mutants is likely mediated by genes regulated by Msn2. Studying the general stress response, mediated by Msn2/4 signalling, has gained renewed importance in light of a recent study examining the role of Hsf1 in the transcriptional response to heat shock [146]. The authors of that study concluded that in yeast, the majority of genes induced by heat shock are activated through Msn2/4 activity and not by Hsf1, as was previously believed [146].

While performing *WHI2* addback experiments, we observed that Guk1-7-GFP stability depended upon adequate levels of leucine being present in the media. Amino acids, especially leucine, have been shown to regulate the TOR signaling pathway [236]. Target of rapamycin (TOR) is a conserved serine threonine protein

kinase which as part of the TORC1 complex promotes growth by linking protein synthesis to extrinsic signals such as nutrient levels and environmental stresses. Treating cells with the antifungal rapamycin mimics nutrient starvation and stress, thereby inhibiting TORC1 and allowing a number of stress and growth response transcription factors (such as Msn2) to translocate into the nucleus [237]. We propose a model in which Whi2 is required to maintain Msn2 functional when TORC1 is active (*e.g.*, in the presence of high concentrations of leucine in the media). Under these conditions, mutations in *WHI2* would result in Msn2 remaining phosphorylated and an inhibition of the downstream induction of stress responsive genes, thereby preventing degradation of cytosolic misfolded proteins such as Guk1-7. In cases where leucine levels are low (*e.g.*, in *LEU2* cells deprived of exogenous leucine) an absence or decrease in TORC1 activity allows Msn2 to remain active in a *WHI2* independent manner. In these conditions, Guk1-7-GFP is degraded with similar dynamics as in wild type cells. Our findings of a link between the general stress response and the degradation of our model substrate might help explain some puzzling results we obtained from a previous screen we conducted with Guk1-7-GFP (see Chapter 2) [206]. In that screen, a number of hits were for deletions in *YAK1* and *RIM15*, but we were unable to validate the data after restreaking the deletion strains from the knockout collection. Perhaps these strains are more likely to accumulate *WHI2* mutations for compensatory reasons, which leads to a reduction in Guk1-7 degradation. The kinases Yak1 and Rim15 translocate into the nucleus from the cytoplasm when TORC1 is inhibited and have been shown to directly phosphorylate Msn2 *in vitro*, leading to the induction of Msn2 dependent genes [238, 239]. There is one striking point that remains unanswered; Msn2 is thought to be mostly active after a stress to induce expression of stress response genes. In our conditions, translation of newly expressed genes would be prevented by cycloheximide. Therefore, the impairment of the turnover of our model substrate is either the result of an imbalance of the proteostatic network prior to the stress (*i.e.*, Msn2 basal activity is also required in unstressed conditions), or stress induced mRNA are also directly required for the proper triage and degradation of misfolded proteins (*e.g.*, by mediating the formation of stress granules).

Given that the majority of non-essential E3 ligases tested had negligible effects on Guk1-7-GFP degradation, we then asked whether the essential E3 ligase Rps5

or Hsp40/70 chaperones might play a role in this process. Rsp5, an E3 ligase of the NEDD4 (neural precursor cell expressed, developmentally downregulated 4) family ubiquitinates cytosolic misfolded proteins following heat shock [52]. We found that an absence of Rsp5 resulted in Guk1-7-GFP stabilization similar to that seen in *ubr1*$\Delta$ cells. One possibility is that Rsp5 directly ubiquitinates misfolded Guk1-7-GFP. Interestingly, *WHI2* was identified as a multicopy suppressor of a temperature sensitive allele of *RSP5* and rescues the general stress response phenotype of Rsp5 mutants [235]. Moreover, Rsp5 is required for the nuclear export of Msn2/4 mRNA under stress conditions [225]. Therefore, another possibility is that the observed impaired turnover of Guk1-7-GFP in *rsp5-1* is indirect and caused by reduced Msn2 activity. Hsp70 and its Hsp40 co-chaperones have previously been implicated in degradative protein quality control [48, 74, 167, 240]. Here we provide yet another example of a misfolded cytoplasmic protein whose proteasomal degradation is mediated by Ssa1 and Ydj1. It will be important to determine whether the reduced turnover of misfolded proteins in *WHI2* and *MSN2* defective cells is also mediated by reduce levels of Ydj1 and Ssa1. While in a number of cases Ssa1 and Ydj1 have been shown to target substrates to the nuclear E3 ligase San1, we found no role for San1 in the degradation of the Guk1-7 substrate [48]. Together our data suggests that a number of cytosolic E3 ubiquitin ligases and molecular chaperones potentially work in parallel to target misfolded substrates for degradation. While the need for multiple E3 ligases has been reported before, besides substrates targeted by Ubr1 and San1, few such examples have been reported [100, 167]. Future studies will be needed to address how a variety of misfolded substrates, bound by the same Ssa1 and Ydj1 chaperones, are specifically recognized and ubiquitinated by one or more E3 ligases.

# Chapter 4

# Conclusion

## 4.1 Chapter Summaries

In Chapter 2 we established novel model substrates to further characterize how cytosolic misfolded proteins are targeted for degradation. We first focused on a mutant allele of the yeast guanylate kinase Guk1 and demonstrated that the mutant protein displays temperature dependent stability and has decreased NP-40 solubility compared to the wild type protein. We employed a GFP fusion approach that enabled us to combine observations based on microscopy, biochemical, and flow cytometry methods. At the elevated temperature of 37°C Guk1-7-GFP formed CytoQ-like inclusions that co-localized with the general aggregate marker Hsp104 and the CytoQ specific marker Hsp42. In addition, whereas soluble Guk1-7-GFP was ubiquitinated, the wild type Guk1 was not. We developed a flow cytometry assay to monitor protein stability and then performed a flow cytometry based screen to isolate factors that promote Guk1-7 proteasomal degradation. We identified the E3 ubiquitin ligase Ubr1 and the prefoldin chaperone subunit Gim3. We further characterized how the absence of *GIM3* influenced Guk1-7-GFP stability. While an absence of *GIM3* did not impair proteasomal function or the ubiquitination of Guk1-7-GFP, it led to delayed degradation and the accumulation of the model substrate in cellular inclusions. Interestingly, while Gim3 interacted with Guk1-7, no interaction was found with the wild type Guk1 protein. This suggests that the interaction occurs as the result of protein misfolding and that Gim3 is not

required for Guk1 to attain its native conformation. Prefoldin is known to deliver proteins to the chaperonin complex for folding. We showed that Guk1-7-GFP also formed aggregates in temperature sensitive mutant strains of two essential chaperonin subunits suggesting a possible role for the chaperonin complex in maintaining substrate solubility. Finally, we demonstrated that in addition to Guk1-7, prefoldin can also stabilize other misfolded cytosolic proteins containing missense mutations. By identifying a role for Gim3 to maintain solubility of mutant proteins, our work adds to a growing body of evidence suggesting that prefoldin is important for preventing potentially toxic protein aggregation and underscores its potential importance in maintaining protein homeostasis. As Gim3 is dispensable for the folding of the wild type Guk1, our work also illustrates how complex the relationship between chaperones and their client proteins is, and that it is an adaptive process.

In Chapter 3 we followed on from work in Chapter 2 and performed a second targeted flow cytometry based genetic screen to identify the E3 ubiquitin ligase, or ligases, responsible for the proteasomal degradation of the thermally unstable model protein quality control substrate, Guk1-7. Attempts to validate a number of putative E3 ligase hits pointed to Guk1-7-GFP stability being the result of an indirect effect. Whole genome sequencing revealed secondary mutations in the general stress response gene *WHI2* in a number of hits obtained from the screen. We then demonstrated that an absence of *WHI2* was responsible for the observed impairment in the proteolytic degradation of Guk1-7. We propose a link between mutations in *WHI2* to a deficiency in the Msn2/4 transcriptional response thereby altering the cells capacity to degrade misfolded cytosolic proteins.

## 4.2 General Discussion

### 4.2.1 Using Temperature Sensitive Alleles as Model Protein Quality Control Substrates

Temperature sensitive alleles have proven to be fruitful model substrates used to elucidate the existence and function of protein quality control pathways. Our lab previously identified a panel of temperature sensitive alleles of essential genes en-

coding for cytosolic proteins in *Saccharomyces cerevisiae* [101]. A large fraction of mutant proteins underwent proteasome-mediated degradation when incubated at an elevated temperature of 37°C, whereas the wild type proteins were stable. Approximately one third of the unstable alleles were found to be substrates of the E3 ubiquitin ligase Ubr1. Using four nuclear temperature sensitive mutant proteins (encoded by the *cdc13-1*, *cdc68-1*, *sir3-8*, and *sir4-9* alleles), Gardner and colleagues identified the nuclear protein quality control E3 ligase San1 [70]. As is the case with Ubr1, the wild type proteins were stable and not targeted for degradation by San1. However, our approach remains distinctive, as different model substrates have been employed to characterize cytosolic quality control.

The Guk1-7 allele used in this thesis was produced by mutagenesis of the wild type sequence by error prone PCR [186]. Temperature sensitive mutations are often missense mutations that preserve the function of the essential protein at normal growth temperatures (permissive) but become non-functional at higher temperatures (non-permissive). As missense mutations represent more than half of all mutations in the HGMD we anticipate that understanding the protein quality control pathways that recognize and triage proteins misfolded as the result of missense mutations will gain in importance [158]. Moreover, because most proteins are only marginally stable, it is predicted that most amino acid substitutions are not neutral with respect to protein stability and approximately 70% of rare human missense alleles are predicted to be mildly deleterious [241, 242]. These predictions are underscored by a recent study that found of the human disease associated missense alleles that were tested, approximately 30% displayed increased binding to specific components of the protein homeostasis network. The majority of alleles, however, resulted in disrupted protein-protein interactions [159]. The human mutation ORFeome created as part of this study contains 2,890 human mutant ORFs from 1,140 genes and is the most extensive human mutation collection created to date. It should be noted that while mutant ORFs in the above collection typically contain a single nucleotide change, the temperature sensitive alleles used in this thesis contain a minimum of four nucleotide changes resulting in at least two non-silent amino acid changes per protein, with the exception of the Guk1-11 mutant. Whether proteins destabilized by multiple mutations are recognized and handled by the protein quality control network differently to proteins containing a single mu-

tation remains to be tested, and should be taken into consideration while designing experiments for projects with potential medical or therapeutic applications.

### 4.2.2 Flow Cytometry: An Ideal Method for Identifying and Characterizing Protein Quality Control Factors

Protein degradation is generally assayed by pulse-chase metabolic labeling, or by using protein synthesis inhibitors coupled with downstream biochemical analysis [201]. Prior to starting the work described in this thesis, fluorescently tagged proteins had already been used to monitor protein stability by flow cytometry. Heck *et al.* used a genomically integrated CPY‡-GFP substrate to screen a collection of deletion strains of ubiquitin pathway genes to identify the parallel requirement for Ubr1 and San1 E3 ligases in the degradation of some misfolded cytoplasmic substrates [74]. Years prior, a GFP-tagged Hmg2g had been used to study degradation in the ER [243].

As mentioned earlier in this thesis, flow cytometry has a number of advantages compared to stability assays as measurements are performed *in vivo*, thousands of cells can be analysed in under an hour, and for most purposes no additional processing or cell lysis is required. Perhaps most importantly, in addition to the relative speed and precision flow cytometry provides over Western blotting methods, the assay we have described is sensitive enough to discern partial effects. For instance, we found *ubr1*$\Delta$ leads to minor but statistically significant stabilization of Guk1-7-GFP (15% more protein after a two hour incubation at 37°C in comparison to wild type cells) that was observed in a consistent manner in multiple experiments. Using Western blots, we had previously missed that Ubr1 plays a role in the turnover of the Guk1-7 mutant protein [101]. Another advantage of the GFP-based approach is that it can be used as a screening tool that does not rely on a functional model substrate. As mentioned earlier, Ura3 fusion proteins have been used to study Ubr1 and cytoplasmic protein quality control pathways [98, 167]. These assays rely on a functional Ura3 protein as they are conducted in auxotrophic yeast strains that do not produce uracil. Were our studies to have been based on a functional Guk1 protein, we would have missed Gim3 in our screen. Because our novel model substrates do not need to meet a minimum functional threshold required for cell viability, our assay is far more sensitive and is amenable to detecting protein

quality control components that would be missed by traditional methods. A potential issue arising from the use of GFP fusions for protein degradation studies is that GFP itself might influence stability of the fusion protein. This has been reported previously for the yeast tandem affinity purification (TAP) tag collection. A comparison of protein half-lives between tagged and untagged versions of the same protein showed that the TAP tag versions were degraded more rapidly [244]. While we did not perform CHX chase assays comparing GFP to His tag versions of Guk1-7, we did compare the solubility differences between these tags. We found that Guk1-7 was much less soluble with the smaller six histidine tag, potentially providing a better reflection of the true solubility of this substrate when untagged. This data suggests that at the very least, GFP influences the solubility of Guk1-7, but we did not confirm whether degradation rates are also influenced. Despite the potential drawbacks of relying on a GFP fusion protein, we believe that the work presented in this thesis demonstrates the benefits of using a flow cytometry based approach to studying protein homeostasis networks and identifying protein quality control components.

### 4.2.3 Triage Decisions: Simply a Matter of Kinetic Partitioning?

One of the major unanswered questions in the protein quality control field is what are the mechanisms involved in the changeover from chaperone assisted refolding to targeted degradation of terminally misfolded proteins? One possibility is that kinetic partitioning could dictate the order of sequential events, in which the E3 ligase and associated cofactors would have lower $K_{on}$ compared to components of the folding machinery. In this scenario, efficient refolding would occur when the rate constant of folding ($K_{fold}$) is faster than that of chaperone rebinding to the folding intermediate ($K_{on}$). In this thesis we have demonstrated that an absence of the prefoldin chaperone subunit Gim3 leads to the aggregation of our model misfolded substrate and is accompanied by delayed degradation. This would suggest that prefoldin chaperones, which lack ATP dependent chaperone activity, are important for enabling and/or maintaining substrate solubility such that substrates may be targeted for degradation by the ubiquitin proteasome machinery instead of entering reiterative cycles of chaperone binding. Another strategy in protein quality control

might be that certain E3 ligases only recognize and bind to substrates when they are in a substrate-chaperone complex and, therefore, an absence of the chaperone cofactor abolishes substrate recognition in these cases. By exchanging ADP for ATP, the nucleotide exchange factor Fes1 releases misfolded proteins from Hsp70 increasing their susceptibility to proteasomal degradation [54]. Sse1, another NEF of the Hsp110 family, can bind directly to hydrophobic patches on misfolded substrates which might assist in maintaining substrate solubility, aid in protein refolding, or shield substrates from interacting with the ubiquitination machinery [54]. An example of substrate competition is the nuclear E3 ligase San1, which directly interacts with short hydrophobic stretches on misfolded substrates [69]. *In vitro*, Sse1 binding inhibits ubiquitination of San1 substrates, potentially as the result of competitive binding [53]. Together, the data would suggest a model whereby kinetic partitioning, protein abundance, and intracellular localization converge to dictate protein triage decisions in protein quality control.

### 4.2.4 The Importance Of, and Difficulty In, Maintaining Proteostasis

Many stresses disrupt protein folding prompting transcriptional responses to increase the chaperone and proteostatic capacity of the cell in order to maintain cell viability. These stress response mechanisms act to restore protein homeostatic balance by matching levels of protein quality control factors with the protein folding requirements of the cell. Moreover, the relationship between protein folding and degradation is underscored by the observation that an increase in folding capacity is almost always accompanied by an increase in the degradation machinery [1]. Regulatory mechanisms are required to adequately respond to the pressure of increasing loads of misfolded proteins as excess capacity is not inherent to the system. A number of experimental observations support the hypothesis that folding capacity is tightly regulated. For example, exposure to stresses that induce protein misfolding elicit a stress response that decreases translation of non-essential protein products but induces gene expression of molecular chaperones and other cytoprotective components. In *Caenorhabditis elegans*, expressing an unstable mutant protein prone to aggregate resulted in decreased stability of other proteome members. This suggests that excess folding capacity is not present as the system is

unable to respond to both the increase in a single species of misfolded protein and to maintain the remainder of the proteome [245]. As the system fails to produce an adequate response in some cases, one could reasonably question why the cell does not simply begin with a higher basal folding capacity? A possible answer is that not only would it be costly to the cell to produce additional chaperone proteins but also increased chaperone levels can themselves be detrimental to cellular functions. For instance, abnormally high levels of Hsp70 in *Drosophila melanogaster* cells or larvae can interfere with growth, development, or survival to adulthood [246, 247]. Second, many proteins rely on conformational changes that involve transitions between low energy states in order to perform their functions [248]. These transitions may expose sensitive binding surfaces or pass through less stable intermediates. Were the proteostasis network to have an excessive folding capacity, a number of these states might be shielded, thereby impeding or eliminating many cellular functions. Finally, while HSF1 mediated signaling is vital for the heat shock response in mammals, increased expression of some heat shock proteins is associated with the propagation of some cancers and the emergence of drug resistant viruses [249]. These examples illustrate how important proper regulation of proteostasis is to maintaining proteome integrity and cellular and organism viability.

In this thesis we describe how an absence of a single non-essential chaperone subunit (Gim3) and mutations in the general stress response gene *WHI2* can profoundly impact the cell's capacity to respond to higher levels of misfolded proteins. Notably, *WHI2* mutations are responsible for the impaired proteolysis of the Guk1-7-GFP protein quality control substrate. We linked this phenotype to a deficiency of the Msn2/4 transcription factor response that altered the ability for cells to adequately degrade cytosolic misfolded proteins. Interestingly, our experiments were performed in the presence of cycloheximide that prevents translation of newly synthesized proteins in response to increased temperatures and levels of misfolded proteins. Our work indicates that potentially small changes to the balance of the protein homeostasis network may impact the cell's ability to adapt rapidly to change, such as before the cell can mount a transcriptional response. These findings present a starting point from which we can begin to understand how changes in the protein quality control network can disturb proteostasis. Understanding how the proteostatic network responds to stress is increasingly becoming important for

our understanding of disease and for drug discovery.

## 4.3 Future Directions

In this thesis, we have developed a flow cytometry based approach to screen for protein quality control factors that promote proteasome mediated degradation of unstable model substrates. Work presented in this thesis also presents a number of interesting avenues for future research.

### 4.3.1 Flow Cytometry Screens for E3 Ligases Targeting Human Disease Alleles

Sahni *et al.* created the human mutation ORFeome, a resource of cloning vectors containing human germline mutations associated with Mendelian diseases [159]. We have requested a number of these ORFs, specifically selecting from those that demonstrated an interaction with the chaperone machinery, suggestive of decreased stability. At the same time, we also acquired the DsRed/EGFP vector developed for global protein stability analysis [174]. The plan is to create EGFP fusions with the mutant and wild type human ORFs. The constructs would be tested initially using the CETSA assay as was used in Chapters 2 and 3 to identify those that have the lowest thermal stability. Once an ideal substrate has been identified a screen using flow cytometry to monitor changes in the EGFP/DsRed ratio could be performed to identify the E3 ubiquitin ligases required to target this disease associated protein for degradation. The screen could be performed using a panel of short hairpin RNA (shRNAs) that specifically target and down regulate levels of human E3 ligases or by using a genome-wide clustered regularly interspaced short palindromic repeats (CRISPR-Cas9) approach as developed by the laboratory of Dr. Moffat at the University of Toronto [250].

### 4.3.2 Characterizing the Role of the E3 Ligase Ubr1 in Cytoplasmic Protein Quality Control

Ubr1 was first identified and characterized as the E3 ligase of the N-end rule, a pathway whereby the half-life of a protein correlates with the identity of its N-terminal amino acid residue [97]. A number of studies now suggest that Ubr1

may play a role in protein degradation independent of the N-end rule [74, 99–101]. Furthermore, previous work from the Mayor lab and work presented in this thesis demonstrates that Ubr1 targets proteins destabilized by missense mutations for degradation [101, 206]. How Ubr1 recognizes these substrates, and whether it does so through a mechanism independent from the N-end rule are both questions that remain unanswered. With the exception of Guk1-11, the alleles we have used to assess Ubr1 function contain a number of mutations that could potentially complicate the analysis of Ubr1 substrate binding. It is necessary therefore to create a new set of alleles by site directed mutagenesis that contain a single destabilizing mutation. Going forward, these new alleles that are stabilized by a Ubr1 deletion would be used to address a number of questions.

Ubr1 recognizes N-end rule substrates through two domains: the UBR box and the ClpS domain [98]. We have generated overexpression plasmids containing the full length Ubr1 protein with point mutations in either the UBR box or ClpS domain. My hypothesis is that the UBR box is responsible for mediating substrate degradation. To further assess the role of the UBR box (or the ClpS domain), I would use dipeptides to block Type I and Type II binding sites thereby inhibiting N-end rule activity, and possibly degradation of the misfolded model substrates. If mutations in either of these domains show no effect on the degradation of model substrates, Ubr1 truncations would be created to define the region involved in substrate recognition. It is also possible that through proteolytic cleavage misfolded proteins are recognized as N-end rule substrates. To assess whether this is the case, dual N-and C-terminally tagged temperature sensitive alleles could be created that have an N-terminal HA tag and a C-terminal His tag, similar to experiments previously performed [74]. In the absence of cleavage, both tags should remain present after pulling down the ubiquitinated misfolded substrate. Currently, we have identified a limited number of Ubr1 model substrates. It would be helpful to identify which misfolded proteins are normally targeted by Ubr1. We could express a Ubr1 mutant that cannot recognize the misfolded model substrate (developed above). Using stable isotope labelling with amino acids in cell culture (SILAC) we could then identify which proteins are no longer ubiquitinated in the presence of the Ubr1 mutant in comparison to cells expressing the wild type Ubr1 using mass spectrometry. Validation could be performed using the flow cytometry assay developed in

this thesis and pulldown analysis.

There is currently great interest in understanding how proteostasis networks maintain proteome integrity. In this thesis we describe the development of a flow cytometry based assay to exploit novel model substrates to study proteostasis. Using this approach we identified the prefoldin subunit Gim3 and the general stress response factor Whi2 and characterized their roles in promoting protein homeostasis. This work underscores the complexity of the systems required to maintain proteostasis and the development of novel model substrates provides a valuable resource for future studies of protein quality control.

# Bibliography


[1] W. E. Balch, R. I. Morimoto, A. Dillin, and J. W. Kelly. Adapting proteostasis for disease intervention. *Science*, 319(5865):916–9, 2008.

[2] D. A. Drummond and C. O. Wilke. The evolutionary consequences of erroneous protein synthesis. *Nat Rev Genet*, 10(10):715–24, 2009.

[3] A. L. Goldberg. Protein degradation and protection against misfolded or damaged proteins. *Nature*, 426(6968):895–9, 2003.

[4] K. A. Geiler-Samerotte, M. F. Dion, B. A. Budnik, S. M. Wang, D. L. Hartl, and D. A. Drummond. Misfolded proteins impose a dosage-dependent fitness cost and trigger a cytosolic unfolded protein response in yeast. *Proc Natl Acad Sci U S A*, 108(2):680–5, 2011.

[5] H. Olzscha, S. M. Schermann, A. C. Woerner, S. Pinkert, M. H. Hecht, G. G. Tartaglia, M. Vendruscolo, M. Hayer-Hartl, F. U. Hartl, and R. M. Vabulas. Amyloid-like aggregates sequester numerous metastable proteins with essential cellular functions. *Cell*, 144(1):67–78, 2011.

[6] Y. E. Kim, F. Hosp, F. Frottin, H. Ge, M. Mann, M. Hayer-Hartl, and F. U. Hartl. Soluble oligomers of polyq-expanded huntingtin target a multiplicity of key cellular factors. *Mol Cell*, 2016.

[7] F. Chiti and C. M. Dobson. Protein misfolding, functional amyloid, and human disease. *Annu Rev Biochem*, 75:333–66, 2006.

[8] T. J. Kamerzell and C. R. Middaugh. The complex inter-relationships between protein flexibility and stability. *J Pharm Sci*, 97(9):3494–517, 2008.

[9] T. W. Mu, D. S. Ong, Y. J. Wang, W. E. Balch, 3rd Yates, J. R., L. Segatori, and J. W. Kelly. Chemical and biological approaches synergize to ameliorate protein-folding diseases. *Cell*, 134(5):769–81, 2008.

[10] F. U. Hartl and M. Hayer-Hartl. Converging concepts of protein folding in vitro and in vivo. *Nat Struct Mol Biol*, 16(6):574–81, 2009.

[11] R. I. Morimoto. Proteotoxic stress and inducible chaperone networks in neurodegenerative disease and aging. *Genes Dev*, 22(11):1427–38, 2008.

[12] A. Ben-Zvi, E. A. Miller, and R. I. Morimoto. Collapse of proteostasis represents an early molecular event in caenorhabditis elegans aging. *Proc Natl Acad Sci U S A*, 106(35):14914–9, 2009.

[13] A. H. Elcock. Molecular simulations of cotranslational protein folding: fragment stabilities, folding cooperativity, and trapping in the ribosome. *PLoS Comput Biol*, 2(7):e98, 2006.

[14] V. Albanese, S. Reissmann, and J. Frydman. A ribosome-anchored chaperone network that facilitates eukaryotic ribosome biogenesis. *J Cell Biol*, 189(1):69–81, 2010.

[15] F. Brandt, L. A. Carlson, F. U. Hartl, W. Baumeister, and K. Grunewald. The three-dimensional organization of polyribosomes in intact human cells. *Mol Cell*, 39(4):560–9, 2010.

[16] H. Otto, C. Conz, P. Maier, T. Wolfle, C. K. Suzuki, P. Jeno, P. Rucknagel, J. Stahl, and S. Rospert. The chaperones mpp11 and hsp70l1 form the mammalian ribosome-associated complex. *Proc Natl Acad Sci U S A*, 102 (29):10064–9, 2005.

[17] S. Preissler and E. Deuerling. Ribosome-associated chaperones as key players in proteostasis. *Trends Biochem Sci*, 37(7):274–83, 2012.

[18] F. Willmund, M. del Alamo, S. Pechmann, T. Chen, V. Albanese, E. B. Dammer, J. Peng, and J. Frydman. The cotranslational function of ribosome-associated hsp70 in eukaryotic protein homeostasis. *Cell*, 152 (1-2):196–209, 2013.

[19] A. Koplin, S. Preissler, Y. Ilina, M. Koch, A. Scior, M. Erhardt, and E. Deuerling. A dual function for chaperones ssb-rac and the nac nascent polypeptide-associated complex on ribosomes. *J Cell Biol*, 189(1):57–68, 2010.

[20] M. P. Mayer and B. Bukau. Hsp70 chaperones: cellular functions and molecular mechanism. *Cell Mol Life Sci*, 62(6):670–84, 2005.

[21] H. H. Kampinga and E. A. Craig. The hsp70 chaperone machinery: J proteins as drivers of functional specificity. *Nat Rev Mol Cell Biol*, 11(8): 579–92, 2010.

[22] E. B. Sarbeng, Q. Liu, X. Tian, J. Yang, H. Li, J. L. Wong, and L. Zhou. A functional dnak dimer is essential for the efficient interaction with hsp40 heat shock protein. *J Biol Chem*, 290(14):8849–62, 2015.

[23] P. Walsh, D. Bursac, Y. C. Law, D. Cyr, and T. Lithgow. The j-protein family: modulating protein assembly, disassembly and translocation. *EMBO Rep*, 5(6):567–71, 2004.

[24] H. Raviol, H. Sadlish, F. Rodriguez, M. P. Mayer, and B. Bukau. Chaperone network in the yeast cytosol: Hsp110 is revealed as an hsp70 nucleotide exchange factor. *EMBO J*, 25(11):2510–8, 2006.

[25] J. Cuellar, J. Martin-Benito, S. H. Scheres, R. Sousa, F. Moro, E. Lopez-Vinas, P. Gomez-Puertas, A. Muga, J. L. Carrascosa, and J. M. Valpuesta. The structure of cct-hsc70 nbd suggests a mechanism for hsp70 delivery of substrates to the chaperonin. *Nat Struct Mol Biol*, 15(8): 858–64, 2008.

[26] M. Taipale, D. F. Jarosz, and S. Lindquist. Hsp90 at the hub of protein homeostasis: emerging mechanistic insights. *Nat Rev Mol Cell Biol*, 11(7): 515–28, 2010.

[27] Y. E. Kim, M. S. Hipp, A. Bracher, M. Hayer-Hartl, and F. U. Hartl. Molecular chaperone functions in protein folding and proteostasis. *Annu Rev Biochem*, 82:323–55, 2013.

[28] A. J. Caplan, A. K. Mandal, and M. A. Theodoraki. Molecular chaperones and protein kinase quality control. *Trends Cell Biol*, 17(2):87–92, 2007.

[29] C. Dekker, P. C. Stirling, E. A. McCormack, H. Filmore, A. Paul, R. L. Brost, M. Costanzo, C. Boone, M. R. Leroux, and K. R. Willison. The interaction network of the chaperonin cct. *EMBO J*, 27(13):1827–39, 2008.

[30] M. A. Kabir, W. Uddin, A. Narayanan, P. K. Reddy, M. A. Jairajpuri, F. Sherman, and Z. Ahmad. Functional subunits of eukaryotic chaperonin cct/tric in protein folding. *J Amino Acids*, 2011:843206, 2011.

[31] T. Lopez, K. Dalton, and J. Frydman. The mechanism and function of group ii chaperonins. *J Mol Biol*, 427(18):2919–30, 2015.

[32] F. Russmann, M. J. Stemp, L. Monkemeyer, S. A. Etchells, A. Bracher, and F. U. Hartl. Folding of large multidomain proteins by partial encapsulation in the chaperonin tric/cct. *Proc Natl Acad Sci U S A*, 109(52):21208–15, 2012.

[33] S. Reissmann, L. A. Joachimiak, B. Chen, A. S. Meyer, A. Nguyen, and J. Frydman. A gradient of atp affinities generates an asymmetric power stroke driving the chaperonin tric/cct folding cycle. *Cell Rep*, 2(4):866–77, 2012.

[34] L. A. Joachimiak, T. Walzthoeni, C. W. Liu, R. Aebersold, and J. Frydman. The structural basis of substrate recognition by the eukaryotic chaperonin tric/cct. *Cell*, 159(5):1042–55, 2014.

[35] M. W. Melville, A. J. McClellan, A. S. Meyer, A. Darveau, and J. Frydman. The hsp70 and tric/cct chaperone systems cooperate in vivo to assemble the von hippel-lindau tumor suppressor complex. *Mol Cell Biol*, 23(9): 3141–51, 2003.

[36] A. Y. Yam, Y. Xia, H. T. Lin, A. Burlingame, M. Gerstein, and J. Frydman. Defining the tric/cct interactome links chaperonin function to stabilization of newly made proteins with complex topologies. *Nat Struct Mol Biol*, 15 (12):1255–62, 2008.

[37] A. Bouhouche, A. Benomar, N. Bouslam, T. Chkili, and M. Yahyaoui. Mutation in the epsilon subunit of the cytosolic chaperonin-containing t-complex peptide-1 (cct5) gene causes autosomal recessive mutilating sensory neuropathy with spastic paraplegia. *J Med Genet*, 43(5):441–3, 2006.

[38] Y. Inoue, H. Aizaki, H. Hara, M. Matsuda, T. Ando, T. Shimoji, K. Murakami, T. Masaki, I. Shoji, S. Homma, Y. Matsuura, T. Miyamura, T. Wakita, and T. Suzuki. Chaperonin tric/cct participates in replication of hepatitis c virus genome via interaction with the viral ns5b protein. *Virology*, 410(1):38–47, 2011.

[39] A. G. Trinidad, P. A. Muller, J. Cuellar, M. Klejnot, M. Nobis, J. M. Valpuesta, and K. H. Vousden. Interaction of p53 with the cct complex promotes protein folding and wild-type p53 activity. *Mol Cell*, 50(6): 805–17, 2013.

[40] H. Zhou, M. Xu, Q. Huang, A. T. Gates, X. D. Zhang, J. C. Castle, E. Stec, M. Ferrer, B. Strulovici, D. J. Hazuda, and A. S. Espeseth. Genome-scale

rnai screen for host factors required for hiv replication. *Cell Host Microbe*, 4(5):495–504, 2008.

[41] I. E. Vainberg, S. A. Lewis, H. Rommelaere, C. Ampe, J. Vandekerckhove, H. L. Klein, and N. J. Cowan. Prefoldin, a chaperone that delivers unfolded proteins to cytosolic chaperonin. *Cell*, 93(5):863–73, 1998.

[42] R. Siegert, M. R. Leroux, C. Scheufler, F. U. Hartl, and I. Moarefi. Structure of the molecular chaperone prefoldin: unique interaction of multiple coiled coil tentacles with unfolded proteins. *Cell*, 103(4):621–32, 2000.

[43] M. Takano, E. Tashiro, A. Kitamura, H. Maita, S. M. Iguchi-Ariga, M. Kinjo, and H. Ariga. Prefoldin prevents aggregation of alpha-synuclein. *Brain Res*, 1542:186–94, 2014.

[44] E. Tashiro, T. Zako, H. Muto, Y. Itoo, K. Sorgjerd, N. Terada, A. Abe, M. Miyazawa, A. Kitamura, H. Kitaura, H. Kubota, M. Maeda, T. Momoi, S. M. Iguchi-Ariga, M. Kinjo, and H. Ariga. Prefoldin protects neuronal cells from polyglutamine toxicity by preventing aggregation formation. *J Biol Chem*, 288(27):19958–72, 2013.

[45] A. Shiber, W. Breuer, M. Brandeis, and T. Ravid. Ubiquitin conjugation triggers misfolded protein sequestration into quality-control foci when hsp70 chaperone levels are limiting. *Mol Biol Cell*, 2013.

[46] D. W. Summers, K. J. Wolfe, H. Y. Ren, and D. M. Cyr. The type ii hsp40 sis1 cooperates with hsp70 and the e3 ligase ubr1 to promote degradation of terminally misfolded cytosolic protein. *PLoS One*, 8(1):e52099, 2013.

[47] Q. Wang, Y. Liu, N. Soetandyo, K. Baek, R. Hegde, and Y. Ye. A ubiquitin ligase-associated chaperone holdase maintains polypeptides in soluble states for proteasome degradation. *Mol Cell*, 42(6):758–70, 2011.

[48] C. J. Guerriero, K. F. Weiberth, and J. L. Brodsky. Hsp70 targets a cytoplasmic quality control substrate to the san1p ubiquitin ligase. *J Biol Chem*, 2013.

[49] G. C. Meacham, C. Patterson, W. Zhang, J. M. Younger, and D. M. Cyr. The hsc70 co-chaperone chip targets immature cftr for proteasomal degradation. *Nat Cell Biol*, 3(1):100–5, 2001.

[50] A. J. McClellan, M. D. Scott, and J. Frydman. Folding and quality control of the vhl tumor suppressor proceed through distinct chaperone pathways. *Cell*, 121(5):739–48, 2005.

[51] A. K. Mandal, P. A. Gibney, N. B. Nillegoda, M. A. Theodoraki, A. J. Caplan, and K. A. Morano. Hsp110 chaperones control client fate determination in the hsp70-hsp90 chaperone system. *Mol Biol Cell*, 21(9): 1439–48, 2010.

[52] N. N. Fang, G. T. Chan, M. Zhu, S. A. Comyn, A. Persaud, R. J. Deshaies, D. Rotin, J. Gsponer, and T. Mayor. Rsp5/nedd4 is the main ubiquitin ligase that targets cytosolic misfolded proteins following heat stress. *Nat Cell Biol*, 16(12):1227–37, 2014.

[53] S. H. Park, N. Bolender, F. Eisele, Z. Kostova, J. Takeuchi, P. Coffino, and D. H. Wolf. The cytoplasmic hsp70 chaperone machinery subjects misfolded and endoplasmic reticulum import-incompetent proteins to degradation via the ubiquitin-proteasome system. *Mol Biol Cell*, 18(1): 153–65, 2007.

[54] N. K. Gowda, G. Kandasamy, M. S. Froehlich, R. J. Dohmen, and C. Andreasson. Hsp70 nucleotide exchange factor fes1 is essential for ubiquitin-dependent degradation of misfolded cytosolic proteins. *Proc Natl Acad Sci U S A*, 110(15):5975–80, 2013.

[55] R. Minami, A. Hayakawa, H. Kagawa, Y. Yanagi, H. Yokosawa, and H. Kawahara. Bag-6 is essential for selective elimination of defective proteasomal substrates. *J Cell Biol*, 190(4):637–50, 2010.

[56] C. M. Pickart and M. J. Eddins. Ubiquitin: structures, functions, mechanisms. *Biochim Biophys Acta*, 1695(1-3):55–72, 2004.

[57] R. J. Deshaies and C. A. Joazeiro. Ring domain e3 ubiquitin ligases. *Annu Rev Biochem*, 78:399–434, 2009.

[58] D. M. Wenzel and R. E. Klevit. Following ariadne's thread: a new perspective on rbr ubiquitin ligases. *BMC Biol*, 10:24, 2012.

[59] M. B. Metzger, V. A. Hristova, and A. M. Weissman. Hect and ring finger families of e3 ubiquitin ligases at a glance. *J Cell Sci*, 125(Pt 3):531–7, 2012.

[60] C. B. Lucking, A. Durr, V. Bonifati, J. Vaughan, G. De Michele, T. Gasser, B. S. Harhangi, G. Meco, P. Denefle, N. W. Wood, Y. Agid, and A. Brice. Association between early-onset parkinson's disease and mutations in the parkin gene. *N Engl J Med*, 342(21):1560–7, 2000.

[61] D. Finley. Recognition and processing of ubiquitin-protein conjugates by the proteasome. *Annu Rev Biochem*, 78:477–513, 2009.

[62] D. Finley, H. D. Ulrich, T. Sommer, and P. Kaiser. The ubiquitin-proteasome system of saccharomyces cerevisiae. *Genetics*, 192 (2):319–60, 2012.

[63] A. Buchberger, B. Bukau, and T. Sommer. Protein quality control in the cytosol and the endoplasmic reticulum: brothers in arms. *Mol Cell*, 40(2): 238–52, 2010.

[64] S. S. Vembar and J. L. Brodsky. One step at a time: endoplasmic reticulum-associated degradation. *Nat Rev Mol Cell Biol*, 9(12):944–57, 2008.

[65] A. Ruggiano, O. Foresti, and P. Carvalho. Quality control: Er-associated degradation: protein quality control and beyond. *J Cell Biol*, 204(6): 869–79, 2014.

[66] P. Carvalho, V. Goder, and T. A. Rapoport. Distinct ubiquitin-ligase complexes define convergent pathways for the degradation of er proteins. *Cell*, 126(2):361–73, 2006. Carvalho, Pedro Goder, Veit Rapoport, Tom A GM052586/GM/NIGMS NIH HHS/United States Comparative Study Research Support, N.I.H., Extramural Research Support, Non-U.S. Gov't United States Cell Cell. 2006 Jul 28;126(2):361-73.

[67] V. Denic, E. M. Quan, and J. S. Weissman. A luminal surveillance complex that selects misfolded glycoproteins for er-associated degradation. *Cell*, 126(2):349–59, 2006. Denic, Vladimir Quan, Erin M Weissman, Jonathan S Research Support, Non-U.S. Gov't Research Support, U.S. Gov't, Non-P.H.S. United States Cell Cell. 2006 Jul 28;126(2):349-59.

[68] C. Wojcik and G. N. DeMartino. Intracellular localization of proteasomes. *Int J Biochem Cell Biol*, 35(5):579–89, 2003.

[69] E. K. Fredrickson, J. C. Rosenbaum, M. N. Locke, T. I. Milac, and R. G. Gardner. Exposed hydrophobicity is a key determinant of nuclear quality control degradation. *Mol Biol Cell*, 22(13):2384–95, 2011.

[70] R. G. Gardner, Z. W. Nelson, and D. E. Gottschling. Degradation-mediated protein quality control in the nucleus. *Cell*, 120(6):803–15, 2005.

[71] R. Ibarra, D. Sandoval, E. K. Fredrickson, R. G. Gardner, and G. Kleiger. The san1 ubiquitin ligase functions preferentially with ubiquitin-conjugating enzyme ubc1 during protein quality control. *J Biol Chem*, 291(36):18778–90, 2016.

[72] J. C. Rosenbaum, E. K. Fredrickson, M. L. Oeser, C. M. Garrett-Engele, M. N. Locke, L. A. Richardson, Z. W. Nelson, E. D. Hetrick, T. I. Milac, D. E. Gottschling, and R. G. Gardner. Disorder targets misorder in nuclear quality control degradation: a disordered ubiquitin ligase directly recognizes its misfolded substrates. *Mol Cell*, 41(1):93–106, 2011.

[73] P. S. Gallagher, S. V. Clowes Candadai, and R. G. Gardner. The requirement for cdc48/p97 in nuclear protein quality control degradation depends on the substrate and correlates with substrate insolubility. *J Cell Sci*, 127(Pt 9):1980–91, 2014.

[74] J. W. Heck, S. K. Cheung, and R. Y. Hampton. Cytoplasmic protein quality control degradation mediated by parallel actions of the e3 ubiquitin ligases ubr1 and san1. *Proc Natl Acad Sci U S A*, 107(3):1106–11, 2010.

[75] S. H. Park, Y. Kukushkin, R. Gupta, T. Chen, A. Konagai, M. S. Hipp, M. Hayer-Hartl, and F. U. Hartl. Polyq proteins interfere with nuclear degradation of cytosolic proteins by sequestering the sis1p chaperone. *Cell*, 154(1):134–45, 2013.

[76] R. Prasad, S. Kawaguchi, and D. T. Ng. A nucleus-based quality control mechanism for cytosolic proteins. *Mol Biol Cell*, 21(13):2117–27, 2010.

[77] S. B. Miller, C. T. Ho, J. Winkler, M. Khokhrina, A. Neuner, M. Y. Mohamed, D. L. Guilbride, K. Richter, M. Lisby, E. Schiebel, A. Mogk, and B. Bukau. Compartment-specific aggregases direct distinct nuclear and cytoplasmic aggregate deposition. *EMBO J*, 34(6):778–97, 2015.

[78] E. Grossman, O. Medalia, and M. Zwerger. Functional architecture of the nuclear pore complex. *Annu Rev Biophys*, 41:557–84, 2012.

[79] R. D. Jones and R. G. Gardner. Protein quality control in the nucleus. *Curr Opin Cell Biol*, 40:81–9, 2016.

[80] A. Khmelinskii, E. Blaszczak, M. Pantazopoulou, B. Fischer, D. J. Omnus, G. Le Dez, A. Brossard, A. Gunnarsson, J. D. Barry, M. Meurer, D. Kirrmaier, C. Boone, W. Huber, G. Rabut, P. O. Ljungdahl, and M. Knop. Protein quality control at the inner nuclear membrane. *Nature*, 516(7531):410–3, 2014.

[81] M. K. Sung, T. R. Porras-Yakushi, J. M. Reitsma, F. M. Huber, M. J. Sweredoski, A. Hoelz, S. Hess, and R. J. Deshaies. A conserved quality-control pathway that mediates degradation of unassembled ribosomal proteins. *Elife*, 5, 2016.

[82] P. Connell, C. A. Ballinger, J. Jiang, Y. Wu, L. J. Thompson, J. Hohfeld, and C. Patterson. The co-chaperone chip regulates protein triage decisions mediated by heat-shock proteins. *Nat Cell Biol*, 3(1):93–6, 2001.

[83] C. Graf, M. Stankiewicz, R. Nikolay, and M. P. Mayer. Insights into the conformational dynamics of the e3 ubiquitin ligase chip in complex with chaperones and e2 enzymes. *Biochemistry*, 49(10):2121–9, 2010.

[84] L. Kundrat and L. Regan. Balance between folding and degradation for hsp90-dependent client proteins: a key role for chip. *Biochemistry*, 49(35): 7428–38, 2010.

[85] V. Arndt, C. Daniel, W. Nastainczyk, S. Alberti, and J. Hohfeld. Bag-2 acts as an inhibitor of the chaperone-associated ubiquitin ligase chip. *Mol Biol Cell*, 16(12):5891–900, 2005.

[86] Q. Dai, S. B. Qian, H. H. Li, H. McDonough, C. Borchers, D. Huang, S. Takayama, J. M. Younger, H. Y. Ren, D. M. Cyr, and C. Patterson. Regulation of the cytoplasmic quality control protein degradation pathway by bag2. *J Biol Chem*, 280(46):38673–81, 2005.

[87] S. Alberti, J. Demand, C. Esser, N. Emmerich, H. Schild, and J. Hohfeld. Ubiquitylation of bag-1 suggests a novel regulatory mechanism during the sorting of chaperone substrates to the proteasome. *J Biol Chem*, 277(48): 45920–7, 2002.

[88] N. Kettern, C. Rogon, A. Limmer, H. Schild, and J. Hohfeld. The hsc/hsp70 co-chaperone network controls antigen aggregation and presentation during maturation of professional antigen presenting cells. *PLoS One*, 6(1):e16398, 2011.

[89] K. M. Scaglione, E. Zavodszky, S. V. Todi, S. Patury, P. Xu, E. Rodriguez-Lebron, S. Fischer, J. Konen, A. Djarmati, J. Peng, J. E. Gestwicki, and H. L. Paulson. Ube2w and ataxin-3 coordinately regulate the ubiquitin ligase chip. *Mol Cell*, 43(4):599–612, 2011.

[90] T. M. Durcan and E. A. Fon. Ataxin-3 and its e3 partners: implications for machado-joseph disease. *Front Neurol*, 4:46, 2013.

[91] N. R. Jana, P. Dikshit, A. Goswami, S. Kotliarova, S. Murata, K. Tanaka, and N. Nukina. Co-chaperone chip associates with expanded polyglutamine protein and promotes their degradation by proteasomes. *J Biol Chem*, 280(12):11635–40, 2005.

[92] Y. Imai, M. Soda, and R. Takahashi. Parkin suppresses unfolded protein stress-induced cell death through its e3 ubiquitin-protein ligase activity. *J Biol Chem*, 275(46):35661–4, 2000.

[93] J. Niwa, S. Ishigaki, N. Hishikawa, M. Yamamoto, M. Doyu, S. Murata, K. Tanaka, N. Taniguchi, and G. Sobue. Dorfin ubiquitylates mutant sod1 and prevents mutant sod1-mediated neurotoxicity. *J Biol Chem*, 277(39): 36793–8, 2002.

[94] Y. C. Tsai, P. S. Fishman, N. V. Thakor, and G. A. Oyler. Parkin facilitates the elimination of expanded polyglutamine proteins and leads to preservation of proteasome function. *J Biol Chem*, 278(24):22044–55, 2003.

[95] C. Vives-Bauza and S. Przedborski. Mitophagy: the latest problem for parkinson's disease. *Trends Mol Med*, 17(3):158–65, 2011.

[96] C. Vives-Bauza, C. Zhou, Y. Huang, M. Cui, R. L. de Vries, J. Kim, J. May, M. A. Tocilescu, W. Liu, H. S. Ko, J. Magrane, D. J. Moore, V. L. Dawson, R. Grailhe, T. M. Dawson, C. Li, K. Tieu, and S. Przedborski. Pink1-dependent recruitment of parkin to mitochondria in mitophagy. *Proc Natl Acad Sci U S A*, 107(1):378–83, 2010.

[97] A. Varshavsky. The n-end rule: functions, mysteries, uses. *Proc Natl Acad Sci U S A*, 93(22):12142–9, 1996.

[98] Z. Xia, A. Webster, F. Du, K. Piatkov, M. Ghislain, and A. Varshavsky. Substrate-binding sites of ubr1, the ubiquitin ligase of the n-end rule pathway. *J Biol Chem*, 283(35):24011–28, 2008.

[99] A. Stolz, S. Besser, H. Hottmann, and D. H. Wolf. Previously unknown role for the ubiquitin ligase ubr1 in endoplasmic reticulum-associated protein degradation. *Proc Natl Acad Sci U S A*, 110(38):15271–6, 2013.

[100] M. A. Theodoraki, N. B. Nillegoda, J. Saini, and A. J. Caplan. A network of ubiquitin ligases is important for the dynamics of misfolded protein aggregates in yeast. *J Biol Chem*, 287(28):23911–22, 2012.

[101] F. Khosrow-Khavar, N. N. Fang, A. H. Ng, J. M. Winget, S. A. Comyn, and T. Mayor. The yeast ubr1 ubiquitin ligase participates in a prominent pathway that targets cytosolic thermosensitive mutants for degradation. *G3 (Bethesda)*, 2(5):619–28, 2012.

[102] B. Bartel, I. Wunning, and A. Varshavsky. The recognition component of the n-end rule pathway. *EMBO J*, 9(10):3179–89, 1990.

[103] F. Eisele and D. H. Wolf. Degradation of misfolded protein in the cytoplasm is mediated by the ubiquitin ligase ubr1. *FEBS Lett*, 582(30): 4143–6, 2008.

[104] N. B. Nillegoda, M. A. Theodoraki, A. K. Mandal, K. J. Mayo, H. Y. Ren, R. Sultana, K. Wu, J. Johnson, D. M. Cyr, and A. J. Caplan. Ubr1 and ubr2 function in a quality control pathway for degradation of unfolded cytosolic proteins. *Mol Biol Cell*, 21(13):2102–16, 2010.

[105] R. Sultana, M. A. Theodoraki, and A. J. Caplan. Ubr1 promotes protein kinase quality control and sensitizes cells to hsp90 inhibition. *Exp Cell Res*, 318(1):53–60, 2012.

[106] C. S. Hwang, M. Sukalo, O. Batygin, M. C. Addor, H. Brunner, A. P. Aytes, J. Mayerle, H. K. Song, A. Varshavsky, and M. Zenker. Ubiquitin ligases of the n-end rule pathway: assessment of mutations in ubr1 that cause the johanson-blizzard syndrome. *PLoS One*, 6(9):e24925, 2011.

[107] B. Medicherla and A. L. Goldberg. Heat shock and oxygen radicals stimulate ubiquitin-dependent degradation mainly of newly synthesized proteins. *J Cell Biol*, 182(4):663–73, 2008.

[108] A. H. Ng, N. N. Fang, S. A. Comyn, J. Gsponer, and T. Mayor. System-wide analysis reveals intrinsically disordered proteins are prone to ubiquitylation after misfolding stress. *Mol Cell Proteomics*, 2013.

[109] N. N. Fang, A. H. Ng, V. Measday, and T. Mayor. Hul5 hect ubiquitin ligase plays a major role in the ubiquitylation and turnover of cytosolic misfolded proteins. *Nat Cell Biol*, 13(11):1344–52, 2011.

[110] B. Crosas, J. Hanna, D. S. Kirkpatrick, D. P. Zhang, Y. Tone, N. A. Hathaway, C. Buecker, D. S. Leggett, M. Schmidt, R. W. King, S. P. Gygi, and D. Finley. Ubiquitin chains are remodeled at the proteasome by opposing ubiquitin ligase and deubiquitinating activities. *Cell*, 127(7): 1401–13, 2006.

[111] D. S. Leggett, J. Hanna, A. Borodovsky, B. Crosas, M. Schmidt, R. T. Baker, T. Walz, H. Ploegh, and D. Finley. Multiple associated proteins regulate proteasome structure and function. *Mol Cell*, 10(3):495–507, 2002.

[112] R. Dunn and L. Hicke. Domains of the rsp5 ubiquitin-protein ligase required for receptor-mediated and fluid-phase endocytosis. *Mol Biol Cell*, 12(2):421–35, 2001.

[113] P. Kaliszewski, T. Ferreira, B. Gajewska, A. Szkopinska, T. Berges, and T. Zoladek. Enhanced levels of pis1p (phosphatidylinositol synthase) improve the growth of saccharomyces cerevisiae cells deficient in rsp5 ubiquitin ligase. *Biochem J*, 395(1):173–81, 2006.

[114] M. S. Rodriguez, C. Gwizdek, R. Haguenauer-Tsapis, and C. Dargemont. The hect ubiquitin ligase rsp5p is required for proper nuclear export of mrna in saccharomyces cerevisiae. *Traffic*, 4(8):566–75, 2003.

[115] M. H. Bengtson and C. A. Joazeiro. Role of a ribosome-associated e3 ubiquitin ligase in protein quality control. *Nature*, 467(7314):470–3, 2010.

[116] S. Shao, K. von der Malsburg, and R. S. Hegde. Listerin-dependent nascent protein ubiquitination relies on ribosome subunit dissociation. *Mol Cell*, 2013.

[117] K. von der Malsburg, S. Shao, and R. S. Hegde. The ribosome quality control pathway can access nascent polypeptides stalled at the sec61 translocon. *Mol Biol Cell*, 26(12):2168–80, 2015.

[118] O. Brandman, J. Stewart-Ornstein, D. Wong, A. Larson, C. C. Williams, G. W. Li, S. Zhou, D. King, P. S. Shen, J. Weibezahn, J. G. Dunn, S. Rouskin, T. Inada, A. Frost, and J. S. Weissman. A ribosome-bound quality control complex triggers degradation of nascent peptides and signals translation stress. *Cell*, 151(5):1042–54, 2012.

[119] Q. Defenouillere, Y. Yao, J. Mouaikel, A. Namane, A. Galopier, L. Decourty, A. Doyen, C. Malabat, C. Saveanu, A. Jacquier, and M. Fromont-Racine. Cdc48-associated complex bound to 60s particles is required for the clearance of aberrant translation products. *Proc Natl Acad Sci U S A*, 110(13):5046–51, 2013.

[120] S. Shao, A. Brown, B. Santhanam, and R. S. Hegde. Structure and assembly pathway of the ribosome quality control complex. *Mol Cell*, 57 (3):433–44, 2015.

[121] R. Verma, R. S. Oania, N. J. Kolawa, and R. J. Deshaies. Cdc48/p97 promotes degradation of aberrant nascent polypeptides bound to the ribosome. *Elife*, 2:e00308, 2013.

[122] J. J. Crowder, M. Geigges, R. T. Gibson, E. S. Fults, B. W. Buchanan, N. Sachs, A. Schink, S. G. Kreft, and E. M. Rubenstein. Rkr1/ltn1 ubiquitin ligase-mediated degradation of translationally stalled endoplasmic reticulum proteins. *J Biol Chem*, 290(30):18454–66, 2015.

[123] D. Lyumkis, S. K. Doamekpor, M. H. Bengtson, J. W. Lee, T. B. Toro, M. D. Petroski, C. D. Lima, C. S. Potter, B. Carragher, and C. A. Joazeiro. Single-particle em reveals extensive conformational variability of the ltn1 e3 ligase. *Proc Natl Acad Sci U S A*, 110(5):1702–7, 2013.

[124] J. Chu, N. A. Hong, C. A. Masuda, B. V. Jenkins, K. A. Nelms, C. C. Goodnow, R. J. Glynne, H. Wu, E. Masliah, C. A. Joazeiro, and S. A. Kay. A mouse forward genetics screen identifies listerin as an e3 ubiquitin ligase involved in neurodegeneration. *Proc Natl Acad Sci U S A*, 106(7): 2097–103, 2009.

[125] D. Glick, S. Barth, and K. F. Macleod. Autophagy: cellular and molecular mechanisms. *J Pathol*, 221(1):3–12, 2010.

[126] X. Chen and X. M. Yin. Coordination of autophagy and the proteasome in resolving endoplasmic reticulum stress. *Vet Pathol*, 48(1):245–53, 2011.

[127] C. Kraft, A. Deplazes, M. Sohrmann, and M. Peter. Mature ribosomes are selectively degraded upon starvation by an autophagy pathway requiring the ubp3p/bre5p ubiquitin protease. *Nat Cell Biol*, 10(5):602–10, 2008.

[128] R. S. Marshall, F. Li, D. C. Gemperline, A. J. Book, and R. D. Vierstra. Autophagic degradation of the 26s proteasome is mediated by the dual atg8/ubiquitin receptor rpn10 in arabidopsis. *Mol Cell*, 58(6):1053–66,

2015. Marshall, Richard S Li, Faqiang Gemperline, David C Book, Adam J Vierstra, Richard D T32 GM007133/GM/NIGMS NIH HHS/United States Research Support, U.S. Gov't, Non-P.H.S. United States Molecular cell Nihms771991 Mol Cell. 2015 Jun 18;58(6):1053-66. doi: 10.1016/j.molcel.2015.04.023. Epub 2015 May 21.

[129] R. S. Marshall, F. McLoughlin, and R. D. Vierstra. Autophagic turnover of inactive 26s proteasomes in yeast is directed by the ubiquitin receptor cue5 and the hsp42 chaperone. *Cell Rep*, 16(6):1717–32, 2016. Marshall, Richard S McLoughlin, Fionn Vierstra, Richard D United States Cell reports Cell Rep. 2016 Aug 9;16(6):1717-32. doi: 10.1016/j.celrep.2016.07.015. Epub 2016 Jul 28.

[130] B. Ossareh-Nazari, C. A. Nino, M. H. Bengtson, J. W. Lee, C. A. Joazeiro, and C. Dargemont. Ubiquitylation by the ltn1 e3 ligase protects 60s ribosomes from starvation-induced selective autophagy. *J Cell Biol*, 204 (6):909–17, 2014.

[131] I. Kim, S. Rodriguez-Enriquez, and J. J. Lemasters. Selective degradation of mitochondria by mitophagy. *Arch Biochem Biophys*, 462(2):245–53, 2007.

[132] D. Narendra, A. Tanaka, D. F. Suen, and R. J. Youle. Parkin-induced mitophagy in the pathogenesis of parkinson disease. *Autophagy*, 5(5): 706–8, 2009.

[133] G. Bjorkoy, T. Lamark, A. Brech, H. Outzen, M. Perander, A. Overvatn, H. Stenmark, and T. Johansen. p62/sqstm1 forms protein aggregates degraded by autophagy and has a protective effect on huntingtin-induced cell death. *J Cell Biol*, 171(4):603–14, 2005.

[134] J. A. Johnston, C. L. Ward, and R. R. Kopito. Aggresomes: a cellular response to misfolded proteins. *J Cell Biol*, 143(7):1883–98, 1998.

[135] D. Kaganovich, R. Kopito, and J. Frydman. Misfolded proteins partition between two distinct quality control compartments. *Nature*, 454(7208): 1088–95, 2008.

[136] S. Escusa-Toret, W. I. Vonk, and J. Frydman. Spatial sequestration of misfolded proteins by a dynamic chaperone pathway enhances cellular fitness during stress. *Nat Cell Biol*, 15(10):1231–43, 2013.

[137] S. Specht, S. B. Miller, A. Mogk, and B. Bukau. Hsp42 is required for sequestration of protein aggregates into deposition sites in saccharomyces cerevisiae. *J Cell Biol*, 195(4):617–29, 2011.

[138] M. Haslbeck, N. Braun, T. Stromer, B. Richter, N. Model, S. Weinkauf, and J. Buchner. Hsp42 is the general small heat shock protein in the cytosol of saccharomyces cerevisiae. *EMBO J*, 23(3):638–49, 2004.

[139] D. Wotton, K. Freeman, and D. Shore. Multimerization of hsp42p, a novel heat shock protein of saccharomyces cerevisiae, is dependent on a conserved carboxyl-terminal sequence. *J Biol Chem*, 271(5):2717–23, 1996.

[140] L. Malinovska, S. Kroschwald, M. C. Munder, D. Richter, and S. Alberti. Molecular chaperones and stress-inducible protein-sorting factors coordinate the spatiotemporal distribution of protein aggregates. *Mol Biol Cell*, 23(16):3041–56, 2012.

[141] J. Verghese, J. Abrams, Y. Wang, and K. A. Morano. Biology of the heat shock response and protein chaperones: budding yeast (saccharomyces cerevisiae) as a model system. *Microbiol Mol Biol Rev*, 76(2):115–58, 2012.

[142] Y. Sanchez and S. L. Lindquist. Hsp104 required for induced thermotolerance. *Science*, 248(4959):1112–5, 1990.

[143] K. A. Morano, C. M. Grant, and W. S. Moye-Rowley. The response to heat shock and oxidative stress in saccharomyces cerevisiae. *Genetics*, 190(4): 1157–95, 2012.

[144] D. B. Berry and A. P. Gasch. Stress-activated genomic expression changes serve a preparative role for impending stress in yeast. *Mol Biol Cell*, 19 (11):4580–7, 2008.

[145] S. B. Ferguson, E. S. Anderson, R. B. Harshaw, T. Thate, N. L. Craig, and H. C. Nelson. Protein kinase a regulates constitutive expression of small heat-shock genes in an msn2/4p-independent and hsf1p-dependent manner in saccharomyces cerevisiae. *Genetics*, 169(3):1203–14, 2005.

[146] E. J. Solis, J. P. Pandey, X. Zheng, D. X. Jin, P. B. Gupta, E. M. Airoldi, D. Pincus, and V. Denic. Defining the essential function of yeast hsf1 reveals a compact transcriptional program for maintaining eukaryotic proteostasis. *Mol Cell*, 63(1):60–71, 2016.

[147] A. P. Gasch, P. T. Spellman, C. M. Kao, O. Carmel-Harel, M. B. Eisen, G. Storz, D. Botstein, and P. O. Brown. Genomic expression programs in the response of yeast cells to environmental changes. *Mol Biol Cell*, 11 (12):4241–57, 2000.

[148] A. P. Schmitt and K. McEntee. Msn2p, a zinc finger dna-binding protein, is the transcriptional activator of the multistress response in saccharomyces cerevisiae. *Proc Natl Acad Sci U S A*, 93(12):5777–82, 1996.

[149] A. Sadeh, D. Baran, M. Volokh, and A. Aharoni. Conserved motifs in the msn2-activating domain are important for msn2-mediated yeast stress response. *J Cell Sci*, 125(Pt 14):3333–42, 2012.

[150] W. Gorner, E. Durchschlag, J. Wolf, E. L. Brown, G. Ammerer, H. Ruis, and C. Schuller. Acute glucose starvation activates the nuclear localization signal of a stress-specific yeast transcription factor. *EMBO J*, 21(1-2): 135–44, 2002.

[151] E. Durchschlag, W. Reiter, G. Ammerer, and C. Schuller. Nuclear localization destabilizes the stress-regulated transcription factor msn2. *J Biol Chem*, 279(53):55425–32, 2004.

[152] A. Santhanam, A. Hartley, K. Duvel, J. R. Broach, and S. Garrett. Pp2a phosphatase activity is required for stress and tor kinase regulation of yeast stress response factor msn2p. *Eukaryot Cell*, 3(5):1261–71, 2004.

[153] M. Jacquet, G. Renault, S. Lallet, J. De Mey, and A. Goldbeter. Oscillatory nucleocytoplasmic shuttling of the general stress response transcriptional activators msn2 and msn4 in saccharomyces cerevisiae. *J Cell Biol*, 161(3): 497–505, 2003.

[154] S. Ghaemmaghami, W. K. Huh, K. Bower, R. W. Howson, A. Belle, N. Dephoure, E. K. O'Shea, and J. S. Weissman. Global analysis of protein expression in yeast. *Nature*, 425(6959):737–41, 2003.

[155] Y. Liu, S. Ye, and A. M. Erkine. Analysis of saccharomyces cerevisiae genome for the distributions of stress-response elements potentially affecting gene expression by transcriptional interference. *In Silico Biol*, 9 (5-6):379–89, 2009.

[156] J. Stewart-Ornstein, C. Nelson, J. DeRisi, J. S. Weissman, and H. El-Samad. Msn2 coordinates a stoichiometric gene expression program. *Curr Biol*, 23(23):2336–45, 2013.

[157] B. Chen, M. Retzlaff, T. Roos, and J. Frydman. Cellular strategies of protein quality control. *Cold Spring Harb Perspect Biol*, 3(8):a004374, 2011.

[158] P. D. Stenson, M. Mort, E. V. Ball, K. Shaw, A. Phillips, and D. N. Cooper. The human gene mutation database: building a comprehensive mutation repository for clinical and molecular genetics, diagnostic testing and personalized genomic medicine. *Hum Genet*, 133(1):1–9, 2014.

[159] N. Sahni, S. Yi, M. Taipale, J. I. Fuxman Bass, J. Coulombe-Huntington, F. Yang, J. Peng, J. Weile, G. I. Karras, Y. Wang, I. A. Kovacs, A. Kamburov, I. Krykbaeva, M. H. Lam, G. Tucker, V. Khurana, A. Sharma, Y. Y. Liu, N. Yachie, Q. Zhong, Y. Shen, A. Palagi, A. San-Miguel, C. Fan, D. Balcha, A. Dricot, D. M. Jordan, J. M. Walsh, A. A. Shah, X. Yang, A. K. Stoyanova, A. Leighton, M. A. Calderwood, Y. Jacob, M. E. Cusick, K. Salehi-Ashtiani, L. J. Whitesell, S. Sunyaev, B. Berger, A. L. Barabasi, B. Charloteaux, D. E. Hill, T. Hao, F. P. Roth, Y. Xia, A. J. Walhout, S. Lindquist, and M. Vidal. Widespread macromolecular interaction perturbations in human genetic disorders. *Cell*, 161(3):647–60, 2015.

[160] P. G. Richardson, B. Barlogie, J. Berenson, S. Singhal, S. Jagannath, D. Irwin, S. V. Rajkumar, G. Srkalovic, M. Alsina, R. Alexanian, D. Siegel, R. Z. Orlowski, D. Kuter, S. A. Limentani, S. Lee, T. Hideshima, D. L. Esseltine, M. Kauffman, J. Adams, D. P. Schenkein, and K. C. Anderson. A phase 2 study of bortezomib in relapsed, refractory myeloma. *N Engl J Med*, 348(26):2609–17, 2003.

[161] G. Nalepa, M. Rolfe, and J. W. Harper. Drug discovery in the ubiquitin-proteasome system. *Nat Rev Drug Discov*, 5(7):596–613, 2006.

[162] S. Khare, A. S. Nagle, A. Biggart, Y. H. Lai, F. Liang, L. C. Davis, S. W. Barnes, C. J. Mathison, E. Myburgh, M. Y. Gao, J. R. Gillespie, X. Liu, J. L. Tan, M. Stinson, I. C. Rivera, J. Ballard, V. Yeh, T. Groessl, G. Federe, H. X. Koh, J. D. Venable, B. Bursulaya, M. Shapiro, P. K. Mishra, G. Spraggon, A. Brock, J. C. Mottram, F. S. Buckner, S. P. Rao, B. G. Wen, J. R. Walker, T. Tuntland, V. Molteni, R. J. Glynne, and F. Supek. Proteasome inhibition for treatment of leishmaniasis, chagas disease and sleeping sickness. *Nature*, 537(7619):229–233, 2016.

[163] T. Kirkegaard, J. Gray, D. A. Priestman, K. L. Wallom, J. Atkins, O. D. Olsen, A. Klein, S. Drndarski, N. H. Petersen, L. Ingemann, D. A. Smith,

L. Morris, C. Bornaes, S. H. Jorgensen, I. Williams, A. Hinsby, C. Arenz, D. Begley, M. Jaattela, and F. M. Platt. Heat shock protein-based therapy as a potential candidate for treating the sphingolipidoses. *Sci Transl Med*, 8 (355):355ra118, 2016.

[164] K. Kuk and J. L. Taylor-Cousar. Lumacaftor and ivacaftor in the management of patients with cystic fibrosis: current evidence and future prospects. *Ther Adv Respir Dis*, 9(6):313–26, 2015. Kuk, Kelly Taylor-Cousar, Jennifer L Research Support, N.I.H., Extramural Research Support, Non-U.S. Gov't Review England Therapeutic advances in respiratory disease Ther Adv Respir Dis. 2015 Dec;9(6):313-26. doi: 10.1177/1753465815601934. Epub 2015 Sep 28.

[165] A. R. Schoenfeld, E. J. Davidowitz, and R. D. Burk. Elongin bc complex prevents degradation of von hippel-lindau tumor suppressor gene products. *Proc Natl Acad Sci U S A*, 97(15):8507–12, 2000.

[166] M. Knop, A. Finger, T. Braun, K. Hellmuth, and D. H. Wolf. Der1, a novel protein specifically required for endoplasmic reticulum degradation in yeast. *EMBO J*, 15(4):753–63, 1996.

[167] M. J. Maurer, E. D. Spear, A. T. Yu, E. J. Lee, S. Shahzad, and S. Michaelis. Degradation signals for ubiquitin-proteasome dependent cytosolic protein quality control (cytoqc) in yeast. *G3 (Bethesda)*, 2016.

[168] W. Seufert, B. Futcher, and S. Jentsch. Role of a ubiquitin-conjugating enzyme in degradation of s- and m-phase cyclins. *Nature*, 373(6509): 78–81, 1995.

[169] J. Betting and W. Seufert. A yeast ubc9 mutant protein with temperature-sensitive in vivo function is subject to conditional proteolysis by a ubiquitin- and proteasome-dependent pathway. *J Biol Chem*, 271(42): 25790–6, 1996.

[170] O. Shimomura, F. H. Johnson, and Y. Saiga. Extraction, purification and properties of aequorin, a bioluminescent protein from the luminous hydromedusan, aequorea. *J Cell Comp Physiol*, 59:223–39, 1962.

[171] R. Heim, D. C. Prasher, and R. Y. Tsien. Wavelength mutations and posttranslational autoxidation of green fluorescent protein. *Proc Natl Acad Sci U S A*, 91(26):12501–4, 1994.

[172] D. C. Prasher, V. K. Eckenrode, W. W. Ward, F. G. Prendergast, and M. J. Cormier. Primary structure of the aequorea victoria green-fluorescent protein. *Gene*, 111(2):229–33, 1992.

[173] R. Heim, A. B. Cubitt, and R. Y. Tsien. Improved green fluorescence. *Nature*, 373(6516):663–4, 1995.

[174] H. C. Yen, Q. Xu, D. M. Chou, Z. Zhao, and S. J. Elledge. Global protein stability profiling in mammalian cells. *Science*, 322(5903):918–23, 2008.

[175] H. C. Yen and S. J. Elledge. Identification of scf ubiquitin ligase substrates by global protein stability profiling. *Science*, 322(5903):923–9, 2008.

[176] A. Khmelinskii, P. J. Keller, A. Bartosik, M. Meurer, J. D. Barry, B. R. Mardin, A. Kaufmann, S. Trautmann, M. Wachsmuth, G. Pereira, W. Huber, E. Schiebel, and M. Knop. Tandem fluorescent protein timers for in vivo analysis of protein dynamics. *Nat Biotechnol*, 30(7):708–14, 2012.

[177] J. F. Morley, H. R. Brignull, J. J. Weyers, and R. I. Morimoto. The threshold for polyglutamine-expansion protein aggregation and cellular toxicity is dynamic and influenced by aging in caenorhabditis elegans. *Proc Natl Acad Sci U S A*, 99(16):10417–22, 2002.

[178] S. A. Comyn, G. T. Chan, and T. Mayor. False start: cotranslational protein ubiquitination and cytosolic protein quality control. *J Proteomics*, 100: 92–101, 2014.

[179] F. U. Hartl, A. Bracher, and M. Hayer-Hartl. Molecular chaperones in protein folding and proteostasis. *Nature*, 475(7356):324–32, 2011.

[180] K. Schneider and A. Bertolotti. Surviving protein quality control catastrophes - from cells to organisms. *J Cell Sci*, 128(21):3861–9, 2015.

[181] G. Kleiger and T. Mayor. Perilous journey: a tour of the ubiquitin-proteasome system. *Trends Cell Biol*, 24(6):352–9, 2014.

[182] N. N. Fang and T. Mayor. Hul5 ubiquitin ligase: good riddance to bad proteins. *Prion*, 6(3):240–4, 2012.

[183] J. Tyedmers, S. Treusch, J. Dong, J. M. McCaffery, B. Bevis, and S. Lindquist. Prion induction involves an ancient system for the sequestration of aggregated proteins and heritable changes in prion fragmentation. *Proc Natl Acad Sci U S A*, 107(19):8633–8, 2010.

[184] U. Lenk and T. Sommer. Ubiquitin-mediated proteolysis of a short-lived regulatory protein depends on its cellular localization. *J Biol Chem*, 275 (50):39403–10, 2000.

[185] S. Ben-Aroya, C. Coombes, T. Kwok, K. A. O'Donnell, J. D. Boeke, and P. Hieter. Toward a comprehensive temperature-sensitive mutant repository of the essential genes of saccharomyces cerevisiae. *Mol Cell*, 30(2): 248–58, 2008.

[186] S. Ben-Aroya, X. Pan, J. D. Boeke, and P. Hieter. Making temperature-sensitive mutants. *Methods Enzymol*, 470:181–204, 2010.

[187] A. Berger, E. Schiltz, and G. E. Schulz. Guanylate kinase from saccharomyces cerevisiae. isolation and characterization, crystallization and preliminary x-ray analysis, amino acid sequence and comparison with adenylate kinases. *Eur J Biochem*, 184(2):433–43, 1989.

[188] J. Blaszczyk, Y. Li, H. Yan, and X. Ji. Crystal structure of unligated guanylate kinase from yeast reveals gmp-induced conformational changes. *J Mol Biol*, 307(1):247–57, 2001.

[189] Y. Shimma, A. Nishikawa, B. bin Kassim, A. Eto, and Y. Jigami. A defect in gtp synthesis affects mannose outer chain elongation in saccharomyces cerevisiae. *Mol Gen Genet*, 256(5):469–80, 1997.

[190] J. Schymkowitz, J. Borg, F. Stricher, R. Nys, F. Rousseau, and L. Serrano. The foldx web server: an online force field. *Nucleic Acids Res*, 33(Web Server issue):W382–8, 2005.

[191] M. J. Gallagher, L. Ding, A. Maheshwari, and R. L. Macdonald. The gabaa receptor alpha1 subunit epilepsy mutation a322d inhibits transmembrane helix formation and causes proteasomal degradation. *Proc Natl Acad Sci U S A*, 104(32):12999–3004, 2007.

[192] A. L. Pey, F. Stricher, L. Serrano, and A. Martinez. Predicted effects of missense mutations on native-state stability account for phenotypic outcome in phenylketonuria, a paradigm of misfolding diseases. *Am J Hum Genet*, 81(5):1006–24, 2007.

[193] D. Martinez Molina, R. Jafari, M. Ignatushchenko, T. Seki, E. A. Larsson, C. Dan, L. Sreekumar, Y. Cao, and P. Nordlund. Monitoring drug target engagement in cells and tissues using the cellular thermal shift assay. *Science*, 341(6141):84–7, 2013.

[194] C. Guerrero, T. Milenkovic, N. Przulj, P. Kaiser, and L. Huang. Characterization of the proteasome interaction network using a qtax-based tag-team strategy and protein interaction network analysis. *Proc Natl Acad Sci U S A*, 105(36):13333–8, 2008.

[195] C. Zhou, B. D. Slaughter, J. R. Unruh, F. Guo, Z. Yu, K. Mickey, A. Narkar, R. T. Ross, M. McClain, and R. Li. Organelle-based aggregation and retention of damaged proteins in asymmetrically dividing cells. *Cell*, 159(3):530–42, 2014.

[196] J. M. Daran, N. Dallies, D. Thines-Sempoux, V. Paquet, and J. Francois. Genetic and biochemical characterization of the ugp1 gene encoding the udp-glucose pyrophosphorylase from saccharomyces cerevisiae. *Eur J Biochem*, 233(2):520–30, 1995.

[197] D. G. Yi and W. K. Huh. Udp-glucose pyrophosphorylase ugp1 is involved in oxidative stress response and long-term survival during stationary phase in saccharomyces cerevisiae. *Biochem Biophys Res Commun*, 467(4): 657–63, 2015.

[198] M. Delarue. Aminoacyl-trna synthetases. *Curr Opin Struct Biol*, 5(1): 48–55, 1995.

[199] K. Galani, H. Grosshans, K. Deinert, E. C. Hurt, and G. Simos. The intracellular location of two aminoacyl-trna synthetases depends on complex formation with arc1p. *EMBO J*, 20(23):6889–98, 2001.

[200] M. C. Brandriss and D. A. Falvey. Proline biosynthesis in saccharomyces cerevisiae: analysis of the pro3 gene, which encodes delta 1-pyrroline-5-carboxylate reductase. *J Bacteriol*, 174(11):3782–8, 1992.

[201] J. W. Yewdell, J. R. Lacsina, M. C. Rechsteiner, and C. V. Nicchitta. Out with the old, in with the new? comparing methods for measuring protein degradation. *Cell Biol Int*, 35(5):457–62, 2011.

[202] A. Abe, K. Takahashi-Niki, Y. Takekoshi, T. Shimizu, H. Kitaura, H. Maita, S. M. Iguchi-Ariga, and H. Ariga. Prefoldin plays a role as a clearance factor in preventing proteasome inhibitor-induced protein aggregation. *J Biol Chem*, 288(39):27764–76, 2013.

[203] H. Lee do, M. Y. Sherman, and A. L. Goldberg. The requirements of yeast hsp70 of ssa family for the ubiquitin-dependent degradation of short-lived and abnormal proteins. *Biochem Biophys Res Commun*, 475(1):100–6, 2016.

[204] M. Sakono, T. Zako, H. Ueda, M. Yohda, and M. Maeda. Formation of highly toxic soluble amyloid beta oligomers by the molecular chaperone prefoldin. *FEBS J*, 275(23):5982–93, 2008.

[205] K. M. Sorgjerd, T. Zako, M. Sakono, P. C. Stirling, M. R. Leroux, T. Saito, P. Nilsson, M. Sekimoto, T. C. Saido, and M. Maeda. Human prefoldin inhibits amyloid-beta (abeta) fibrillation and contributes to formation of nontoxic abeta aggregates. *Biochemistry*, 52(20):3532–42, 2013.

[206] S. A. Comyn, B. P. Young, C. J. Loewen, and T. Mayor. Prefoldin promotes proteasomal degradation of cytosolic proteins with missense mutations by maintaining substrate solubility. *PLoS Genet*, 12(7):e1006184, 2016.

[207] F. Tsukahara and Y. Maru. Bag1 directly routes immature bcr-abl for proteasomal degradation. *Blood*, 116(18):3582–92, 2010.

[208] D. Sambrook J., Russell. *Molecular Cloning: A Laboratory Manual*. Cold Spring Harbor Laboratory Press, Cold Spring Harbor, NY, 3 edition, 2001.

[209] H. Li and R. Durbin. Fast and accurate long-read alignment with burrows-wheeler transform. *Bioinformatics*, 26(5):589–95, 2010.

[210] H. Li, B. Handsaker, A. Wysoker, T. Fennell, J. Ruan, N. Homer, G. Marth, G. Abecasis, and R. Durbin. The sequence alignment/map format and samtools. *Bioinformatics*, 25(16):2078–9, 2009.

[211] J. T. Robinson, H. Thorvaldsdottir, W. Winckler, M. Guttman, E. S. Lander, G. Getz, and J. P. Mesirov. Integrative genomics viewer. *Nat Biotechnol*, 29(1):24–6, 2011.

[212] H. Thorvaldsdottir, J. T. Robinson, and J. P. Mesirov. Integrative genomics viewer (igv): high-performance genomics data visualization and exploration. *Brief Bioinform*, 14(2):178–92, 2013.

[213] O. Foresti, V. Rodriguez-Vaello, C. Funaya, and P. Carvalho. Quality control of inner nuclear membrane proteins by the asi complex. *Science*, 346(6210):751–5, 2014.

[214] W. C. Cheng, X. Teng, H. K. Park, C. M. Tucker, M. J. Dunham, and J. M. Hardwick. Fis1 deficiency selects for compensatory mutations responsible for cell death and growth control defects. *Cell Death Differ*, 15(12): 1838–46, 2008.

[215] G. I. Lang, D. P. Rice, M. J. Hickman, E. Sodergren, G. M. Weinstock, D. Botstein, and M. M. Desai. Pervasive genetic hitchhiking and clonal interference in forty evolving yeast populations. *Nature*, 500(7464):571–4, 2013.

[216] X. Teng, M. Dayhoff-Brannigan, W. C. Cheng, C. E. Gilbert, C. N. Sing, N. L. Diny, S. J. Wheelan, M. J. Dunham, J. D. Boeke, F. J. Pineda, and J. M. Hardwick. Genome-wide consequences of deleting any single gene. *Mol Cell*, 52(4):485–94, 2013.

[217] M. T. Martinez-Pastor, G. Marchler, C. Schuller, A. Marchler-Bauer, H. Ruis, and F. Estruch. The saccharomyces cerevisiae zinc finger proteins msn2p and msn4p are required for transcriptional induction through the stress response element (stre). *EMBO J*, 15(9):2227–35, 1996.

[218] H. Garreau, R. N. Hasan, G. Renault, F. Estruch, E. Boy-Marcotte, and M. Jacquet. Hyperphosphorylation of msn2p and msn4p in response to heat shock and the diauxic shift is inhibited by camp in saccharomyces cerevisiae. *Microbiology*, 146 ( Pt 9):2113–20, 2000.

[219] W. Gorner, E. Durchschlag, M. T. Martinez-Pastor, F. Estruch, G. Ammerer, B. Hamilton, H. Ruis, and C. Schuller. Nuclear localization of the c2h2 zinc finger protein msn2p is regulated by stress and protein kinase a activity. *Genes Dev*, 12(4):586–97, 1998.

[220] M. G. Buse and S. S. Reid. Leucine. a possible regulator of protein turnover in muscle. *J Clin Invest*, 56(5):1250–61, 1975.

[221] A. K. Said and D. M. Hegsted. Response of adult rats to low dietary levels of essential amino acids. *J Nutr*, 100(11):1363–75, 1970.

[222] S. C. Schriever, M. J. Deutsch, J. Adamski, A. A. Roscher, and R. Ensenauer. Cellular signaling of amino acids towards mtorc1 activation in impaired human leucine catabolism. *J Nutr Biochem*, 24(5):824–31, 2013.

[223] H. Shahsavarani, M. Sugiyama, Y. Kaneko, B. Chuenchit, and S. Harashima. Superior thermotolerance of saccharomyces cerevisiae for efficient bioethanol fermentation can be achieved by overexpression of rsp5 ubiquitin ligase. *Biotechnol Adv*, 30(6):1289–300, 2012.

[224] F. Cardona, A. Aranda, and M. del Olmo. Ubiquitin ligase rsp5p is involved in the gene expression changes during nutrient limitation in saccharomyces cerevisiae. *Yeast*, 26(1):1–15, 2009.

[225] Y. Haitani and H. Takagi. Rsp5 is required for the nuclear export of mrna of hsf1 and msn2/4 under stress conditions in saccharomyces cerevisiae. *Genes Cells*, 13(2):105–16, 2008.

[226] D. J. Omnus and P. O. Ljungdahl. Latency of transcription factor stp1 depends on a modular regulatory motif that functions as cytoplasmic retention determinant and nuclear degron. *Mol Biol Cell*, 25(23):3823–33, 2014.

[227] B. M. Kus, C. E. Caldon, R. Andorn-Broza, and A. M. Edwards. Functional interaction of 13 yeast scf complexes with a set of yeast e2 enzymes in vitro. *Proteins*, 54(3):455–67, 2004.

[228] A. R. Willems, T. Goh, L. Taylor, I. Chernushevich, A. Shevchenko, and M. Tyers. Scf ubiquitin protein ligases and phosphorylation-dependent proteolysis. *Philos Trans R Soc Lond B Biol Sci*, 354(1389):1533–50, 1999.

[229] J. Kunz, A. Loeschmann, M. Deuter-Reinhard, and M. N. Hall. Fap1, a homologue of human transcription factor nf-x1, competes with rapamycin for binding to fkbp12 in yeast. *Mol Microbiol*, 37(6):1480–93, 2000.

[230] M. Koegl, T. Hoppe, S. Schlenker, H. D. Ulrich, T. U. Mayer, and S. Jentsch. A novel ubiquitination factor, e4, is involved in multiubiquitin chain assembly. *Cell*, 96(5):635–44, 1999.

[231] C. S. Hwang, A. Shemorry, D. Auerbach, and A. Varshavsky. The n-end rule pathway is mediated by a complex of the ring-type ubr1 and hect-type ufd4 ubiquitin ligases. *Nat Cell Biol*, 12(12):1177–85, 2010.

[232] B. Szamecz, G. Boross, D. Kalapis, K. Kovacs, G. Fekete, Z. Farkas, V. Lazar, M. Hrtyan, P. Kemmeren, M. J. Groot Koerkamp, E. Rutkai, F. C. Holstege, B. Papp, and C. Pal. The genomic landscape of compensatory evolution. *PLoS Biol*, 12(8):e1001935, 2014.

[233] N. Mendl, A. Occhipinti, M. Muller, P. Wild, I. Dikic, and A. S. Reichert. Mitophagy in yeast is independent of mitochondrial fission and requires the stress response gene whi2. *J Cell Sci*, 124(Pt 8):1339–50, 2011.

[234] J. van Leeuwen, C. Pons, J. C. Mellor, T. N. Yamaguchi, H. Friesen, J. Koschwanez, M. M. Usaj, M. Pechlaner, M. Takar, M. Usaj, B. VanderSluis, K. Andrusiak, P. Bansal, A. Baryshnikova, C. E. Boone, J. Cao, A. Cote, M. Gebbia, G. Horecka, I. Horecka, E. Kuzmin, N. Legro, W. Liang, N. van Lieshout, M. McNee, B. J. San Luis, F. Shaeri,

E. Shuteriqi, S. Sun, L. Yang, J. Y. Youn, M. Yuen, M. Costanzo, A. C. Gingras, P. Aloy, C. Oostenbrink, A. Murray, T. R. Graham, C. L. Myers, B. J. Andrews, F. P. Roth, and C. Boone. Exploring genetic suppression interactions on a global scale. *Science*, 354(6312), 2016.

[235] D. Kaida, H. Yashiroda, A. Toh-e, and Y. Kikuchi. Yeast whi2 and psr1-phosphatase form a complex and regulate stre-mediated gene expression. *Genes Cells*, 7(6):543–52, 2002.

[236] H. L. Fox, P. T. Pham, S. R. Kimball, L. S. Jefferson, and C. J. Lynch. Amino acid effects on translational repressor 4e-bp1 are mediated primarily by l-leucine in isolated adipocytes. *Am J Physiol*, 275(5 Pt 1): C1232–8, 1998.

[237] T. Beck and M. N. Hall. The tor signalling pathway controls nuclear localization of nutrient-regulated transcription factors. *Nature*, 402(6762): 689–92, 1999.

[238] P. Lee, B. R. Cho, H. S. Joo, and J. S. Hahn. Yeast yak1 kinase, a bridge between pka and stress-responsive transcription factors, hsf1 and msn2/msn4. *Mol Microbiol*, 70(4):882–95, 2008.

[239] P. Lee, M. S. Kim, S. M. Paik, S. H. Choi, B. R. Cho, and J. S. Hahn. Rim15-dependent activation of hsf1 and msn2/4 transcription factors by direct phosphorylation in saccharomyces cerevisiae. *FEBS Lett*, 587(22): 3648–55, 2013.

[240] D. H. Lee, M. Y. Sherman, and A. L. Goldberg. Involvement of the molecular chaperone ydj1 in the ubiquitin-dependent degradation of short-lived and abnormal proteins in saccharomyces cerevisiae. *Mol Cell Biol*, 16(9):4773–81, 1996.

[241] M. A. DePristo, D. M. Weinreich, and D. L. Hartl. Missense meanderings in sequence space: a biophysical view of protein evolution. *Nat Rev Genet*, 6(9):678–87, 2005.

[242] G. V. Kryukov, L. A. Pennacchio, and S. R. Sunyaev. Most rare missense alleles are deleterious in humans: implications for complex disease and association studies. *Am J Hum Genet*, 80(4):727–39, 2007.

[243] R. G. Gardner and R. Y. Hampton. A highly conserved signal controls degradation of 3-hydroxy-3-methylglutaryl-coenzyme a (hmg-coa) reductase in eukaryotes. *J Biol Chem*, 274(44):31671–8, 1999.

[244] A. Belle, A. Tanay, L. Bitincka, R. Shamir, and E. K. O'Shea. Quantification of protein half-lives in the budding yeast proteome. *Proc Natl Acad Sci U S A*, 103(35):13004–9, 2006.

[245] T. Gidalevitz, A. Ben-Zvi, K. H. Ho, H. R. Brignull, and R. I. Morimoto. Progressive disruption of cellular protein folding in models of polyglutamine diseases. *Science*, 311(5766):1471–4, 2006.

[246] J. H. Feder, J. M. Rossi, J. Solomon, N. Solomon, and S. Lindquist. The consequences of expressing hsp70 in drosophila cells at normal temperatures. *Genes Dev*, 6(8):1402–13, 1992.

[247] R. A. Krebs and M. E. Feder. Deleterious consequences of hsp70 overexpression in drosophila melanogaster larvae. *Cell Stress Chaperones*, 2(1):60–71, 1997.

[248] H. Frauenfelder, S. G. Sligar, and P. G. Wolynes. The energy landscapes and motions of proteins. *Science*, 254(5038):1598–603, 1991.

[249] L. Whitesell and S. L. Lindquist. Hsp90 and the chaperoning of cancer. *Nat Rev Cancer*, 5(10):761–72, 2005.

[250] T. Hart, M. Chandrashekhar, M. Aregger, Z. Steinhart, K. R. Brown, G. MacLeod, M. Mis, M. Zimmermann, A. Fradet-Turcotte, S. Sun, P. Mero, P. Dirks, S. Sidhu, F. P. Roth, O. S. Rissland, D. Durocher, S. Angers, and J. Moffat. High-resolution crispr screens reveal fitness genes and genotype-specific cancer liabilities. *Cell*, 163(6):1515–26, 2015.